University of Coimbra University of Liege University Politehnica of Timisoara Technical University of Lulea University Federico II of Naples Czech Technical University in Prague
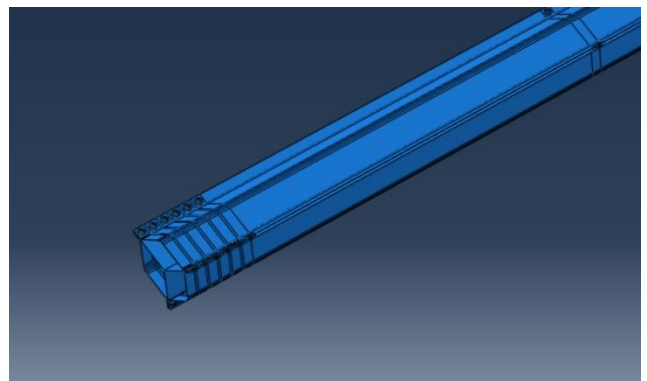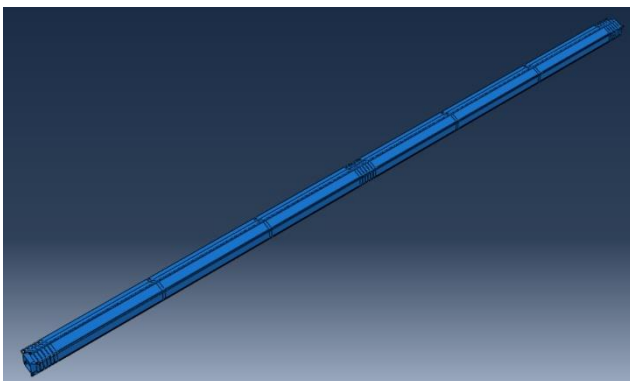
suscos

Master Thesis

Resistance of Polygonal Cross sections of Lattice Wind Tower

Bicen Jia

2017

Supervisor: Panagiotis Manoleas

Preface

This report is presented by Bicen Jia as the master thesis under Erasmus

Mundus Master Programme Sustainable Constructions Under Natural Hazards and Catastrophic

Events (SUSCOS).

First of all, I would like to thank my supervisor, Panagiotis Manoleas for his patience and time

spent on guidance through the work on this master thesis. Also, I would like to express my gratitude to Efthymios Koltsakis for his supervision and guidance.

At last, I would like to thank to people who supported and guided me throughout the education time.

Luleå, January 2017

Bicen Jia

Abstract

Wind energy is one of the most efficient renewable energies. The most used wind towers are tubular and lattice wind towers. Parts of lattice are easier to transfer, especially in the inland areas. Also, it is easier to build higher lattice tower in order to have more efficient energy conversion in inland areas. However, most of the cross sections for lattice tower are tubular cross sections.

This thesis represents the parametric study of polygonal cross section of lattice tower. It consists of the numerical analysis based on finite element method (ABAQUS) and analysis based on EN 1993-1-3. The objective of this thesis is to find regular patterns of parametric influences on polygonal cross section, and to compare them against calculation based on EN 1993-1-3. Also, to find regular patterns of parametric influences on the stiffness of the bolts on the lips.

Table of Contents

1. Introduction

1.1 Background

Google recently announced that as of 2017 it will have 100 percent renewable energy for its operations – and it's got a lot to do with Norwegian wind [1]. Renewable energy sources, which has grown strongly in EU in recent years, play important roles in sustainable development. Renewable energy sources include wind power, solar power, hydroelectric power, tidal power, geothermal energy, biofuels and the renewable part of waste.

The wind energy is a renewable energy that can be used directly or be transformed to other types of energy, such as electricity. According to Eurostat, primary production of energy, gross electricity generation and electricity generation capacity of wind have increased from 1990 to 2014 [2]. Wind in Power, 2015 European Statistics mentions that the wind energy has overtaken hydro as the third largest source of power generation and it accounts for one third of all new power installations since 2000 in the EU [3]. European Wind Energy Roadmap 2013 updated the long term target that wind would generate 15% to 18% of global electricity [4]. Therefore, more projects and researches about wind turbines and wind towers have been done in past years. This thesis presents the resistance of polygonal cross-section lattice tower under variable parameters based on both finite element method and Eurocode.

1.2 Wind tower

Wind tower is the structure that supports a wind turbine. The most common used wind towers are tubular wind tower and lattice tower as well as called truss tower. Lattice towers were quite commonly used in the early history of wind energy system. During the period of 1930-1980s, free-standing lattice towers were the major structure for supporting wind turbines. Then wind towers were then slowly replaced by the tubular towers since mid-1980s.

1.2.1 Tubular wind tower

Most of the wind towers are tubular steel structures. Generally, tubular towers are made of sections with a length of 20-30m. The sections are connected by either welded or bolted. Currently, the sections of tubular towers are mostly connected by bolted ring flange connection. According to C. Heistermann and W. Husson & M,Veljkovic's study in 2009, the flange connection might be replaced by a friction connection with long slotted holes. The advantage of friction connection is the big cost saving since it uses smaller bolts produced in large series, while ring flange connections require a big number of bolts and thick plates in order to meet the stiffness requirement requirements. Also, steel rings of ring flange connections are welded at both tube ends, which costs more. Furthermore, friction connections are less sensitive to fatigue. [5] Figure 1.1 shows the tubular tower and the connection types.

Resistance of Polygonal Cross Section of Lattice Wind Tower

Tubular tower
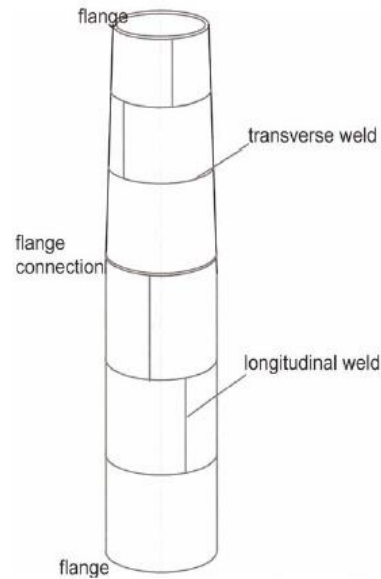
Welded steel shell tower
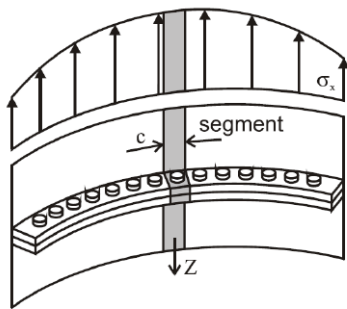
Bolted ring flange connection

Friction connection (HISTWIN project)

Figure 1.1 Tubular wind tower

Tubular wind towers have following advantages:

- Tubular towers are mostly welded, which leads to more rigid structures and improves the efficiency of the sections. Also, welding has less concentrated stress comparing to bolt connection.
- It has good torsional stiffness.
- It has the same bending stiffness in all direction due to its circular cross section [6].
- The inner volume of the tubular tower offers a protected area for equipment [7].
- The shape of tubular tower is more aesthetical.

However, in order to withstand the increased loading, the dimensions of the tower have to be increased, such as the diameter of the tube, the thickness of the plate. It leads to difficult transportation, practically in onshore areas. Also, it has technical difficulties to roll the plates thicker than 50mm and weld.

1.2.2 Lattice wind tower

Generally, tubular wind towers have a maximum height of 80-100m, however, it is necessary to have higher towers in inland arears in order to avoid non-uniform winds and get larger wind so as to have

2

more efficient and economical energy production. On the other hand, it is also necessary to have a stable supporting structure for wind turbines, especially in offshore areas [7]. Lattice tower (Figure 1.2) tends to be a better solution for building higher and stiffer wind towers due to its stability and simpler construction method.

| Lattice tower | Topview of lattice tower |

Figure 1.2: Lattice wind tower

Lattice towers for onshore wind turbines are comparably light-weight support structures and are constructed using connected steel beams. They offer a cost advantage since less steel is used in their construction comparing to the tubular towers of same resistance. Also, they allow the wind to flow through them to have less lateral loads caused by wind. However, lattice towers have a lower aesthetic appeal than tubular towers [8].

Most offshore lattice towers have been built with tubular steel pipes due to the corrosion of offshore environment, which makes it also necessary to weld the connections, thereby removing some of the most important advantages of onshore lattice structures. Furthermore, welding requires higher cost since lattice structures include a large number of joints [7].

This thesis studies the behaviour of a polygonal section of lattice tower. Folded steel plates (Figure 1.3) of the polygonal section are made by cold formed steel technology. Bolt connection between the sectors is used instead of welding.
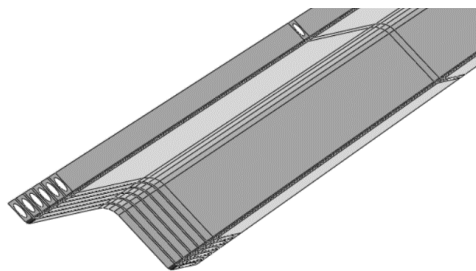
Figure 1.3: Folded steel plate

Lattice towers have following advantages:

- Onshore lattice towers are typically bolted steel frames, which are easier and more cost-efficient to produce comparing to welding.

- Lattice towers are cheaper since they use less structural steel than tubular towers which have the same stiffness.
- Lattice towers are more stable for higher wind towers. A higher tower is beneficial to generate more energy since the wind speed increases with height in inshore areas. Also, the fatigue loads on the turbine on a higher tower are smaller than on a short tower since the wind speed variation between the bottom and top positions the rotor blades passing through is smaller [3].
- A lattice tower does not buckle like shell structure, the risk of buckling of the individual members is controlled [9].
- Pieces of lattice towers are easier to be transported, especially in inshore areas.
- The tubular towers have a problem with tower shadow effect. A tubular tower is more influenced by the horizontal wind load whereas lattice towers are likely transparent to it. Also, lattice towers require less volume in the foundation than tubular towers since tubular towers spread the lattice wind tower to a wider area. [8]

Lattice towers have following disadvantages:

- The basic disadvantage of lattice towers is their visual appearance. For aesthetic reasons, lattice towers have almost disappeared from use for larger, modern wind turbines.
- A high number of bolts are exposed to the open air and each bolt must be inspected three times during its 20-year service life, so maintenance is
- Torsion stiffness is weaker comparing to tubular towers.

1.3 World's tallest wind tower
1) Tallest wind tower

The world's tallest wind turbine, installed by Nordex in 2016, is in Hausbay, Germany. It has a hub height of 164m and a rotor length of 65.5m, the wind power system is N131/3300. The tower consists of a 100m concrete tower and two tubular steel tower segments [10].

2) Tallest lattice wind tower

The tallest lattice wind tower with a height of 160m was installed in 2006 near Laasow, Germany. It has got a tower width of 2.9m at the tower top and 29m at the bottom. It carries a rotor of 90m diameter. This wind turbine is capable of generating 2500 KW if there is enough wind [11].

World's tallest wind tower   World's tallest lattice tower

Figure 1.4: World's tallest towers

1.4 Research achievements (objectives)

The aim of this thesis is listed as below:

1) Build finite element models of polygonal cross sections with different paraments - cross-sectional diameter, thickness, length of the tube and bolt spacing. Study the parametric effects on the resistance.
2) Calculate the resistance based on EN 1993-1-3.
3) Compare the results between finite element analysis and Eurocode.
4) Calculate stiffness of bolts on the lips.

1.5 Limitation

The limitations in this thesis are listed as below:

1) S355 steel is used instead of the high strength steel. Properties of high strength steel are not taken into consideration.
2) Only the results between finite element analysis and Eurocode are compared, experimental test results are excluded.
3) Only two load modes which are pure compression and compression with moment are analysed. Other loads, such as lateral wind, are not taken into consideration.
4) Moments are taken as 0.05, 0.1 and 0.15 of the moment resistance. So the N+M interaction diagram is not completed, the effects of moments on compressive resistance are not significant.
5) Packing plates are not considered in the ABAQUS model
6) Linear buckling analysis (LBA) is assumed to find the first eigenmode as the pattern with the most unfavourable effect on the buckling behaviour for geometrically and materially nonlinear analysis with imperfection included (GMNIA) analysis. However, eigenmode from LBA is always not the worst (most unfavourable) imperfection. Material non-linearity also has effects on geometrically and materially nonlinear analysis (GMNIA) analysis. In order to have the most realistic mode, it is more accurate to use GMNA analysis for finding the most unfavourable imperfection for GMNIA.

1.6 Structure of the thesis

The thesis is to study the parametric effects on polygonal cross-sections and comparison between the resistance calculated based on finite element analysis and Eurocode. This thesis is divided into 7 chapters as shown below:

Chapter 1: Gives the background of wind turbine development; brief introduction of lattice wind tower; objectives and limitations of this thesis.

Chapter 2: Gives the literature review of wind towers. It describes the previous researches about lattice wind tower; method of calculating resistance according to Eurocode; properties of cold form steel and geometric imperfection.

Chapter 3: Gives the introduction of materials and profiles.

Chapter 4: Gives the brief description of and theory used to build finite element models.

Chapter 5: Gives the method and result of calculating bolt stiffness.

Chapter 6: Gives the results from ABAQUS and resistance calculated based on Eurocode, and the comparison between them.

Chapter 7: Conclusion

2. Literature review

2.1 Previous studies of lattice tower and cold formed steel

2.1.1 Loads acting on lattice towers

Basically, there are two type of loads acting on a lattice tower:

1) Gravity loads
   - i) Weight of members
   - ii) Weight of platforms, railings, ladders, lifts
   - iii) Weight of instruments, appliances
   - iv) Weights of gussets and secondary bracings
   - v) Live loads
2) Lateral loads
   - i) Wind load
   - ii) Seismic loads
3) Erection loads

Maximum wind pressure is the major factor for the design of lattice tower. The flow of air over the members cause them to oscillate along or across the wind steam or cause them in torsional flutter, depending on the cross-sectional shape and natural frequency of the members. Stress created by these repeated deflections are the main reason of failure fatigue.

The gravity loads are almost fixed. Earthquake forces may be considered in the design of towers in regions where earthquakes happen frequently [12]. In some regions are experienced snow frequently, it is assumed that all members of a lattice tower are covered with a certain ice thickness, which considered as ice loading [13].

2.1.2 Structural components

Lattice towers can be built with different number of struts [14]. Figure 2.1 shows different variants of lattice towers of onshore wind turbines.
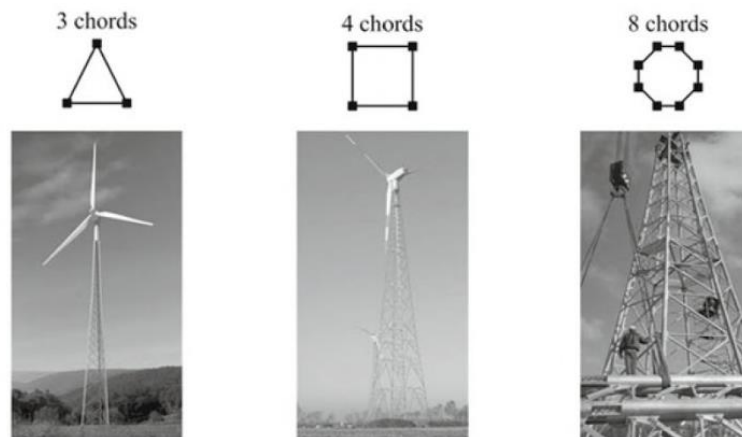
Figure 2.1 Lattice tower variants

The chords transfer the loads from top to the bottom. The most commonly used one is lattice tower with 4 chords. The framework is realised by diagonal and horizontal bracings. The load bearing behaviour of the lattice tower is dominated by the chosen type of bracing. Figure 2.2 shows the structural components of lattice tower.
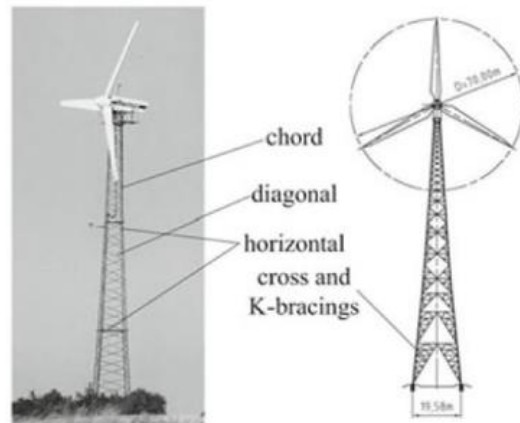
Figure 2.2: Structural components

2.1.3 Load bearing behaviour

The following assessments have to be done for lattice towers:

1) Stress design
2) Bar buckling
3) Design of bolted connections
4) Fatigue

As shown in Figure 2.3, the load of the trestle is mainly carried by the inclination of the chords. Diagonal members are unnecessary. The vertical loads are transferred to the foundation.

Parallel chords transfer the horizontal loads, especially wind loads, by compression or tension forces from the top of the tower to foundation.

Trestle chord   Parallel chord
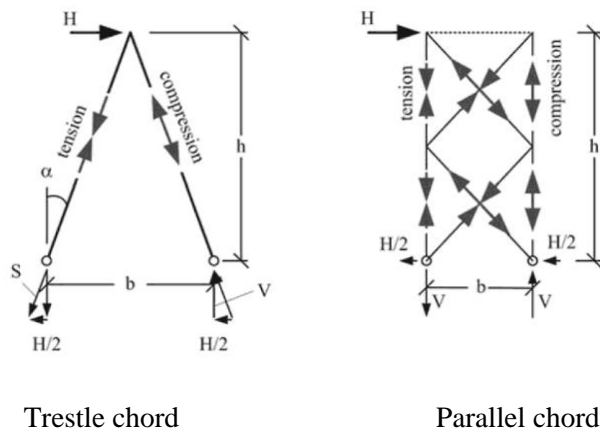
Figure 2.3 Load bearing behaviour

It is important to distinguish members in tension and in compression. For members in compression, lateral torsional buckling may become decisive. For members in tension the load bearing capacity of the bolted joint has to be taken care of. Fatigue has to be assessed in both compression and tension members.

2.1.4 Cross sections

The selection of cross section of the members of structure depends on bending moments. Bending moments increase from the top to foundation. The diameter of tower sections near rotor blades are limited due to necessary clearance. Torsional moments, which are caused by inclined flow on rotor

blades, are along the tower height. Lattice towers have smaller torsional stiffness comparing to tubular towers.

Generally, angle sections are used for members. Figure 2.4 shows different types of angle sections
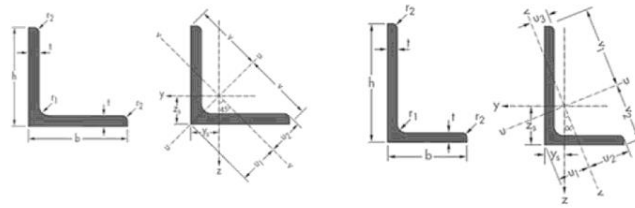
Equal and unequal angle sections
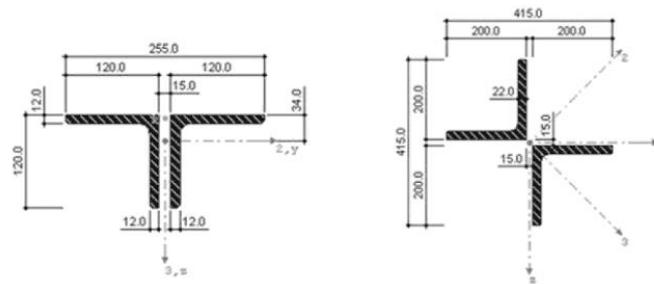
Double angle sections

Figure 2.4 Angle sections

2.1.5 Bolt connections for cold formed steel

Bolted connection is a common fastener in steel structure which can be applied to both hot-rolled and cold-formed steel [15]. The structural behaviour and application of bolted connections for cold formed steel are different from hot rolled steel since the connected sheets are thin. The cold formed connection uses bearing type connection only while hot rolled steel allows both slip critical and bearing types of connections [16]. Figure 2.5 shows the typical failure modes of cold formed steel bolted connections.

Type I Shear Failure of Sheet

Type II Bearing Failure of Sheet

Type III Rupture in Net Section

Type IV Shear Failure of Bolt
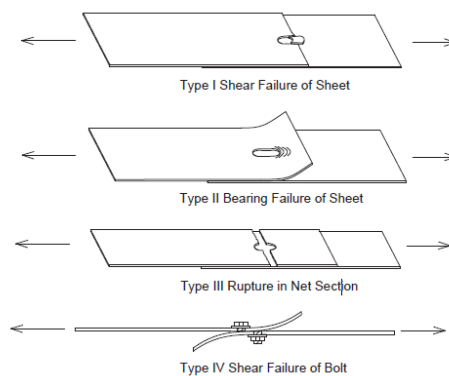
Figure 2.5: Failure mode of bolted connection

Generally, bolted connections are sheet-to-sheet connections (Figure 2.6). The connected sheets of sheet-to-sheet connections are restrained on both sides by the bolt head and nut with or without washers. However, in many cases of cold formed steel, the bolted connections have gaps between the plates (or lips) in some sections. In 2013, Yu developed a modified bearing strength method for cold formed steel bolted connection with a gap based on AISI S100 and experimental tests.
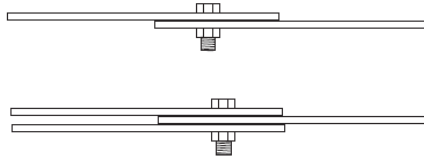
Figure 2.6: Sheet-to-sheet bolted connection

2.1.6 Rounded corner of cold formed steel

The production of cold formed steel requires cold bending of the sheet, which causes the round corners in the cross sections [19]. Regarding to the influences of rounded corner, AISI-S100-07 assumes that all corners remain fully effective regardless of their size or slenderness; Eurocode 1993-1-6 suggests to use nominal cross sectional date in calculation.

2.1.7 Packing plates at joints

Packing plate can increase the load carrying capacity of the bolted section subjected to axial force. According to V.M. Vaghe's experimental test in 2013, bearing failure can be avoided with the use of thicker packing plates [17]. The advantages of packing plates are shown as follows:

- Increasing the thickness of packing plates at the joints increases the strength of the joint.
- Larger packing plate increase the stiffness width and stiffness to against the horizontal force which might cause the deformation of the section.

Generally, packing plate is added between two lips of cold formed steel section. In some cases, more than one packing plate are added between lips and above and below lips in order to increase the stiffness (Figure 2.7).
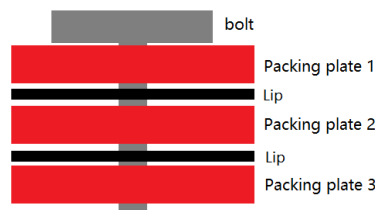
Figure 2.7 Joints with more than one packing plates

2.2 Calculation of resistance based on Eurocode
2.2.3 EN 1993-1-3 Cold formed & EN 1995-1-5 Plated structure
2.2.3.1 Material properties of cold formed sections and sheeting

According to EN 1993-1-3 section 3.2.2, the yield strength is influenced by either cold formed or heat treatment, so it is specified using the symbol f_y the average yield strength f_{ya}. Cold forming increases the yield strength, which may be taken into account as follows:

- in axially loaded members in which the effective cross-sectional area A_{eff} equals the gross are A_g;
- in determining A_{eff} the yield strength f_y should be as taken as f_{yb}.

The increased average yield strength f_{ya} may be determined by calculation using:

$$f_{ya} = f_{yb} + (f_u - f_{yb}) \frac{knt^2}{A_g}$$

9

But

$$f_{ya} \leq \frac{(f_u + f_{yb})}{2}$$

(3.1)

where

A_g is the gross cross-section area;

k is a numerical coefficient that depends on the type of forming as follows:

- k = 7 for rolling forming;
- k = 5 for other methods of forming;

n is the number of $90°$ bends in the cross-section with an internal radius $r \leq 5t$ (fractions of $90°$ bends should be counted as fractions of n);

t is the design thickness of the steel material before cold-forming.

Yield strength may be reduced lower than the basic yield strength as f_{yb} due to heat treatment. In order cases, the basic yield strength f_{yb} should be used.

The average yield strength f_{ya} may be utilised in determining:

- the cross-section resistance of an axially loaded tension member;
- the cross-section resistance and the buckling resistance of an axially loaded compression member with a fully effective cross-section;
- the moment resistance of a cross-section with fully effective flanges.

2.2.3.2 Influence of rounded corner

According to EN 1993-1-3, section 5.1, in cross section with rounded corners, the calculation of section properties should be based on the nominal geometry of the cross section. the notional flat widths b_p of the plane elements should be measured from the midpoints of the adjacent corner elements as indicated in Figure 2.6.
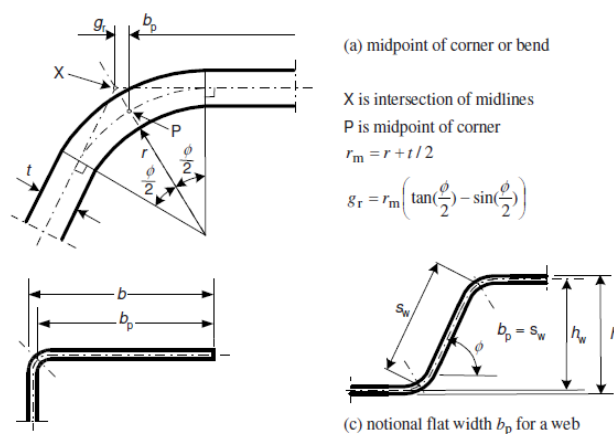
Figure 2.6: Notional widths of plane cross section parts b_p allowing for corner radii

The influence of rounder corners on cross section resistance may be neglected if the internal radius $r \leq 5t$ and $r \leq 0.10b_p$ and the cross section may be assumed to consist of plane elements with sharp corners.

For cross-section stiffness properties, the influence of rounded corners should always be taken into account.

The influence of rounded corners on section properties may be taken into account by reducing the properties calculated as follows:

$$A_g \approx A_{g,sh}(1 - \delta)$$

$$I_g \approx I_{g,sh}(1 - 2\delta)$$

$$I_w \approx I_{g,sh}(1 - 2\delta)$$

with:

$$\delta = 0.43 \frac{\sum_{j=1}^{n} r_j \frac{\Phi_j}{90°}}{\sum_{i=1}^{m} b_{p,i}}$$

where:

A_g is the area of the gross cross-section;

$A_{g,sh}$ is the value of A_g for a cross-section with sharp corners;

$b_{p,i}$ is the notional flat width of plane element I for a cross-section with sharp corners;

I_g is the second moment of area of the gross cross-section;

$I_{g,sh}$ is the value of I_g for a cross-section with sharp corners;

I_w is the warping constant of the gross cross-section;

$I_{w,sh}$ is the value of I_w for a cross-section with sharp corners;

Φ is the angle between two plane elements;

m is the number of plane elements;

n is the number of curved elements;
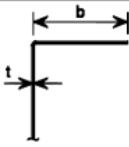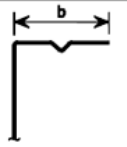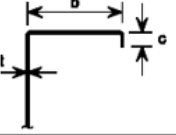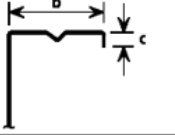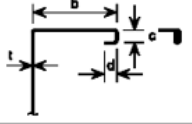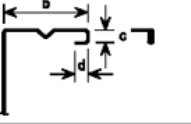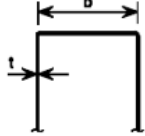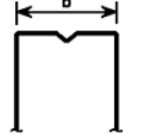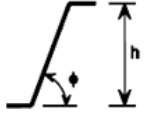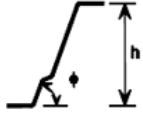
r_j is the internal radius of curved element j.

To be noticed, the reductions may also be applied in calculating the effective section properties A_{eff}, $I_{y,eff}$, $I_{z,eff}$ and $I_{w,eff}$. Where the internal radius $r > 0.04tE/f_y$ then the resistance of the cross-section should be determined by tests.

2.2.3.3 Geometrical proportions

According to EN 1993-1-3, section 5.2, the design based on EN 1993-1-3 should not be applied to cross sections out of the range of width-to-thickness ratios b/t, h/t, c/t and d/t which is shown in Table 2.1.

Table 2.1 Maximum width-to-thickness ratios

Element of cross-section		Maximum value
		$b/t \leq 50$
		$b/t \leq 60$ $c/t \leq 50$
		$b/t \leq 90$ $c/t \leq 60$ $d/t \leq 50$
		$b/t \leq 500$
		$45° \leq \phi \leq 90°$ $h/t \leq 500 \sin\phi$

In order to avoid primary buckling of the stiffener itself, ths sizes of stiffeners should be within the following ranges:

$0.2 \leq c/b \leq 0.6$

$0.1 \leq d/b \leq 0.1$

in which the dimensions b,c and d are as indicated in table 5.1. If $c/b < 0.2$ or $d/b < 0.1$ the lip should be ignored (c=0 or d=0).

2.2.3.4 Calculation of local and distortional buckling

According to EN 1993-1-3 section 5.1, the effects of local and distortional buckling should be taken into consideration in determining the resistance and stiffness of cold-formed members and sheeting. Local buckling effects may be calculated based on EN 1993-1-5. Distortional buckling is considered based on EN 1993-1-3.

2.2.3.4.1   Local buckling and reduction factor (EN1993-1-5)

The effective area of the compression zone of a plate with the gross cross section area A_c should be obtained from:

$$A_{c,eff} = \rho A_c$$

The reduction factor ρ for plate buckling is calculated as follows:

For internal compression elements:

$\rho = 1$ for $\bar{\lambda}_p \leq 0.673$
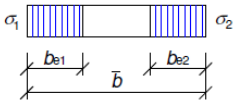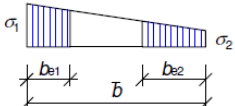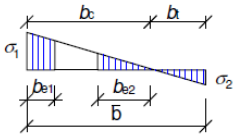
$\rho = \dfrac{\bar{\lambda}_p - 0.055(3 + \psi)}{\bar{\lambda}_p^{\ 2}} \leq 1$ for $\bar{\lambda}_p > 0.673$, where $(3 + \psi) \geq 0$

where

$$\bar{\lambda}_p = \sqrt{\frac{f_y}{\sigma_{cr}}} = \frac{\bar{b}/t}{28.4\varepsilon\sqrt{k_\sigma}}$$

Ψ is the stress ratio which is shown in Table 2.2.

Table 2.2: Internal compression elements

Stress distribution (compression positive)				Effective[p] width b_{eff}		
				$\psi = 1$: $b_{eff} = \rho\ \bar{b}$ $b_{e1} = 0.5\ b_{eff}$ $b_{e2} = 0.5\ b_{eff}$		
				$1 > \psi \geq 0$: $b_{eff} = \rho\ \bar{b}$ $b_{e1} = \dfrac{2}{5-\psi} b_{eff}$ $b_{e2} = b_{eff} - b_{e1}$		
				$\psi < 0$: $b_{eff} = \rho\ b_c = \rho\ \bar{b} / (1-\psi)$ $b_{e1} = 0.4\ b_{eff}$ $b_{e2} = 0.6\ b_{eff}$		
$\psi = \sigma_2/\sigma_1$	1	$1 > \psi > 0$	0	$0 > \psi > -1$	-1	[AC1]$-1 > \psi \geq -3$[AC1]
Buckling factor k_σ	4,0	8,2 / (1,05 + ψ)	7,81	7,81 - 6,29ψ + 9,78ψ^2	23,9	5,98 (1 - ψ)^2

$\bar{b}$ is the appropriate width.

k_σ is the buckling factor corresponding to the stress ratio ψ and boundary conditions. For long plate k_σ is given in Table 2.2.

t is the thickness.

σ_{cr} is the elastic critical plate buckling stress given as:

$$\sigma_{cr} = k_\sigma 189800(\frac{t}{\bar{b}})^2$$

2.2.3.4.2   Plane elements with edge stiffener
Distortional buckling, as well as called stiffener buckling or local-torsional buckling, is characterized by rotation of the flange in members with edge stiffeners. In members with intermediately stiffeners, distortional buckling is characterized by displacement of the intermediate stiffener [20].

According to EN 1993-1-3 section 5.5.3.3, the reduction factor χ_d for the distortional buckling resistance should be calculated from the relative slenderness $\overline{\lambda_d}$ as shown:

$\chi_d = 1$ if $\overline{\lambda_d} \leq 0.65$

$\chi_d = 1.47 - 0.723\ \overline{\lambda_d}$ if $0.65 \leq \overline{\lambda_d} \leq 1.38$

$\chi_d = 0.66/\overline{\lambda_d}$ if $\overline{\lambda_d} \geq 1.38$

where $\overline{\lambda_d} = \sqrt{f_{yb}/\sigma_{cr,s}}$

$\sigma_{cr,s}$ is the elastic critical stress. Critical stress for intermediate stiffeners is given as:

Resistance of Polygonal Cross Section of Lattice Wind Tower

$$\sigma_{cr,s} = \frac{2\sqrt{KEI_s}}{A_s}$$

where K is the spring stiffness per unit length which is given as follows:

The spring stiffness for edge stiffeners of lipped sections is given as:

$$K_1 = \frac{Et^3}{4(1-v^2)} * \frac{1}{b_1{}^2 h_w + b_1{}^3 + 0.5 b_1 b_2 h_w k_f}$$

where b_1 is the distance from the web-to-flange junction to the gravity centre of the effective area of the edge stiffener (including effective part b_{e2} of the flange) of flange 1, see Figure 2.7;

b_2 is the distance from the web-to-flange junction to the gravity centre of the effective area of the edge stiffener (including effective part of the flange) of flange 2;

h_w is the web depth;

$k_f = 1$ for a symmetric section in compression.
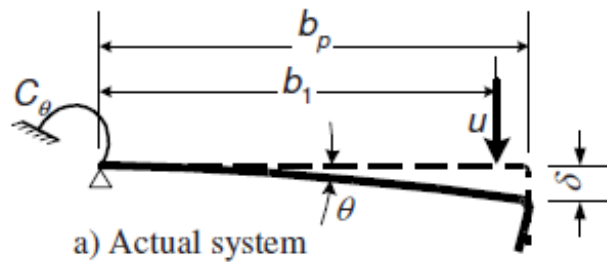
Figure 2.7: Determination of spring stiffness
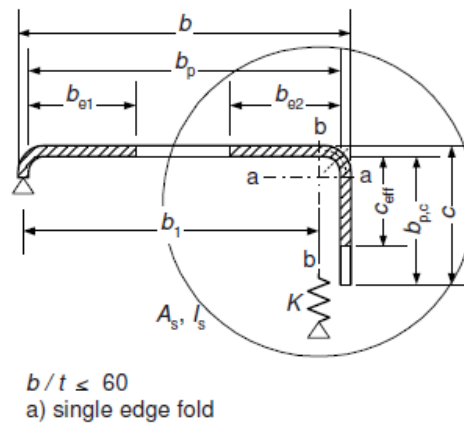
Figure 2.8: Edge stiffeners

The effective area of web is calculated based on EN 1995-1-5. The reduction factor of edge stiffener is also calculated based on EN 1995-1-5, using buckling factor k_σ given by following:

- If $b_{p,c}/b_p \leq 0.35$:

$$k_\sigma = 0.5$$

- If $0.35 < b_{p,c}/b_p \leq 0.6$:

14

Resistance of Polygonal Cross Section of Lattice Wind Tower

$$k_\sigma = 0.5 + 0.83\sqrt{(b_{p,c}/b_p - 0.35)^2}$$

2.2.3.5 Axial compressive resistance of cross section (ULS)

According to EN 1993-1-3 section 6, the design resistance of cross-section with a axial load acting at the centroid of its effective cross section for compression $N_{c,Rd}$ should be determined from:

- if the effective area A_{eff} is less than the gross area A_g (section with reduction due to local and/or distortional buckling)

$$N_{c,Rd} = A_{eff}f_{yb}/\Upsilon_{M0}$$

- if the effective area A_{eff} is equal to the gross area A_g (section with no reduction due to local or distortional buckling)

$$N_{c,Rd} = A_g(f_{yb} + (f_{ya} - f_{yb})4\left(1 - \frac{\overline{\lambda_e}}{\overline{\lambda_{e0}}}\right))/\Upsilon_{M0}$$

but not more than $A_g f_{ya}/\Upsilon_{M0}$

where

A_{eff} is the effective area of the cross-section, assuming a uniform compressive stress equal to f_{yb};

f_{ya} is the average yield strength;

f_{yb} is the basic yield strength;

For plane elements $\overline{\lambda_e} = \overline{\lambda_p}$ and $\overline{\lambda_{e0}} = 0.673$;

For stiffened elements $\overline{\lambda_e} = \overline{\lambda_d}$ and $\overline{\lambda_{e0}} = 0.65$.

2.2.3.6 Buckling resistance (ULS)

According to EN 1993-1-3, in members with cross sections which are sensitive to cross sectional distortion, the lateral buckling of compression flanges and lateral bending of flanges should be taken into consideration. The effects of local and distortional buckling should be checked.

According to EN 1993-1-1 section 6.3, a compression member should be verified against buckling as follows:

$$N_{Ed}/N_{b,Rd} \leq 1$$

where

N_{Ed} is the design value of the compression force;

$N_{b,Rd}$ is the design buckling resistance of the compression member.

The design buckling resistance of a compression member should be taken as:

$N_{b,Rd} = \dfrac{\chi A f_y}{\Upsilon_{M1}}$ for class 1,2 and 3 cross sections

$N_{b,Rd} = \dfrac{\chi A_{eff} f_y}{\Upsilon_{M1}}$ for class 4 cross sections

where χ is the reduction factor for the relevant buckling mode.

Resistance of Polygonal Cross Section of Lattice Wind Tower

$$\chi = \frac{1}{\Phi + \sqrt{\Phi^2 - \bar{\lambda}^2}} \text{ but } \chi \leq 1$$

where $\Phi = 0.5[1 + \alpha(\bar{\lambda}^2 - 0.2) + \bar{\lambda}^2]$

α is the imperfection factor, shown in Table 2.4:

Table 2.4: Imperfection factors for buckling curves

Buckling curve	a_0	a	b	c	d
Imperfection factor α	0,13	0,21	0,34	0,49	0,76

Figure 2.9 gives the buckling curve.
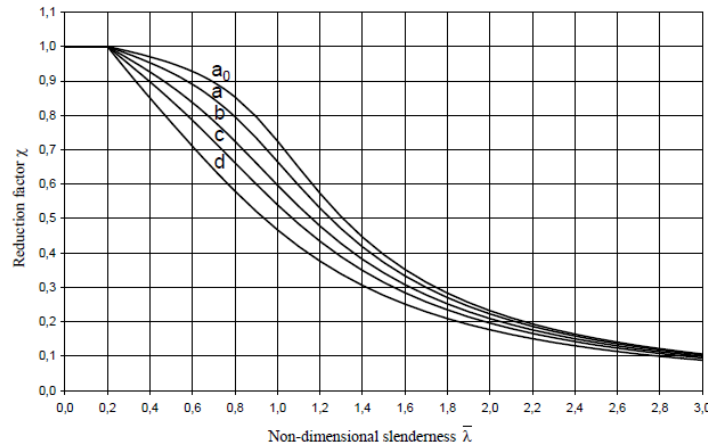
Figure 2.9: Buckling curve

(1) Flexural buckling

For slenderness for flexural buckling, the non-dimensional slenderness $\bar{\lambda}$ is given by:

$$\bar{\lambda} = \sqrt{\frac{Af_y}{N_{cr}}} = \frac{L_{cr}}{i} \frac{1}{\lambda_1} \qquad \text{for class 1, 2 and 3 cross section}$$

$$\bar{\lambda} = \sqrt{\frac{A_{eff}f_y}{N_{cr}}} = \frac{L_{cr}}{i} \frac{\sqrt{\frac{A_{eff}}{A}}}{\lambda_1} \qquad \text{for class 4 cross section}$$

where i is the radius of gyration about the relevant axis, calculated as follows:

$$i = \sqrt{\frac{I}{A}}$$

L_{cr} is the buckling length in the buckling plane

N_{cr} is the elastic critical force for the relevant buckling mode based on the gross cross sectional properties.
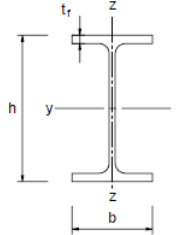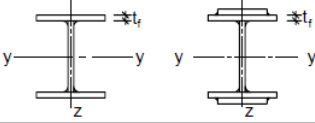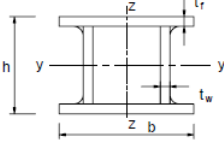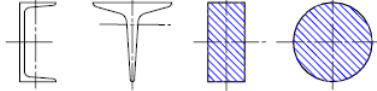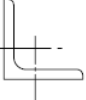
$N_{cr} = A\sigma_{cr}$

$$\sigma_{cr} = \frac{\pi^2 E}{\lambda_1^{\,2}}$$

$$\lambda_1 = \pi \sqrt{\frac{E}{f_y}} = 93.9\varepsilon$$

For flexural buckling the appropriate buckling curve should be determined by Table 2.3.

Table 2.3: Selection of buckling curve for a cross section

	Cross section		Limits	Buckling about axis	Buckling curve S 235 S 275 S 355 S 420	S 460
Rolled sections		$h/b > 1,2$	$t_f \leq 40$ mm	$y-y$ $z-z$	a b	a_0 a_0
			40 mm $< t_f \leq 100$	$y-y$ $z-z$	b c	a a
		$h/b \leq 1,2$	$t_f \leq 100$ mm	$y-y$ $z-z$	b c	a a
			$t_f > 100$ mm	$y-y$ $z-z$	d d	c c
Welded I-sections			$t_f \leq 40$ mm	$y-y$ $z-z$	b c	b c
			$t_f > 40$ mm	$y-y$ $z-z$	c d	c d
Hollow sections			hot finished	any	a	a_0
			cold formed	any	c	c
Welded box sections			generally (except as below)	any	b	b
			thick welds: $a > 0,5t_f$ $b/t_f < 30$ $h/t_w < 30$	any	c	c
U-, T- and solid sections				any	c	c
L-sections				any	b	b

2.2.4 EN 1993-1-6 Shell structure
2.2.4.1 Types of finite element analysis

Generally, there are two types of buckling analysis:

- Linear buckling analysis

Linear buckling analysis is used to determine the critical stress and buckling shape. No imperfections are allowed to be included. It provides the eigenvalue solution of the elastic system, which should be considered using geometrical stiffness and certain load conditions.

- Non-linear buckling analysis

Resistance of Polygonal Cross Section of Lattice Wind Tower

The static analysis of non-leaner buckling analysis should use the geometrical nonlinearity theory. Applied load increases incrementally until a small change in load level causes a large change in displacement. Initial imperfections can be included.

EN1993-1-6 provides the following types of analysis when linear elastic analysis for buckling is unreasonable:

- MNA/LBA: Linear elastic bifurcation analysis in combination with materially nonlinear analysis
- GMNIA: Geometrically and materially nonlinear analysis with imperfections included
(1) Linear elastic bifurcation analysis (LBA)

LBA is based on the linear elastic material law and the linear small deflection theory with the perfect geometry of the thin-walled shell structure. Small deflection theory gives that the assumed geometry remains as the undeformed structure. LBA analysis obtains the lowest eigen value where shell structure may buckle. Change of geometry, change in the direction of action of the loads and material degradation are assumed not to be considered. Imperfections in LBA are not taken into account.

LBA can be used for:

- Determination of elastic critical buckling resistance.
- Definition of equivalent geometrical imperfections for non-linear buckling analysis (GMNIA)

Requirements of LBA:

- Proper geometry and boundary conditions
- Design loads

Results of LBA:

- Deformed shapes of the model
- Corresponding eigen values (critical load amplification factors) $r_{R_{cr}}$

Critical load or stress for certain buckling shape is:

$$F_{cr} = r_{R_{cr}} F_{applied}$$

$$\rho_{cr} = r_{R_{cr}} \rho_{applied}$$

(2) Materially nonlinear analysis (MNA)

MNA analysis is based on shell bending theory and small deflection theory, applied to a perfect structure. It follows the nonlinear elasto-plastic material law. MNA analysis gives the plastic limit load. It is used to determine the load amplification factor $r_{R_{pl}}$ that is needed to achieve the plastic limit state. The design value of the loads F_{Ed} should be used as input. This analysis provides the plastic reference resistance ratio $r_{R_{pl}}$.

(3) Geometrically and materially nonlinear analysis with imperfection included (GMNIA)

A geometrically and materially nonlinear analysis of the imperfect shell is the numerical analysis which is closest to reality. GMNIA will become a more significant analysis method in the future because it can replace some experiments so that time and cost can be reduced [23].

According to EN 1993-1-6, a GMNIA analysis is based on the principles of shell bending theory applied to the imperfect structure, including nonlinear large deflection theory for the displacements that accounts full for any change in geometry due to the actions on the shell and a nonlinear elasto-

plastic material law. A GMNIA analysis is used when compression or shear stress are dominant in the shell structure. It provides the elasto-plastic buckling loads for the real imperfect structure.

Requirements of GMNIA:

- LBA analysis is required to obtain eigen mode of shape of imperfection.
- Proper boundary conditions and design value of loads should be used.
- Imperfections are required to apply to the model using eigen mode of shapes got from LBA and amplitudes calculated according to EN 1993-1-6.
- The ultimate load amplification factor $r_{R,GMNIA}$ should be obtained by applying the design value of loads.

Results of GMNIA:

- The ultimate load amplification factor $r_{R,GMNIA}$

2.2.4.2 Imperfections for GMNIA

The realistic reflection of the influence of imperfections is the most difficult problem while using GMNIA analysis. Equivalent geometric imperfection includes the original effects of study subject itself. EN 1993-1-6 suggests that linear buckling analysis (LBA) should be done for finding the eigenmode, which is taken as the most unfavourable effect on buckling behaviour.

Imperfections should be introduced in form of equivalent geometric imperfections covering following effects:

- Geometric imperfections
- Irregularities near welds
- Material imperfections

The pattern of equivalent geometric imperfection which has the most unfavourable effect should be chosen.

2.2.4.3 Shell boundary conditions

The boundary conditions should be chosen properly to ensure the model is closed to real structure. Following constraints should be paid attention:

- Constraint of displacements normal to shell wall (deflections)
- Constraint of the displacements in the plane of the shell wall (Meridional and circumferential plane)

In shell buckling (eigenvalue) calculations, the boundary condition should refer to the incremental displacements during the buckling process, not to total displacements caused by applied load.

2.2.4.4 Materials and geometry

Material properties should be obtained from the relevant standard. To be noticed, the Young's modulus E should be replaced by a reduced value when materials are nonlinear. The secant modulus at the 0.2% proof stress should be used when assessing the elastic critical load or elastic critical stress. Also, the 0.2% proof stress should be used to represent the yield stress f_y in a global analysis using material nonlinearity.

According to EN 1993-1-5 Annex C, the true stress-strain curve modified from the test results as follows:

$$\sigma_{true} = \sigma(1 + \varepsilon)$$

$$\varepsilon_{true} = \ln(1 + \varepsilon)$$

1   *true stress-strain curve*
2   *stress-strain curve from tests*
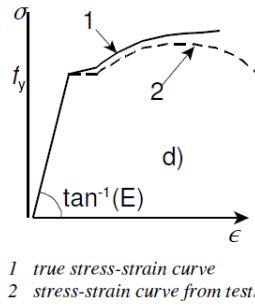
Figure 2.11: Modelling of material behaviour

2.2.4.5 Ultimate limit states in steel shells

2.2.4.6 Plastic limit state (LS1)

The highest membrane stress $\sigma_{eq,Ed}$ determined under the design values of actions F_{Ed} should be limited to the stress resistance given as follows:

$$\sigma_{eq,Ed} \leq f_{eq,Rd}$$

$$f_{eq,Rd} = f_{yd} = f_{yk}/\Upsilon_{M0}$$

where

$$\Upsilon_{M0} = 1$$

The value of the characteristic yield strength f_{yk} should be taken as the 0.2% proof stress where the material is nonlinear.

2.2.4.7 Buckling limit state (LS3)

The buckling reduction factor should be determined as a function of the relative slenderness of the shell $\bar{\lambda}$ from:

$$\chi = 1 \qquad\qquad \text{when } \bar{\lambda} \leq \overline{\lambda_0}$$

$$\chi = 1 - \beta\left(\frac{\bar{\lambda} - \overline{\lambda_0}}{\overline{\lambda_p} - \overline{\lambda_0}}\right)^{\eta} \qquad \text{when } \overline{\lambda_0} < \bar{\lambda} < \overline{\lambda_p}$$

$$\chi = \frac{\alpha}{\bar{\lambda}^2} \qquad\qquad \text{when } \overline{\lambda_p} \leq \bar{\lambda}$$

α is the elastic imperfection reduction factor

β is the plastic range factor

η is the interaction exponent

$\overline{\lambda_0}$ is the squash limit relative slenderness

The value of plastic limit relative slenderness $\overline{\lambda_p}$ should be determined from:

$$\overline{\lambda_p} = \sqrt{\frac{\alpha}{1 - \beta}}$$

The relative shell slenderness parameters for different stress components:

-   Meridional (axial) compression

Resistance of Polygonal Cross Section of Lattice Wind Tower

$$\bar{\lambda}_x = \sqrt{\frac{f_{yk}}{\sigma_{x,Rcr}}}$$

The elastic critical meridional buckling stress is given as follows:

$$\sigma_{x,Rcr} = 0.605 E C_x \frac{t}{r}$$

The length of the shell segment is characterised in terms of the dimensionless length parameter ω:

$$\omega = \frac{l}{r}\sqrt{r/t} = \frac{l}{\sqrt{rt}}$$

- For short cylinders,

$$\omega \leq 1.7$$

The factor C_x may be taken as

$$C_x = 1.36 - \frac{1.83}{\omega} + \frac{2.07}{\omega^2}$$

- For medium-length cylinders,

$$1.7 \leq \omega \leq 0.5\frac{r}{t}$$

The factor C_x may be taken as

$$C_x = 1$$

- For long cylinders,

$$\omega > 0.5\frac{r}{t}$$

The factor C_x may be taken as

$$C_x = C_{x,N}$$

in which $C_{x,N}$ is the great of

$$C_{x,N} = 1 + \frac{0.2}{C_{xb}}[1 - 2\omega\frac{t}{r}]$$

and

$$C_{x,N} = 0.6$$

where C_{xb} is a parameter depending on the boundary conditions as shown in Table 2.4.

Table 2.4: Parameter C_{xb} for the effect of boundary conditions on the elastic critical meridional buckling stress in long cylinders

Case	Cylinder end	Boundary condition	C_{xb}
1	end 1	BC 1	6
	end 2	BC 1	
2	end 1	BC 1	3
	end 2	BC 2	
3	end 1	BC 2|	1
	end 2	BC 2	

21

The meridional elastic imperfection reduction factor α_x should be obtained from:

$$\alpha_x = \frac{0.62}{1 + 1.91(\frac{\Delta w_k}{t})^{1.44}}$$

where Δw_k is the characteristic imperfection amplitude:

$$\Delta w_k = \frac{1}{Q}\sqrt{\frac{r}{t}}\,t$$

where Q is the meridional compression fabrication quality parameter which is shown in Table 2.5.

Table 2.5: Values of fabrication quality parameter Q

Fabrication tolerance quality class	Description	Q
Class A	Excellent	40
Class B	High	25
Class C	Normal	16

The meridional squash limit slenderness $\overline{\lambda_{x0}}$, the plastic range factor β, and the interaction exponent η should be taken as:

$$\overline{\lambda_{x0}} = 0.2$$

$$\beta = 0.6$$

$$\eta = 1$$

2.3 N-M interaction diagram

According to EN 1993-1-1, for member under axial force and moment, the axial force has effects on plastic moment resistance. So, beam-columns under combined compression and bending moment (Figure 2.12) fail before reaching the squash load P_d or the plastic moment M_p [18], where $P_d = A_g f_y$ and $M_p = Z_p f_y$ (Z_p is the plastic section modulus of the cross section).
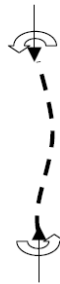
Figure 2.12: Member under N+M

Figure 2.13 shows the stress distributions of cross section under different types of loads.
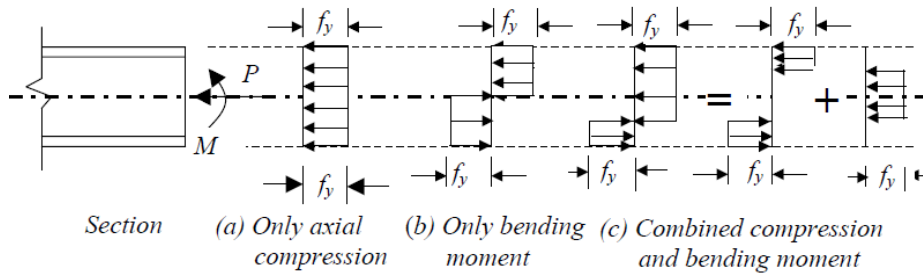
Figure 2.13: Stress distribution of member

When axial compression is small (smaller than 25% of plastic compressive resistance), the area closer to the neutral axis contributes very little to the resistance, so the reduction of moment capacity is negligible. As shown in Figure 2.14, when P/P_d is small, M/M_p tends to 1, moment resistance is not reduced. The typical failure envelope diagram (2D) of a beam-column that subjected to axial compressive load P and bending moment M (single axial) is shown in Figure 2.14
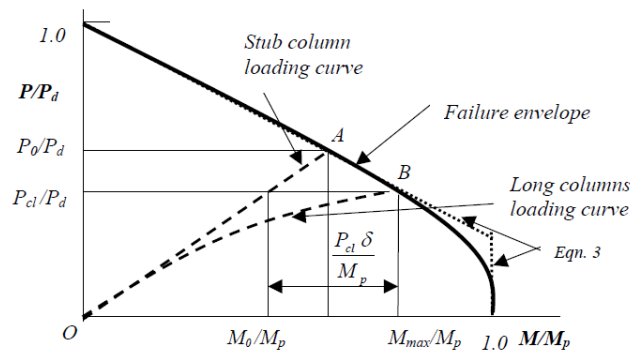
Figure 2.14 Beam-Column Failure Envelop

Line OA and OB in Figure 2.14 represent the loading curves of different columns. The slope of the loading curve is the eccentricity which is given by P/M. When the loading curve reaches the failure envelope, the capacity of the member is reached. The values of P and M (N_1 and $M_{y,1}$ in Figure 2.15) corresponding to point A or B are the compressive and moment capacity under the given compression and moment.
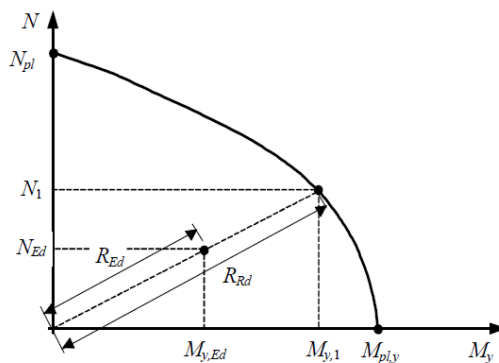
Figure 2.15: N+M interaction diagram

23

Resistance of Polygonal Cross Section of Lattice Wind Tower

EN 1993-1-1 gives the basic interaction formula as [23]:

$$\frac{N_y}{\chi_y N_{pl}} + \frac{\beta M_y}{M_{pl,y}} \leq 1$$

where N_{pl} is the plastic compressive resistance of the member, M_{pl} is the plastic moment resistance of the member.

χ is the buckling reduction factor.

β is the moment distribution factor:

$\beta = 1.1$ for uniform distribution.

$\beta = 0.66$ for triangular distribution.

$\beta = 0.66\_0.44\psi$ for bitriangular distribution, where $\psi = M_1/M_2$.

3. Materials and profiles

3.1 Materials

According to EN 1993-1-3 section 3.1, all steels used for cold formed members and profiled sheets should be suitable for cold forming and welding, if needed [24]. Steel S355 is used in this thesis. Table 3.1 shows the nominal values of basic yield strength f_{yb} and ultimate tensile strength f_u.

Table 3.1 Basic yield strength and ultimate tensile strength of S355

Grade	$f_{yb}N/mm^2$	f_uN/mm^2
S355	355	510

3.2 Profiles

In this thesis, a polygonal column section of lattice tower is taken as the study subject. The section consists of three sectors and three gusset plates which are bolted. Sections with different parameters are modelled in ABAQUS.

Figure 3.1: Polygonal section

Figure 3.2: Side view of the section
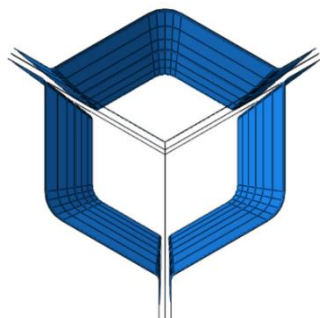
Figure 3.3: Front view of the section   **Figure 3.4: Detailed view of the section**
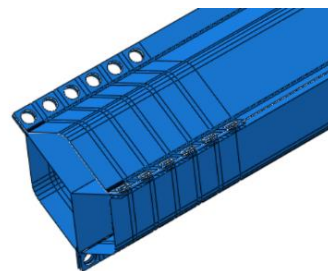
3.2.1   Parameters

Five parameters are taken into account for models.

1) Number of corners (n)

In analysis of buckling and resistance, cross sections with 6 corners (Figure 3.5) are taken into account. The hexagonal cross section consists of three sectors, each sector has lips at both end and the lips are bolted together.

Figure 3.5: Front view of hexagonal cross section

Cross sections with corners of 6, 9 and 12 are taken into account for calculating bolt stiffness.

2) Diameter of the section (d)

Diameters of the cross section are taken as 500mm, 700mm and 900mm.

3) Plate thickness (t)

Cross sections in class 3 and class 4 are chosen in order to save the materials. According to EN 1993-1-1, Table 5.2, slenderness is supposed to be larger than $70\varepsilon^2$. The range of slenderness is shown as follows:

$$70\varepsilon^2 \leq d/t \leq 110\varepsilon^2$$

which gives

$$70 \leq d/\varepsilon^2 t \leq 110$$

The variation of thickness depends on diameter and slenderness.

$$d/70\varepsilon^2 \leq t \leq d/110\varepsilon^2$$

The values of $d/\varepsilon^2 t$ are taken as 90 and 110. Table 3.1 shows the thicknesses under slenderness of $90\varepsilon^2$ and $110\varepsilon^2$.

Table 3.1: Thickness of the section

Diameter (mm)	$d/\varepsilon^2 t$	d/t	t (mm)	Rounded t (mm)
500	90	59.049	8.47	8.00
500	110	72.171	6.93	7.00
700	90	59.049	11.85	12.00
700	110	72.171	9.70	10.00
900	90	59.049	15.24	15.00
900	110	72.171	12.47	12.00

4) Length (l)

The appropriate non-dimensional slenderness $\bar{\lambda}$ is given as:

$$\bar{\lambda} = \sqrt{Af_y/N_{cr}}$$

where

$$N_{cr} = \frac{\pi^2 EI_y}{L_{cr}^2}$$

Combining the equations above,

$$L_{cr} = \bar{\lambda}\pi\sqrt{\frac{EI_y}{Af_y}}$$

Since the section is pinned at both end, the buckling length of it equals to the length.

The length of the section is given by

$$L = \bar{\lambda}\pi\sqrt{\frac{EI_y}{Af_y}}$$

Taking $\bar{\lambda}$ as 0.6, 1 and 1.25. The length of the section is also related to the sectional date (e.g. area, thickness).

For example, take a profile with n = 6; d = 500mm; $d/\varepsilon^2 t = 90$,

$A = 1.4672e + 04mm^2$

$I_{yy} = 4.0977e + 08mm^2$

Lengths of the profile based on different slenderness are shown in Table 3.2.

Table 3.2 Lengths of the example profile

$\bar{\lambda}$	L (mm)	L (m)
0.6	7657.76	7.66
1	12762.93	12.76
1.25	15953.67	15.95

5) Bolt spacing (s)

Sectors are connected by the bolts on lips (Figure 3.6). In this thesis, M16 bolt is selected. Dimensions of M16 bolt are shown in Table 3.3.

Table 3.3: Dimensions of M16 bolt

Bolt	Diameter (mm)	Min. diameter of washer (mm)
M16	16	24.9

The diameter of the hole is based on the diameter of washer which is 30mm.
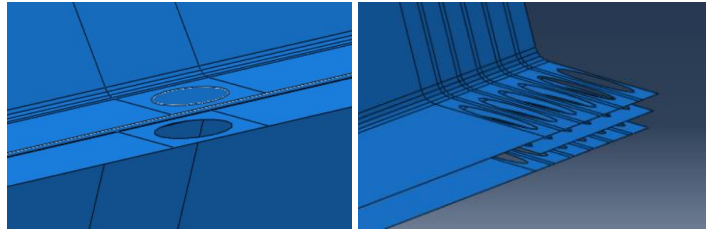
Figure 3.6: Holes for bolts on lips

The regions where the distortional buckling is dominant, are where the bolds matter. Bolts help to increase rotational stiffness so as to increase distortional buckling stress.
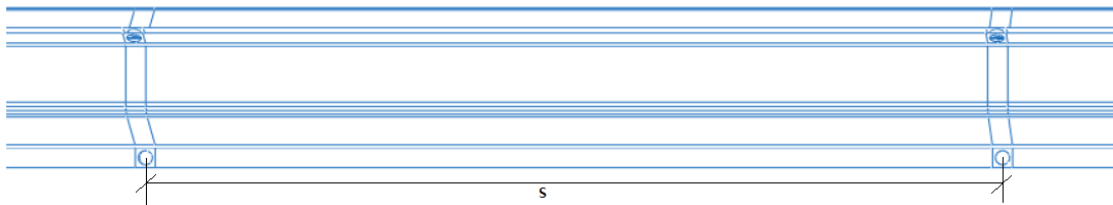
Figure 3.7: Spacing of bolts of column

Bolt spacing s (Figure 3.7) is dependent on distortional buckling. The density of the bolts should be equivalent to the spring stiffness. However, in this thesis, bolt spacing on the column is estimated based on bolt spacing ratio b, then equivalent stiffness is calculated based on the estimated bolt density. b is given as 3, 4 and 5.

$$b = s/d$$

where s is the bolt spacing and d is the diameter of the section.

modified the equation above, gives s = b*d.

Table 3.4 Spacing of the bolts of column

b	d (mm)	s (mm)	s (m)
3	500	1500	1.5
3	700	2100	2.1
3	900	2700	2.7
4	500	2000	2
4	700	2800	2.8
4	900	3600	3.6
5	500	2500	2.5
5	700	3500	3.5
5	900	4500	4.5

Number of bolts n_0 is calculated as follows:

$$n_0 = l/s$$

where l is the length of the section and s is bolt spacing. s_0, which is the remainder of l/s, is the remaining space.
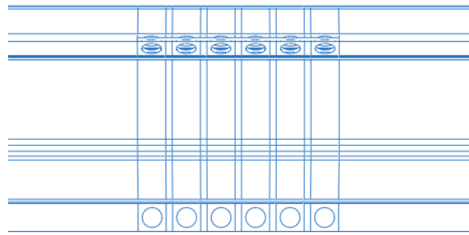
Figure 3.8: Spacing of bolts of joint

Bolt spacing at the joint (Figure 3.8) is taken as the length of the lip.

3.2.2   Sectors

A hexagonal cross section is made of three sectors. A sector (Figure 3.9) consists of two webs and two lips; the corners are rounded.
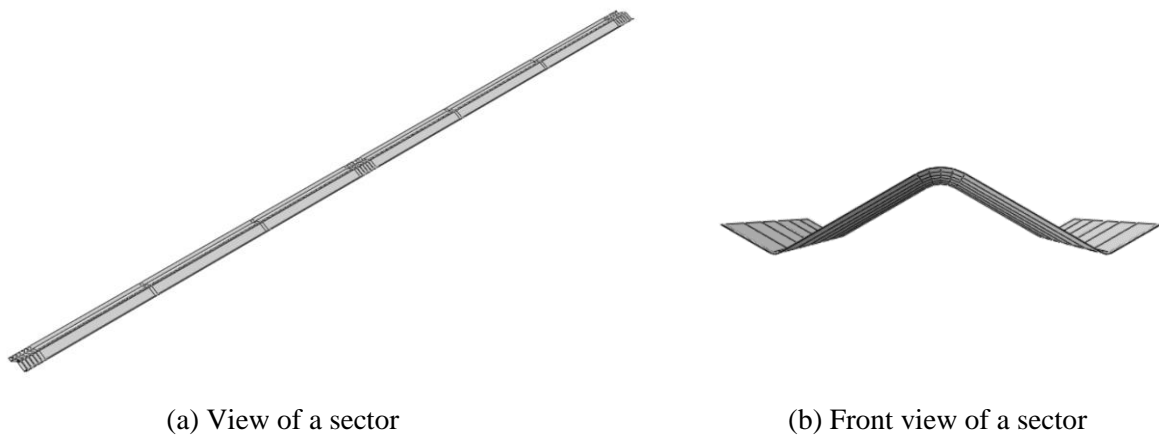
(a) View of a sector   (b) Front view of a sector

Figure 3.9: Sector

Calculation of the coordinates of the cross section of the sector is shown below:

Take cross section (Figure 3.10) of n=6, d=500mm, t=4mm as the example.

Resistance of Polygonal Cross Section of Lattice Wind Tower
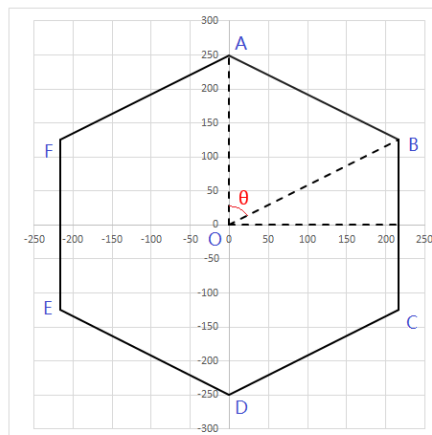
Figure 3.10: Hexagonal cross section with diameter of 500mm

R = 500/2 = 250mm   θ = 2π/6 = 60°
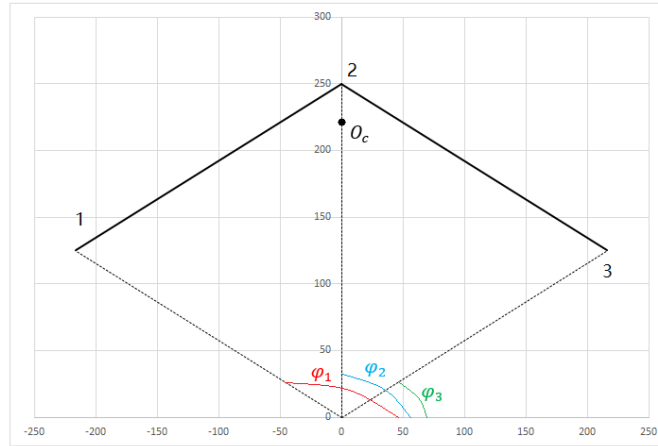
Figure 3.11: Coordinates of a sector

φ_1, φ_2 and φ_3 are the angles between x-axis and edges, where:

$$\varphi_1 = 150°; \ \varphi_2 = 90° ; \ \varphi_3 = 30°$$

Coordinates of point 1, 2 and 3 in a sector are calculated as:

$x_{(1)} = Rcos(150°) = -216.506;$ $y_{(1)} = Rsin(150°) = 125$

$x_{(2)} = Rcos(90°) = 0;$ $y_{(2)} = Rsin(90°) = 250$

$x_{(3)} = Rcos(30°) = 216.506;$ $y_{(3)} = Rsin(30°) = 250$
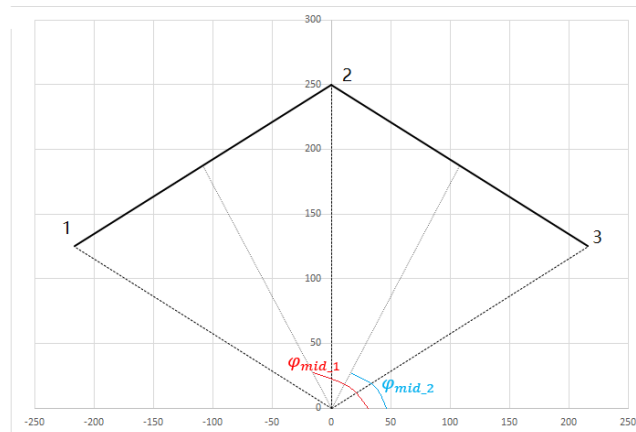
Figure 3.12: Mid-line between edges of sector

φ_{mid_1} and φ_{mid_2} shown in Figure 3.12 are the angles between x-axis and midline of edges.

$$\varphi_{mid\_1} = \ \varphi_1 - \frac{\theta}{2} = \ 150 - 30 = 120°$$

$$\varphi_{mid\_2} = \ \varphi_2 - \frac{\theta}{2} = \ 90 - 30 = 60°$$

Coordinates of rounded corners are calculated as follows:

30

<u>Resistance of Polygonal Cross Section of Lattice Wind Tower</u>

Bending radius of the rounded corner is taken as:

$$r_{bend} = r_{coef}t$$

where r_{coef} is the bending radius to thickness ratio:

$$r_{coef} = 6 \quad r_{bend} = 4 * 6 = 24mm$$
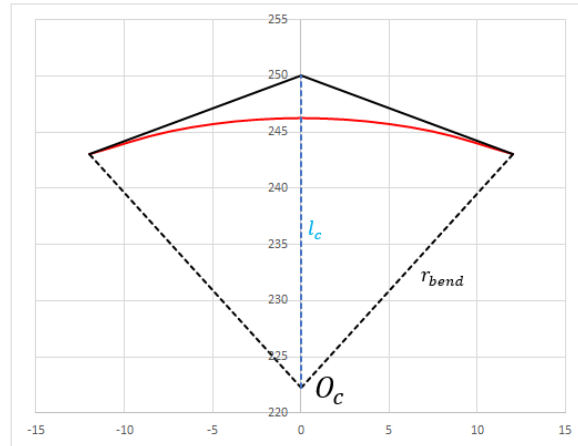
Figure 3.13 Bending radius of the rounded corner

Distance between bending centre and corner l_c:

$$l_c = r_{bend}/\cos(\frac{\theta}{2})$$

$$l_c = \frac{24}{\cos(30)} = 16\sqrt{3}$$

Coordinates of the bending centre:

$$x_c = x_2 - l_c \cos(\varphi_2) = 0 - 16\sqrt{3} * \cos(90°) = 0$$

$$y_c = y_2 - l_c \sin(\varphi_2) = 250 - 16\sqrt{3} * \sin(90°) = 222.278$$

$$O_c(x_c, y_c) = (0, 222.278)$$

Six arc points (Figure 3.14) are calculated as follows:
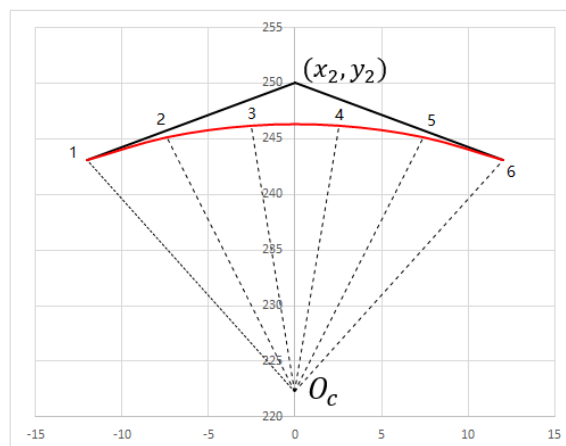
Figure 3.14: Arc points on the rounded corner

31

Resistance of Polygonal Cross Section of Lattice Wind Tower

Coordinates of the points are calculated as follow:

$$x_{arc,1} = x_c + r_{bend} \cos\left(\varphi_{mid_1} - 0 * \frac{\theta}{5}\right) = 0 + 24 * \cos(120) = -12$$

$$x_{arc,2} = x_c + r_{bend} \cos\left(\varphi_{mid_1} - 1 * \frac{\theta}{5}\right) = 0 + 24 * \cos(108) = -7.416$$

$$x_{arc,3} = x_c + r_{bend} \cos\left(\varphi_{mid_1} - 2 * \frac{\theta}{5}\right) = 0 + 24 * \cos(96) = -2.509$$

$$x_{arc,4} = x_c + r_{bend} \cos\left(\varphi_{mid_1} - 3 * \frac{\theta}{5}\right) = 0 + 24 * \cos(84) = 2.509$$

$$x_{arc,5} = x_c + r_{bend} \cos\left(\varphi_{mid_1} - 4 * \frac{\theta}{5}\right) = 0 + 24 * \cos(72) = 7.416$$

$$x_{arc,6} = x_c + r_{bend} \cos\left(\varphi_{mid_1} - 5 * \frac{\theta}{5}\right) = 0 + 24 * \cos(60) = 12$$

$$y_{arc,1} = y_c + r_{bend} \sin\left(\varphi_{mid_1} - 0 * \frac{\theta}{5}\right) = 222.278 + 24 * \sin(120) = 243.063$$

$$y_{arc,2} = y_c + r_{bend} \sin\left(\varphi_{mid_1} - 1 * \frac{\theta}{5}\right) = 222.278 + 24 * \sin(108) = 245.103$$

$$y_{arc,3} = y_c + r_{bend} \sin\left(\varphi_{mid_1} - 2 * \frac{\theta}{5}\right) = 222.278 + 24 * \sin(96) = 246.146$$

$$y_{arc,4} = y_c + r_{bend} \sin\left(\varphi_{mid_1} - 3 * \frac{\theta}{5}\right) = 222.278 + 24 * \sin(84) = 246.146$$

$$y_{arc,5} = y_c + r_{bend} \sin\left(\varphi_{mid_1} - 4 * \frac{\theta}{5}\right) = 222.278 + 24 * \sin(72) = 245.103$$

$$y_{arc,6} = y_c + r_{bend} \sin\left(\varphi_{mid_1} - 5 * \frac{\theta}{5}\right) = 222.278 + 24 * \sin(60) = 243.063$$

Point 1 = (-12, 243.063)   Point 2 = (-7.416, 245.103) Point 3 = (-2.509, 246.146)

Point 4 = (2.509, 246.146) Point 5 = (7.416, 245.103)   Point 6 = (12, 243.063)

3.2.3 Lips

Sectors are bolted on the lips. Also, lips work as the stiffeners of the section. Sector can be considered as the edge stiffened element; the section can be considered as the intermittently stiffened element (Figure 3.11).
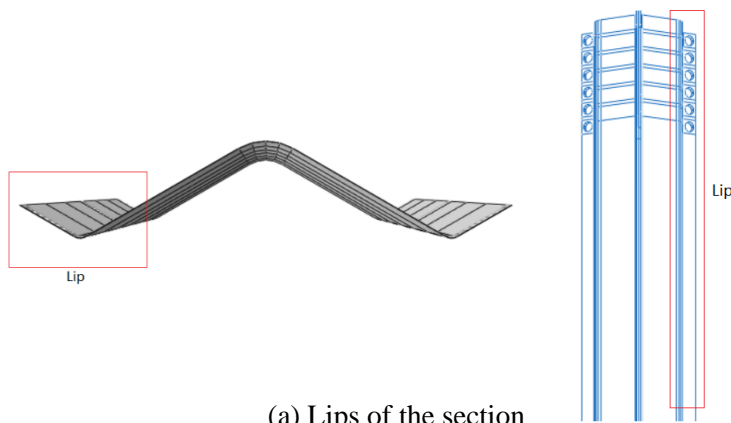
(a) Lips of the section

32
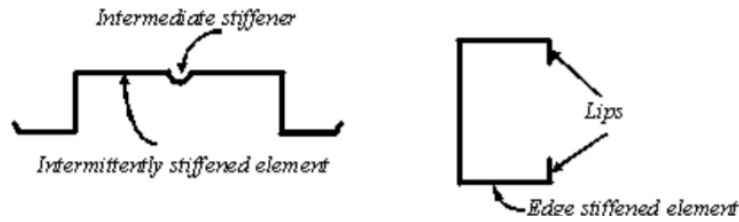
(b) Lips as stiffeners

Figure 3.11: Lips

Wider lips are usually better. When the lip length approaches to the flange width, the highest distortional buckling stress is achieved [25]. Lips are supposed to support along the longitudinal edges, which has benefits of flexural rigidity. A general rule suggests that the length of lip should be at least one-fifth of the adjacent plate width [26].

In this thesis, since the cross section is hexagonal, 1/5 of the radius is 10% of the diameter, width of the lip is taken as 0.1d. Length of the lip is taken as the length of the section. Table 3.4 shows the width of the lips under different diameters.

Table 3.4: Width of lips

d (mm)	0.1d (mm)
500	50
700	70
900	90

The connection between lip and plate is bended as well.

Bending radius is taken as $r_s = r_{bend}/5$. Take the same cross section as the previous one as the example for calculating the coordinates.

(a)

33

(b)

(c)
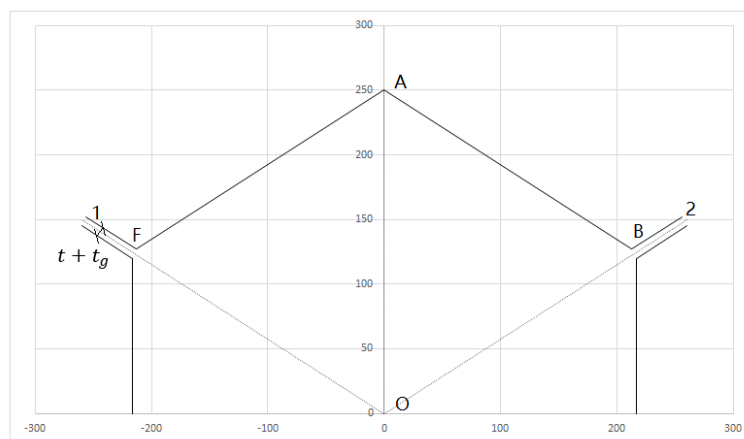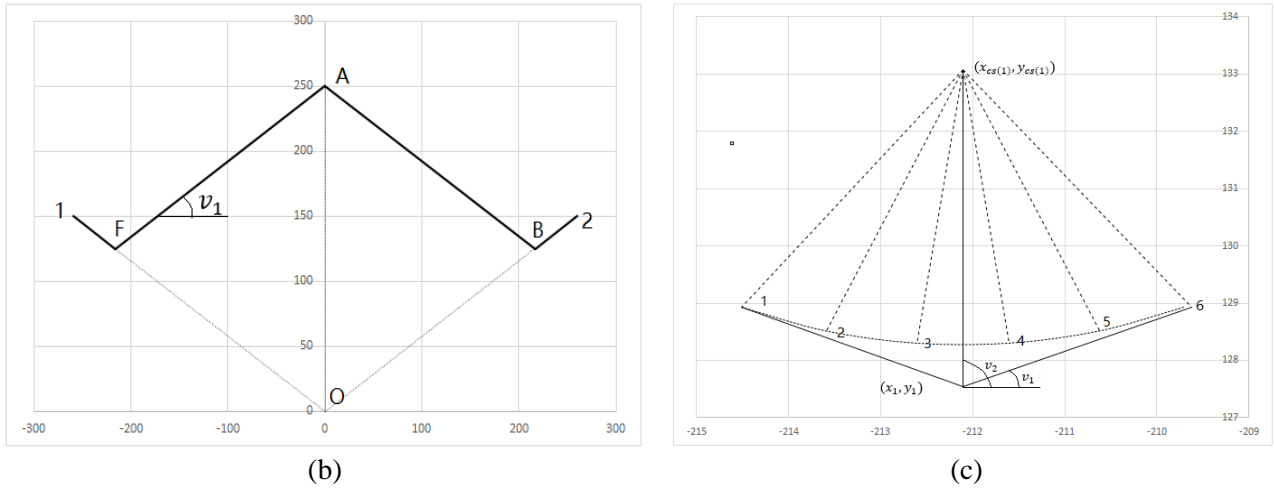
Figure 2.12: Coordinates of lip

$d = 500mm$; $t = 4mm$; $r_{bend} = 24mm$;

$$r_s = \frac{24}{5} = 4.8mm$$

$$\frac{t + t_g}{2} = 4.4$$

$$v_1 = \varphi_{mid\_1} - \frac{\pi}{2} = 120 - 90 = 30°$$

$$v_2 = \frac{\varphi_1 + v_1}{2} = \frac{150 + 30}{2} = 90°$$

$$l_1 = \frac{t + t_g}{2} * \frac{1}{\cos(\varphi_1 - \varphi_{mid_1})}) = 4.4 * \frac{1}{0.866} = 5.08$$

$$l_2 = \frac{r_s}{\sin(v_2 - \varphi_{mid_1} + 90°)} = \frac{4.8}{\sin(60)} = 5.54$$

Coordinates of point F (x_1, y_1) are calculated as:

$$x_1 = x_{(1)} + l_1 \cos(v_1) = -216.506 + 5.08 * \cos(30)$$
$$= -212.106$$

$$y_1 = y_{(1)} + l_1 \sin(v_1) = 125 + 5.08 * \sin(30) = 127.54$$

The bending centre coordinates are calculated as:

$$x_{cs(1)} = x_1 + l_2 \cos(v_2) = -212.106 + 5.54 * \cos(90) = -212.106$$

$$y_{cs(1)} = y_1 + l_2 \sin(v_2) = 127.54 + 5.54 * \sin(90) = 133.08$$

Calculation of the arc points (Figure 2.12 (c)):

$$x_{sarc,1} = x_{cs(1)} + r_s * \cos\left(\frac{4\pi}{3} + 0 * \frac{60°}{5}\right) = -212.106 + 4.8 * \cos\left(240° + 0 * \frac{60°}{5}\right) = -214.506$$

$$x_{sarc,2} = x_{cs(1)} + r_s * \cos\left(\frac{4\pi}{3} + 1 * \frac{60°}{5}\right) = -212.106 + 4.8 * \cos\left(240° + 1 * \frac{60°}{5}\right) = -213.589$$
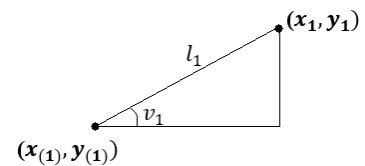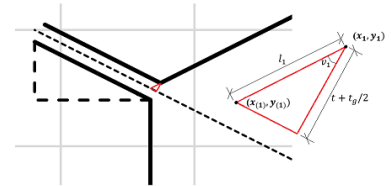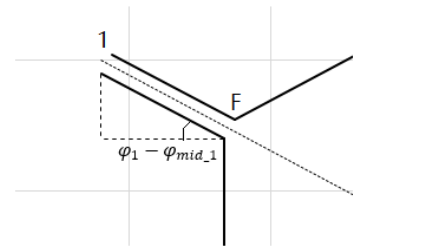
$$x_{sarc,3} = x_{cs(1)} + r_s * \cos\left(\frac{4\pi}{3} + 2 * \frac{60°}{5}\right) = -212.106 + 4.8 * \cos\left(240° + 2 * \frac{60°}{5}\right) = -212.608$$

$$x_{sarc,4} = x_{cs(1)} + r_s * \cos\left(\frac{4\pi}{3} + 3 * \frac{60°}{5}\right) = -212.106 + 4.8 * \cos\left(240° + 3 * \frac{60°}{5}\right) = -211.604$$

$$x_{sarc,5} = x_{cs(1)} + r_s * \cos\left(\frac{4\pi}{3} + 4 * \frac{60°}{5}\right) = -212.106 + 4.8 * \cos\left(240° + 4 * \frac{60°}{5}\right) = -210.623$$

$$x_{sarc,6} = x_{cs(1)} + r_s * \cos\left(\frac{4\pi}{3} + 5 * \frac{60°}{5}\right) = -212.106 + 4.8 * \cos\left(240° + 5 * \frac{60°}{5}\right) = -209.706$$

$$y_{sarc,1} = y_{cs(1)} + r_s * \sin\left(\frac{4\pi}{3} + 0 * \frac{60°}{5}\right) = 133.08 + 4.8 * \sin\left(240° + 0 * \frac{60°}{5}\right) = 128.923$$

$$y_{sarc,2} = y_{cs(1)} + r_s * \sin\left(\frac{4\pi}{3} + 1 * \frac{60°}{5}\right) = 133.08 + 4.8 * \sin\left(240° + 1 * \frac{60°}{5}\right) = 128.515$$

$$y_{sarc,3} = y_{cs(1)} + r_s * \sin\left(\frac{4\pi}{3} + 2 * \frac{60°}{5}\right) = 133.08 + 4.8 * \sin\left(240° + 2 * \frac{60°}{5}\right) = 128.306$$

$$y_{sarc,4} = y_{cs(1)} + r_s * \sin\left(\frac{4\pi}{3} + 3 * \frac{60°}{5}\right) = 133.08 + 4.8 * \sin\left(240° + 3 * \frac{60°}{5}\right) = 128.306$$

$$y_{sarc,5} = y_{cs(1)} + r_s * \sin\left(\frac{4\pi}{3} + 4 * \frac{60°}{5}\right) = 133.08 + 4.8 * \sin\left(240° + 4 * \frac{60°}{5}\right) = 128.515$$

$$y_{sarc,6} = y_{cs(1)} + r_s * \sin\left(\frac{4\pi}{3} + 5 * \frac{60°}{5}\right) = 133.08 + 4.8 * \sin\left(240° + 5 * \frac{60°}{5}\right) = 128.923$$

3.2.4   Gusset plates

Gusset plates are thick steel sheets used at joints to collect the forces [27]. In this thesis, the thickness of gusset plate is $t_g = 1.2*t$.
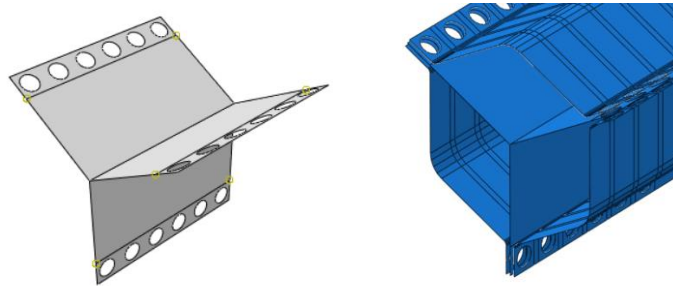
Figure 3.12: Gusset plate

4. Finite element analysis

4.1 Steps of finite element analysis

In this thesis, models of different parameters are analysed. One value of corners; three values of diameters; two values of cross sectional slenderness; three values of length slenderness and three values of bolt spacing are selected, which results in 54 models with different cross sections. Both linear buckling analysis and RIKS are analysed. Also, there are two load modes and three values of moment, which results in 270 files. So, MATLAB and PYTHON are used. Figure 4.1 shows the procedures of finite element analysis. The analysis is achieved by MATLAB, PYTHON script and ABAQUS.

Step	Description
Matlab	•Calculation of the coordinates of cross section profiles
Matlab	•Create the cross sections profiles
Python	•Create ABAQUS models
Custer	•Run ABAQUS models
Python	•Take out the results from ODB. files
Matlab	•Calculation of the resistance
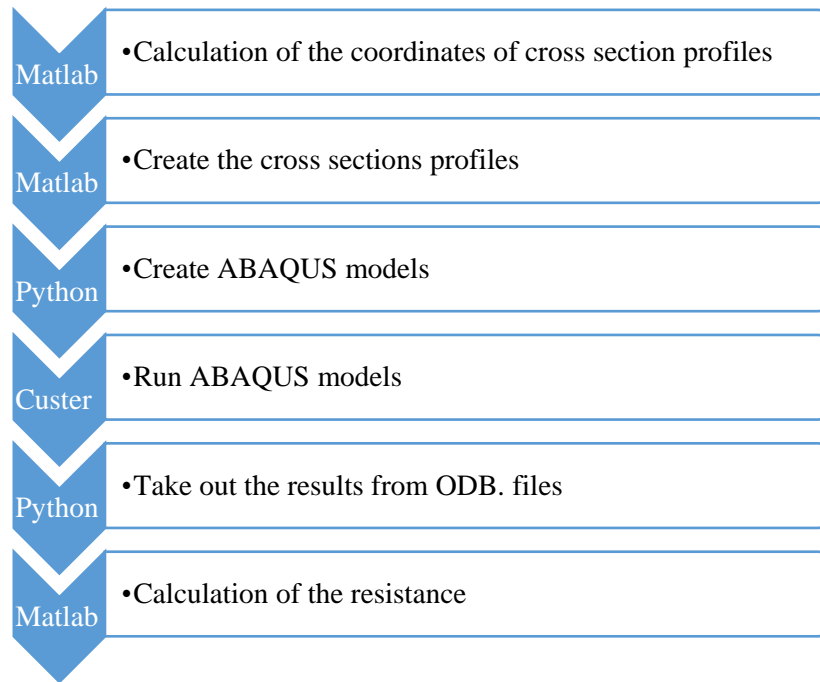
Figure 4.1: Steps of finite element analysis

4.2 MATLAB

MATLAB is used to calculate the coordinates of the cross-sectional profiles, it gives a profile database to import in PYTHON script. File pcoords.m (Annex A) gives the coordinates of the cross section, polygonal.m (Annex B) gives the range of the corresponding parameters, which creates coordinates of all models.

In MATLAB, the corresponding meanings of the names are shown in Table 4.1.

Table 4.1: Meanings of the names in MATLAB

Name	Meaning
nrange	Range of numbers of corners
drange	Range of diameters
slendrange	Range of cross section slenderness (thickness)
fy	Yield strength
rcoef	Radius coefficient of bend of rounded corner
nbend	Number of bending
l_ratio	Ratio of width of lip and diameter
t_ratio	Ratio of thickness of gusset plate
lambda	Slenderness of the length

For loop is used to get values for all models within the given range. Table 4.2 shows the corresponding meanings of i, j, k, l used in for loop.

Table 4.2: i, j, k, l in for loop

i	nrange	k	slendrange
j	drange	l	lambda

4.3 ABAQUS

Models of abaqus are created by running python script (Annex C).

4.3.1   Units

Units used in ABAQUS are shown in Table 4.3.

Table 4.3.: Units used in finite element analysis

Mass	Length	Force	Stress
ton	mm	N	Mpa

4.3.2   Material properties

- Elastic

S355 steel is used in the analysis.

$f_y = 355N/mm^2$

Young's Modulus = $210000N/mm^2$

Poisson's ratio = 0.3

- Plastic

The relationship between yield stress and plastic strain of the plastic material properties of S355 steel is shown in Table 4.4, 10 couples of values are taken from database.

Table 4.4 Plastic material properties of S355

Yield Stress	Plastic Strain
381.1	0.0
391.2	0.0053
404.8	0.0197
418.0	0.0228
444.2	0.0310
499.8	0.0503
539.1	0.0764
562.1	0.1009
584.6	0.1221
594.4	0.1394

4.3.3 Shell element

Shell element is selected in ABAQUS due to the following advantages:

- Shell element has an advantage of saving time since it requires less elements while modelling thin structures comparing to solid elements [28].
- It is easier to mesh.
- Shell element has more realistic boundary conditions as it allows to create boundary conditions on face.
- Shell element requires less disk space for the results, which is important for nonlinear analysis and big models. Also, the processing of shell element analysis is faster comparing to solid element.

4.3.4 Parts, sets and assembly

Sector and gusset plates are created as the individual parts. Parts are created dependently. Dependent part is used since it consumes less memory. Also, ABAQUS applies the same mesh to all dependent instances of the part, hence part needs to be meshed only once.

However, most modifications are not allowed on a dependent part instance. Sets are created in order to modify the geometry and apply loads and boundary conditions of the parts. Note that modifications of mesh of dependent parts are not allowed in mesh module either, the modifications are supposed to be done in part module.

When the model is assembled, it is the part instance being worked with instead of the original part itself. Figure 4.2 shows the parts and assembled model.

(a) Part of a sector   (b) Part of gusset plate
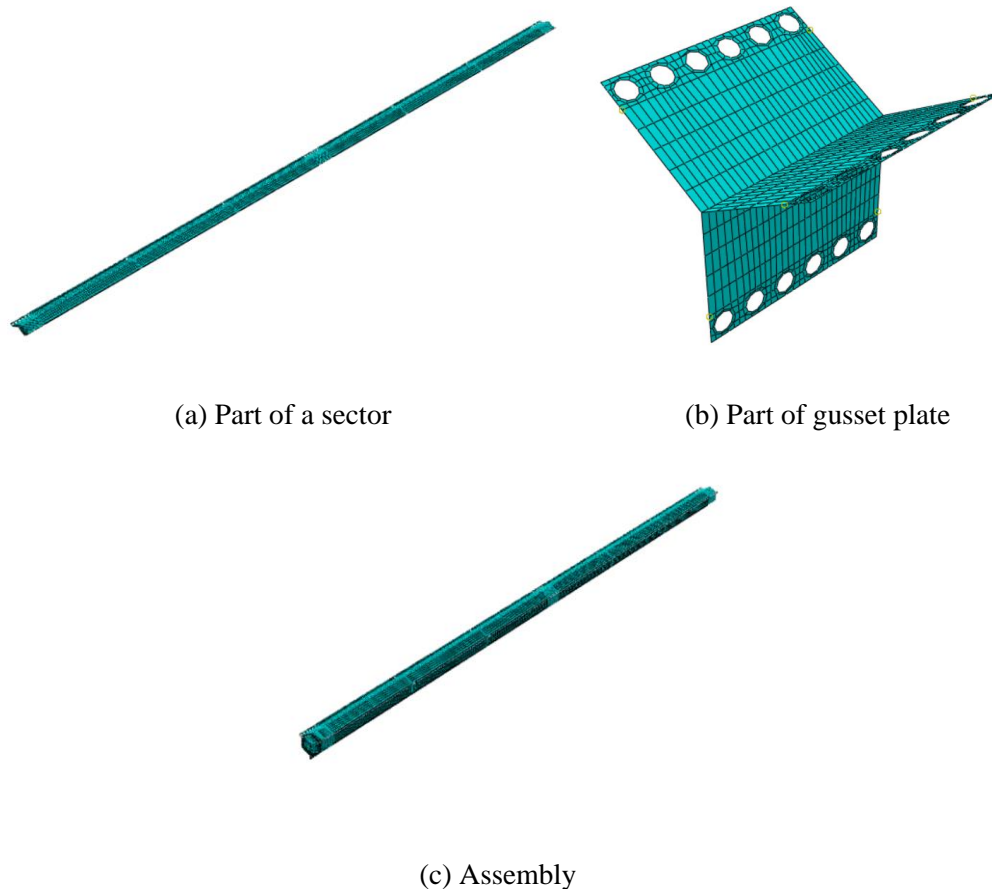
(c) Assembly

Figure 4.2: Parts and assembled model

4.3.5   Holes

Rigid body constraint, which can be used between deformable components, allows the users to constrain the motion of the regions to the motion of reference point [28]. It forces the whole constrained region to behave as a rigid body. The constrained region has the same displacement and rotation corresponding to the reference point.

Since transverse force is not considered in the model, bolt is used only for connecting the sectors. Hence the constrained holes along the lips and gusset plates are modelled instead of bolts. Holes at the same positions are paired to each other. Reference points are made for each set of holes, each hole is tied to the corresponding reference point as shown in Figure 4.3 (c).
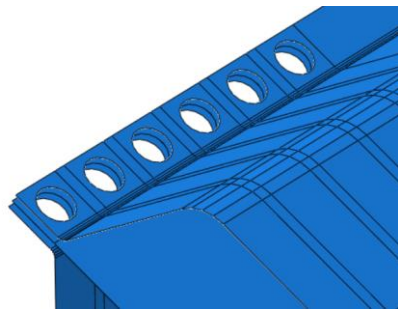
(a) Holes on lips and gusset plate
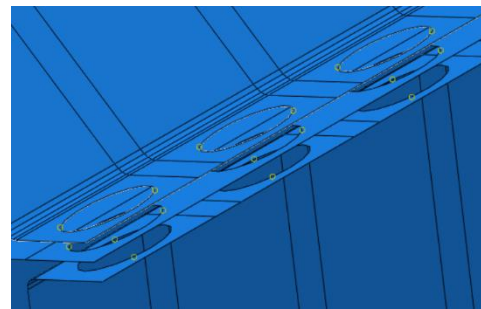
(b) Rigid body constriant
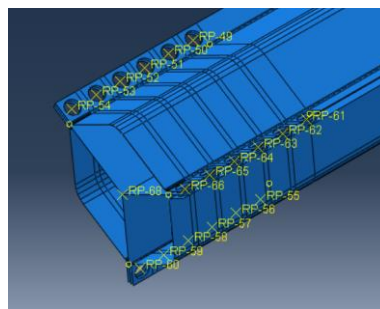
(c) Reference points

Figure 4.3: Holes

In order to obtain the more accurate mesh (Figure 4.5) around the hole, datum planes (Figure 4.5) are created to partition the regions around the holes on the sector and gusset plate.
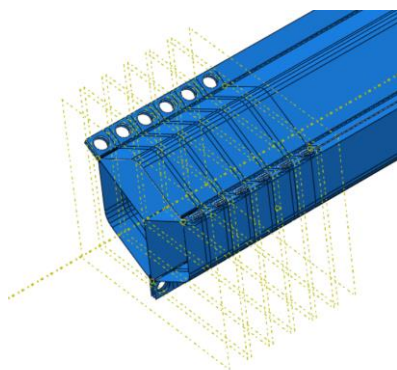
Figure 4.4: Datum planes   **Figure 4.5: Mesh due to datum planes**
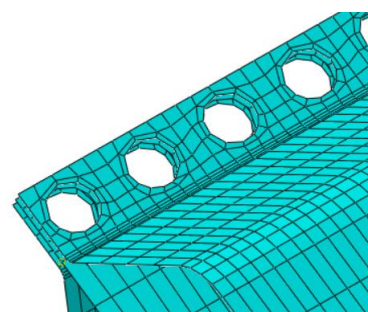
4.3.6 Boundary conditions

Reference points are created at centre of both end planes and middle plane. The reference points at both ends are coupling constrained to the edges of the cross section (Figure 4.6 (a)); the reference point at the middle is coupling constrained to the centre axis of gusset plate (Figure 4.6 (b)). Boundary conditions are added on the reference points.
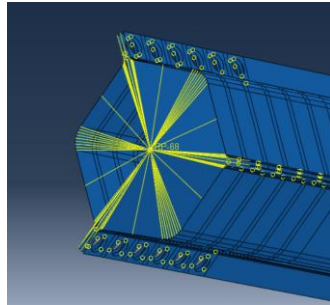
(a) References points and couplings at the both ends
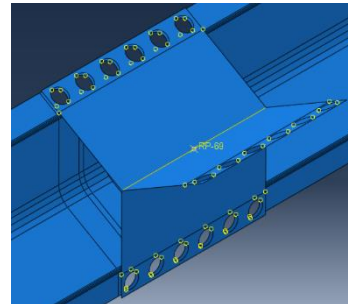
(b) Reference point at the middle

Figure 4.6: Reference points and boundary conditions
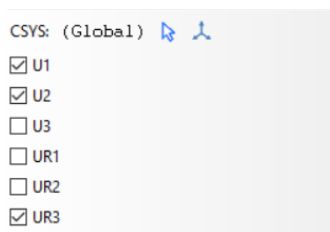
(a) top
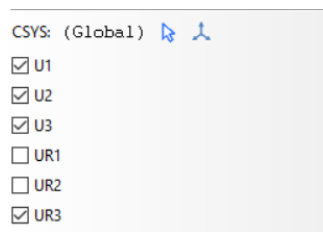
(b) bottom
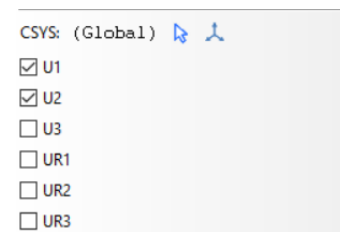
(c) middle

Figure 4.7: Boundary conditions

1: x-axis;

2: y-axis;

3: z-axis

- Boundary conditions at the top

Reference point is translational constrained in both x and y direction; rotational constrained around z axis. Since the section might have displacement under compression load, translational boundary condition in z direction is realised.

- Boundary conditions at the bottom

Reference point is translational constrained in all directions and rotational restrained around z axis.

- Boundary conditions at the middle

The reference point, which is used to be added moment, at the middle is coupled to the middle axis of the gusset plate. The reference point is only translational restrained in x and y axis.

4.3.7   Loads

Two load modes are analysed in the model:

(1) Concentrated load

Concentrated load is estimated as the follows:

$$N_{pl,Rd} = f_u A$$

which gives the highest load that could be applied on the cross section in order to have the resistance lower than it so as to make sure the section collapses.

Concentrated load is added at the reference point of the top end along the z axis.

(2) Concentrated load + moment

Concentrated load is taken as the one used in (1). Added bending moment is taken as 10% of moment resistance of the cross section. Moment resistance is calculated as follows:

$$M_{pl,Rd} = W_{pl} f_y / Y_{M0}$$

where $W_{pl} = I_y / r$.

Moment is added at the centroid of the middle plan on the negative direction of x axis.

4.3.8   Mesh

Mesh is created in part since the part is dependent. Global size of mesh is 30.

4.3.9   Step and procedure type

In ABAQUS, step is defined as a period of time, which calculates the model with a particular set of loads and boundary conditions under a specified analysis method [30]. Procedure type can be chosen in step module. Another importation function of step is either field output or history output can be chosen for each set, and it allows to choose the specified variables for output, such reaction force, rotational moment (Figure 4.8).
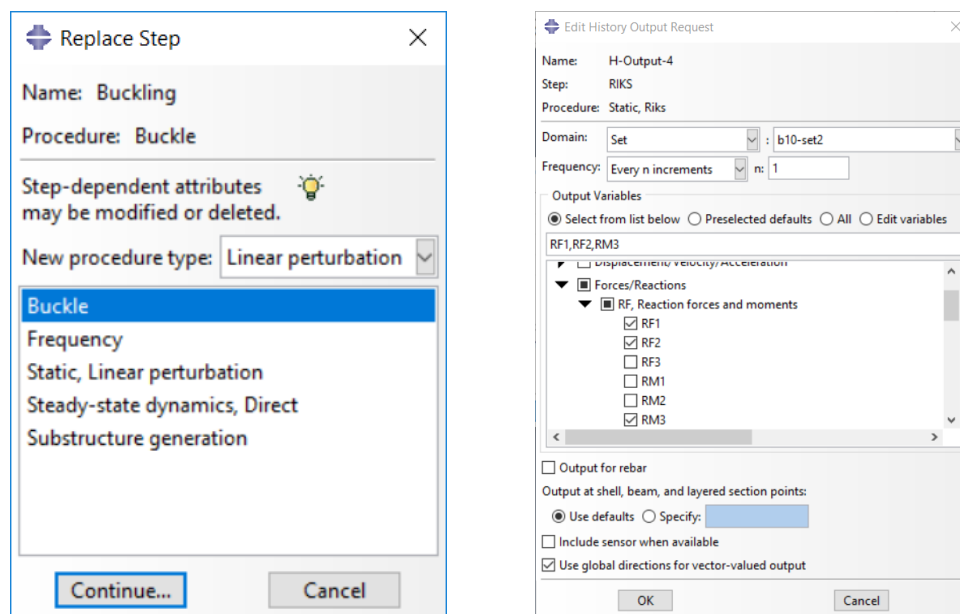
(a) Procedure type   (b) Output variables

Figure 4.8: Step

In this thesis, buckling analysis and static RIKS analysis are used.

- Elastic buckling analysis

Linear elastic buckling analysis is done for

- Static, RIKS analysis

RIKS (load-deflection) analysis is the most suitable method to analyse the problems with unstable collapse and post-buckling. Generally, RIKS is used to predict unstable, geometrically nonlinear collapse of a structure. It also can include nonlinear materials (GMNIA).

RIKS method solves simultaneously for loads and displacements [31]. RIKS uses arc-length method along the static equilibrium to look for the maximum load value when there is a significant change in the structure (collapse).

The initial increment is defined as 0.2 and the maximum number of increments in this thesis is used as 30. The RIKS analysis steps stop when increment reaches to 30.

4.3.10   Imperfections

Eigen mode of shape imperfection is obtained in linear elastic analysis, s/2000 is taken to include the initial imperfection. This estimation is based on the bolt spacing rather than the member length, because the dominant buckling modes are on the local regions (as the LBA buckling analysis shows, shown in chapter 7), not on the member (global regions). The results of LBA analysis of the models show that the wavelengths of the eigen modes are shorter than half wavelengths, the dominant eigen modes are local ones. Half wavelength is the length of the member, eigen modes of half wavelength are given by global buckling. It is more reasonable to have an imperfection value not based on the member length. So, s/2000 is assumed in the RIKS analysis.

5. Stiffness of bolts

5.1. Methodology

General static analysis in ABAQUS is used for calculating the stiffness matrix. The bolt (corresponding hole in the model) in the middle of the section is defined as bolt 1. The following two bolts, either on the left or right, are defined as bolt 2 and bolt 3 (Figure 5.1).
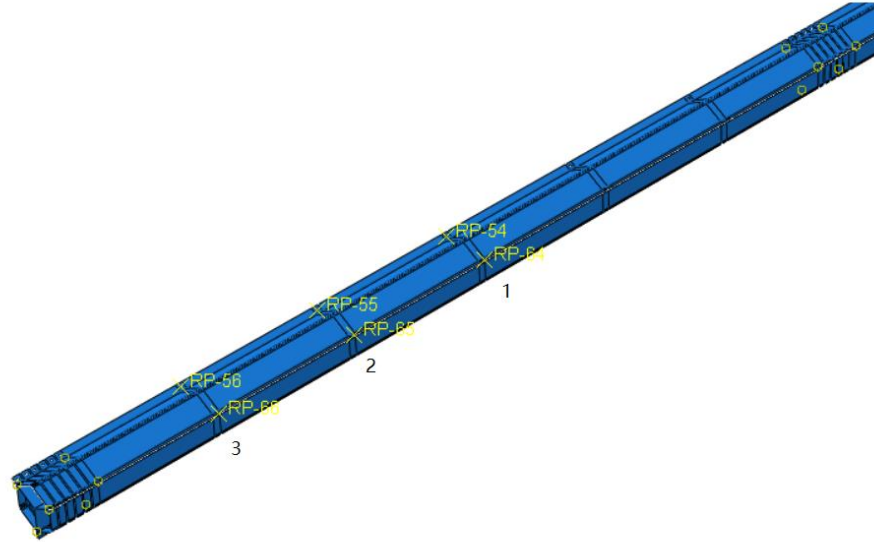
Figure 5.1: Bolts selected for calculation of stiffness

Stiffness matrix of the three bolts are represented as k_{ij}, where $i = 1,2,3$. Either unit displacement (Figure 5.3) and unit rotation (Figure 5.4) is applied on the ith pair of bolts. Displacement and rotation are applied on the reference points which are rigid body constrained to the homologous holes on the lips (Figure 5.2). Loads are applied in boundary condition manager, displacement 1 is divided into $1*\cos(30)=0.866$ in x axis and $1*\sin(30)=0.5$ in y axis. The calculated translational reaction and rotational reaction at the jth ($j = 1,2,3$) bolt are taken as the translational and rotational stiffness of the jth bolt, which results in the stiffness matrix of bolts shown as follow:

$$\begin{matrix} & U_1 \quad U_2 \quad U_3 & UR_1 \ UR_2 \ UR_3 \end{matrix}$$

Displacement applied
$$\begin{bmatrix} k_{11} & k_{12} & k_{13} \\ k_{21} & k_{22} & k_{23} \\ k_{31} & k_{32} & k_{33} \end{bmatrix} \begin{bmatrix} k_{11} & k_{12} & k_{13} \\ k_{21} & k_{22} & k_{23} \\ k_{31} & k_{32} & k_{33} \end{bmatrix}$$

Rotation applied
$$\begin{bmatrix} k_{11} & k_{12} & k_{13} \\ k_{21} & k_{22} & k_{23} \\ k_{31} & k_{32} & k_{33} \end{bmatrix} \begin{bmatrix} k_{11} & k_{12} & k_{13} \\ k_{21} & k_{22} & k_{23} \\ k_{31} & k_{32} & k_{33} \end{bmatrix}$$

where U_j / UR_j means translational / rotational reaction on the jth bolt with the ith loaded bolt.

Since the properties and geometries of all bolts as well as the loaded displacement and rotation are the same, the reactions on the loaded bolts remain the same, which gives:

$$k_{11} = k_{22} = k_{33}$$

Furthermore, since the bolt spacing is equal between any two bolts, the effects on the bolts next to the loaded bolt remain the same. Similarly, the effects on the bolts which have same distance to the loaded bolt remain the same. It gives:

$$k_{21} = k_{23} = k_{12} = k_{32} \text{ and } k_{31} = k_{13}$$

Hence, the stiffness matrix can be written as:

$$\begin{array}{cccccc} U_1 & U_2 & U_3 & UR_1 & UR_2 & UR_3 \end{array}$$

Displacement applied
$$\begin{bmatrix} k_{11} & k_{12} & k_{13} \\ k_{12} & k_{11} & k_{12} \\ k_{13} & k_{12} & k_{11} \end{bmatrix} \begin{bmatrix} k_{11} & k_{12} & k_{13} \\ k_{12} & k_{11} & k_{12} \\ k_{13} & k_{12} & k_{11} \end{bmatrix}$$

Rotation applied
$$\begin{bmatrix} k_{11} & k_{12} & k_{13} \\ k_{12} & k_{11} & k_{12} \\ k_{13} & k_{12} & k_{11} \end{bmatrix} \begin{bmatrix} k_{11} & k_{12} & k_{13} \\ k_{12} & k_{11} & k_{12} \\ k_{13} & k_{12} & k_{11} \end{bmatrix}$$

Figure 5.2: Bolts where to apply loads
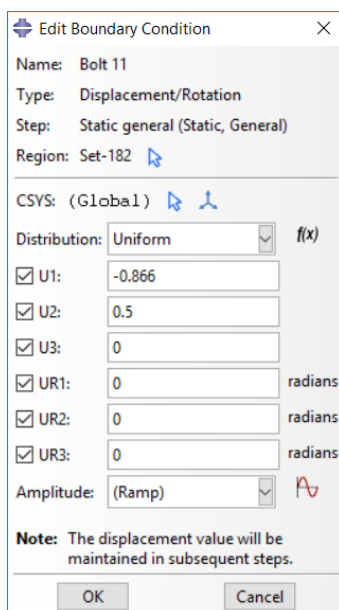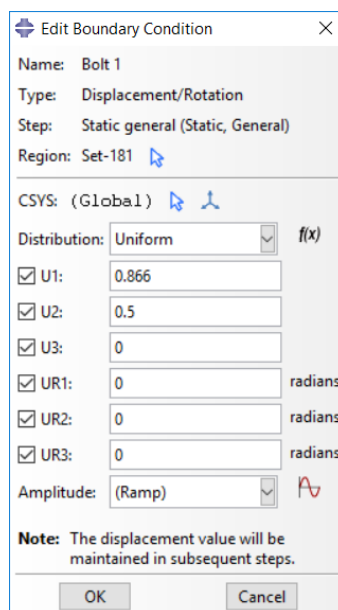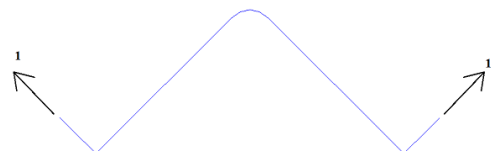
(a) Bolt 1'   (b) Bolt 1   (c) Cross sectional view

Figure 5.3: Displacement
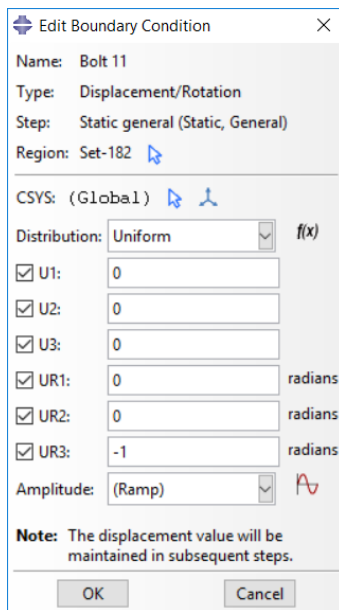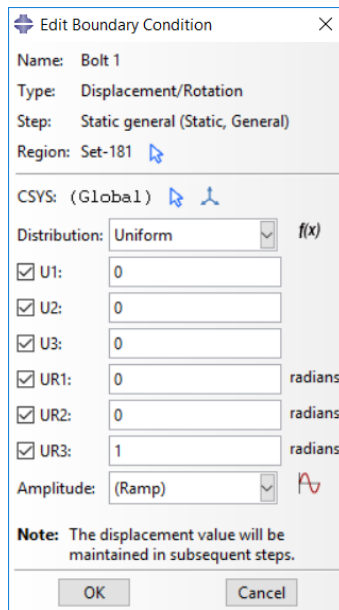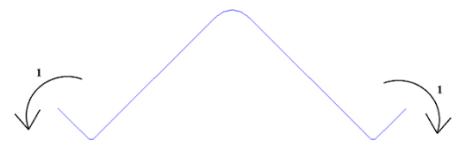
(a) Bolt 1'   (b) Bolt 1   (c) Cross sectional view

Figure 5.4: Rotation

All other bolts on the sector besides the loaded bolts should be fixed (Figure 5.5).
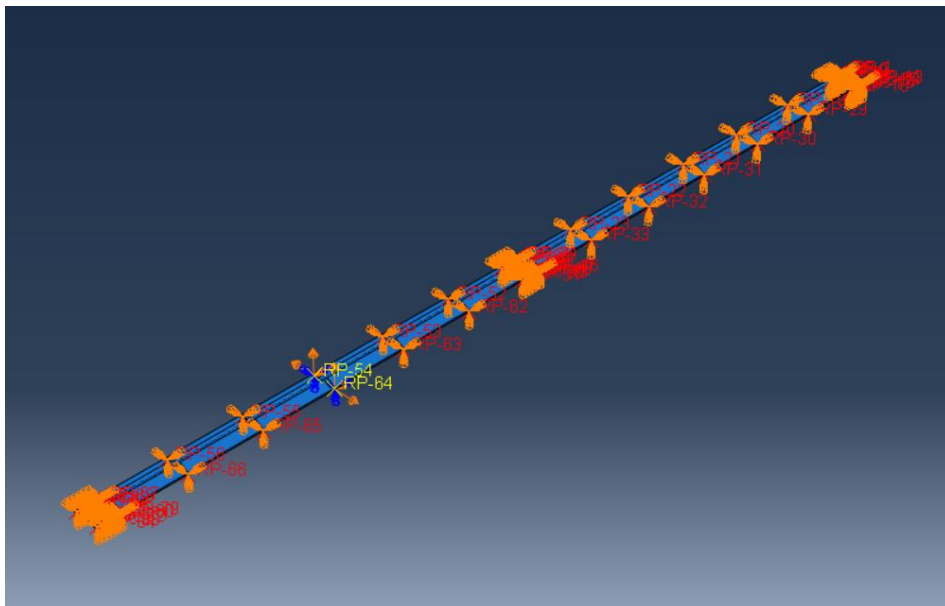
Figure 5.5: Fixed bolts

The steps are shown as follows:

1) Find the bolt in the middle of the section (between two joints), define it as bolt 1.
2) Defines the following two bolts, either on the left or on the right, as bolt 2 and 3.
3) Define the bolt on the opposite side of bolt 1 on the sector as bolt 1'.
4) Apply load on bolt 1 and bolt 1' in boundary condition.
5) Fix all bolts on the sector besides the two loaded bolts.

6) Define sets of bolt 1, 2 and 3 as; create history output with RF1, RF2 and RM3 for each set in step module.
7) Run the model.

5.2. Results and stiffness matrix

Table 5.1 shows the geometrical parameters of the models which are chosen to be analysed for stiffness. Stiffness under different diameter, thickness and bolt spacing are compared.

Table 5.1: Geometries of models

d (mm)	t (mm)	bolt spacing ratio	bolt spacing (mm)
700	11	3	2100
700	12	3	2100
700	13	3	2100

(1) Thickness

500	11	3	1500
700	11	3	2100
900	11	3	2700

(2) Diameter (same bolt spacing ratio)

700	11	3	2100
700	11	5	3500

(3) Bolt spacing

Translational and rotational reactions and stiffness matrix are shown in Table 5.3 – Table 5.10.

Table 5.3: d = 700mm; t = 11mm; bolt spacing = 2100mm

	d=	700	mm	b=	3	
	t=	11	mm	l=	0	
	Displacement applied			Rotation applied		
	bolt1	bolt2	bolt3	bolt1	bolt2	bolt3
RF1(N)	36218.20	-9193.05	861.73	136106.00	-257771.00	71069.40
RF2(N)	21454.60	-10352.50	-1468.85	-937227.00	550748.00	-61788.60
RF(N)	84731.60	-31320.53	-1942.63	-1717287.72	803838.96	-41510.92
RM3(N-mm)	-349934.00	50299.20	33830.00	151657000.00	-20490400.00	3593940.00

Reaction	Translational Reaction (kN)			Rotational Reaction (kNm)		
	U1	U2	U3	UR1	UR2	UR3
	84.73	-31.32	-1.94	-0.35	0.05	0.03
displacement applied	-31.32	84.73	-31.32	0.05	-0.35	0.05
	-1.94	-31.32	84.73	0.03	0.05	-0.35
	-1717.29	803.84	-41.51	151.66	-20.49	3.59
rotation applied	803.84	-1717.29	803.84	-20.49	151.66	-20.49
	-41.51	803.84	-1717.29	3.59	-20.49	151.66

Table 5.4: d = 700mm; t = 12mm; bolt spacing = 2100mm

	d=	700	mm	b=	3	
	t=	12	mm	l=	0	
	Displacement applied			Rotation applied		
	bolt1	bolt2	bolt3	bolt1	bolt2	bolt3
RF1(N)	44200.20	-10326.20	1004.36	86521.90	-285061.00	79946.30
RF2(N)	25020.30	-12271.10	-1618.68	-1004220.00	594889.00	-72739.20
RF(N)	101080.09	-36466.22	-2077.59	-1908530.18	860608.25	-53161.66
RM3(N-mm)	-429236.00	53759.40	35971.00	188201000.00	-21957300.00	4115090.00

Reaction	Translational Reaction (kN)			Rotational Reaction (kNm)		
	U1	U2	U3	UR1	UR2	UR3
displacement applied	101.08	-36.47	-2.08	-0.43	0.05	0.04
	-36.47	101.08	-36.47	0.05	-0.43	0.05
	-2.08	-36.47	101.08	0.04	0.05	-0.43
rotation applied	-1908.53	860.61	-53.16	188.20	-21.96	4.12
	860.61	-1908.53	860.61	-21.96	188.20	-21.96
	-53.16	860.61	-1908.53	4.12	-21.96	188.20

Table 5.5: d = 700; t = 13mm; bolt spacing = 2100mm

	d=	700	mm	b=	3	
	t=	13	mm	l=	0	
	Displacement applied			Rotation applied		
	bolt1	bolt2	bolt3	bolt1	bolt2	bolt3
RF1(N)	53334.30	-11435.20	1151.38	-25692.20	-301975.00	88890.10
RF2(N)	29062.00	-14462.00	-1713.04	-1064840.00	637507.00	-86042.30
RF(N)	119710.95	-42128.62	-2096.54	-2159347.67	926313.08	-69440.14
RM3(N-mm)	-553732.00	57194.50	36062.10	232982000.00	-23131200.00	4645640.00

Reaction	Translational Reaction			Rotational Reaction		
	U1	U2	U3	UR1	UR2	UR3
displacement applied	119.71	-42.13	-2.10	-0.55	0.06	0.04
	-42.13	119.71	-42.13	0.06	-0.55	0.06
	-2.10	-42.13	119.71	0.04	0.06	-0.55
rotation applied	-2159.35	926.31	-69.44	232.98	-23.13	4.65
	926.31	-2159.35	926.31	-23.13	232.98	-23.13
	-69.44	926.31	-2159.35	4.65	-23.13	232.98

Table 5.6: d = 700; t = 11mm; bolt spacing = 3500mm

	d=	700	mm	b=	5	
	t=	11	mm	l=	0	
	Displacement applied			**Rotation applied**		
	bolt1	**bolt2**	**bolt3**	**bolt1**	**bolt2**	**bolt3**
RF1(N)	30009.30	-3127.00	450.67	-63133.20	-73385.70	28102.70
RF2(N)	15501.20	-5711.43	-177.10	-507387.00	213686.00	-26864.00
RF(N)	65655.17	-15033.71	166.20	-1087676.08	342631.01	-21276.85
RM3(N-mm)	-308421.00	42527.30	10677.80	135114000.00	-7125960.00	1509220.00

Reaction	**Translational Reaction**			**Rotational Reaction**		
	U1	**U2**	**U3**	**UR1**	**UR2**	**UR3**
displacement applied	65.66	-15.03	0.17	-0.31	0.04	0.01
	-15.03	65.66	-15.03	0.04	-0.31	0.04
	0.17	-15.03	65.66	0.01	0.04	-0.31
rotation applied	-1087.68	342.63	-21.28	135.11	-7.13	1.51
	342.63	-1087.68	342.63	-7.13	135.11	-7.13
	-21.28	342.63	-1087.68	1.51	-7.13	135.11

Table 5.7: d = 500mm; t = 11mm; bolt spacing = 2100mm

	d=	500	mm	b=	4.2	
	t=	11	mm	l=	0	
	Displacement applied			**Rotation applied**		
	bolt1	**bolt2**	**bolt3**	**bolt1**	**bolt2**	**bolt3**
RF1(N)	50036.70	-4911.74	752.69	-326684.00	-75479.60	29664.10
RF2(N)	17742.30	-10091.80	-50.33	-350292.00	211034.00	-32264.60
RF(N)	93263.70	-25855.36	768.50	-1077817.26	334909.11	-30275.04
RM3(N-mm)	-458361.00	40733.10	11413.20	138745000.00	-5177750.00	1248810.00

Reaction	**Translational Reaction**			**Rotational Reaction**		
	U1	**U2**	**U3**	**UR1**	**UR2**	**UR3**
displacement applied	93.26	-25.86	0.77	-0.46	0.04	0.01
	-25.86	93.26	-25.86	0.04	-0.46	0.04
	0.77	-25.86	93.26	0.01	0.04	-0.46
rotation applied	-1077.82	334.91	-30.28	138.75	-5.18	1.25
	334.91	-1077.82	334.91	-5.18	138.75	-5.18
	-30.28	334.91	-1077.82	1.25	-5.18	138.75

Table 5.8: d = 900mm; t = 11mm; bolt spacing = 2100mm

	d=	900	mm	b=	2.33	
	t=	11	mm	l=	0	
	Displacement applied			**Rotation applied**		
	bolt1	**bolt2**	**bolt3**	**bolt1**	**bolt2**	**bolt3**
RF1(N)	40071.40	-14244.10	292.12	593194.00	-520959.00	73526.80
RF2(N)	24189.10	-10086.90	-2487.37	-1594770.00	862589.00	-16752.10
RF(N)	94650.02	-36621.95	-4637.42	-2504558.48	1123608.72	51399.73
RM3(N-mm)	-282902.00	-21617.20	57534.70	219548000.00	-43521400.00	3093890.00
Reaction	**Translational Reaction**			**Rotational Reaction**		
	U1	**U2**	**U3**	**UR1**	**UR2**	**UR3**
	94.65	-36.62	-4.64	-0.28	-0.02	0.06
displacement applied	-36.62	94.65	-36.62	-0.02	-0.28	-0.02
	-4.64	-36.62	94.65	0.06	-0.02	-0.28
	-2504.56	1123.61	51.40	219.55	-43.52	3.09
rotation applied	1123.61	-2504.56	1123.61	-43.52	219.55	-43.52
	51.40	1123.61	-2504.56	3.09	-43.52	219.55

Table 5.9: d = 900mm; t = 11mm; bolt spacing = 2700mm

	d=	900	mm	b=	3	
	t=	11	mm	l=	0	
	Displacement applied			**Rotation applied**		
	bolt1	**bolt2**	**bolt3**	**bolt1**	**bolt2**	**bolt3**
RF1(N)	31708.90	-9006.49	646.52	292233.00	-333983.00	76802.10
RF2(N)	18672.20	-8480.47	-1686.23	-1104830.00	629993.00	-48456.70
RF(N)	73959.76	-27361.04	-2625.90	-1872208.50	874324.34	-8227.37
RM3(N-mm)	-299286.00	25342.50	48918.10	195120000.00	-30273200.00	4182400.00
Reaction	**Translational Reaction**			**Rotational Reaction**		
	U1	**U2**	**U3**	**UR1**	**UR2**	**UR3**
	73.96	-27.36	-2.63	-0.30	0.03	0.05
displacement applied	-27.36	73.96	-27.36	0.03	-0.30	0.03
	-2.63	-27.36	73.96	0.05	0.03	-0.30
	-1872.21	874.32	-8.23	195.12	-30.27	4.18
	874.32	-1872.21	874.32	-30.27	195.12	-30.27
	-8.23	874.32	-1872.21	4.18	-30.27	195.12

Table 5.10: d = 500mm; t = 11mm; bolt spacing = 1500mm

	d=	500	mm	b=	3	
	t=	11	mm	l=	0	
	Displacement applied			Rotation applied		
	bolt1	bolt2	bolt3	bolt1	bolt2	bolt3
RF1(N)	57158.30	-25971.20	-2128.70	-160779.00	-203280.00	62688.20
RF2(N)	17625.00	-8121.07	-62.34	-740765.00	449421.00	-66322.50
RF(N)	101252.66	-46231.98	-2582.77	-1667187.04	664107.59	-60256.78
RM3(N-mm)	657612.00	-237581.00	-57963.20	148993000.00	-12113600.00	2592230.00
Reaction	Translational Reaction			Rotational Reaction		
	U1	U2	U3	UR1	UR2	UR3
	101.25	-46.23	-2.58	0.66	-0.24	-0.06
displacement applied	-46.23	101.25	-46.23	-0.24	0.66	-0.24
	-2.58	-46.23	101.25	-0.06	-0.24	0.66
	-1667.19	664.11	-60.26	148.99	-12.11	2.59
rotation applied	664.11	-1667.19	664.11	-12.11	148.99	-12.11
	-60.26	664.11	-1667.19	2.59	-12.11	148.99

Figure 5.6 and 5.7 show the deformation of bolts under displacement.
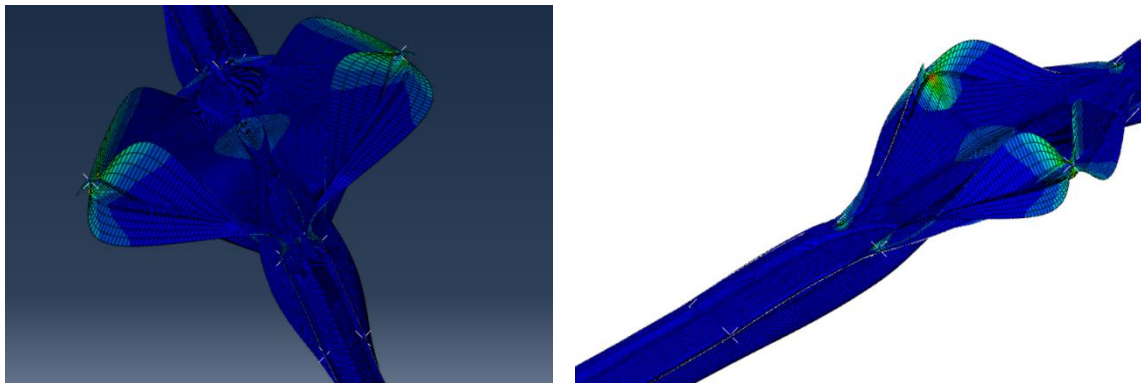
Figure 5.6: Deformation of the bolts
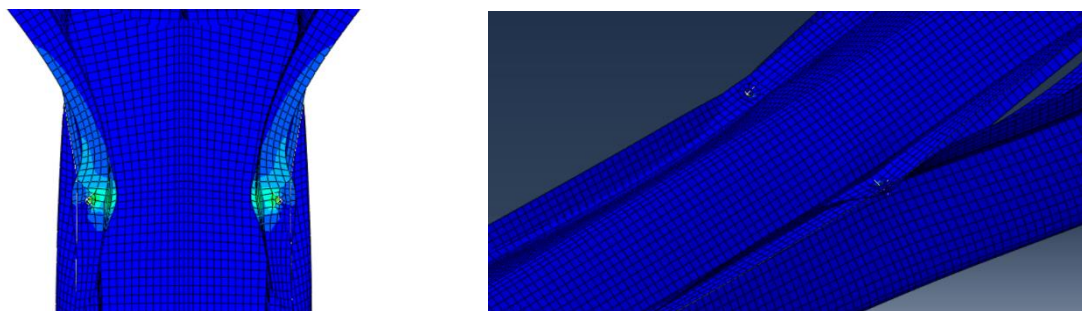
(a) Bolt 2   (b) Bolt 3

Figure 5.7: Detailed deformation

The displacement on bolt 1 and bolt 1' pull the bolts outwards, which are the same directions a=as the displacements, so reactions are in positive sign. As shown in Figure 5.7, the pairs of bolt 2 and bolt 3 are deformed inwards, which are the opposite directions of displacement, so the reactions have negative sign.

Figure 5.8 shows the deformation of bolts under rotation.
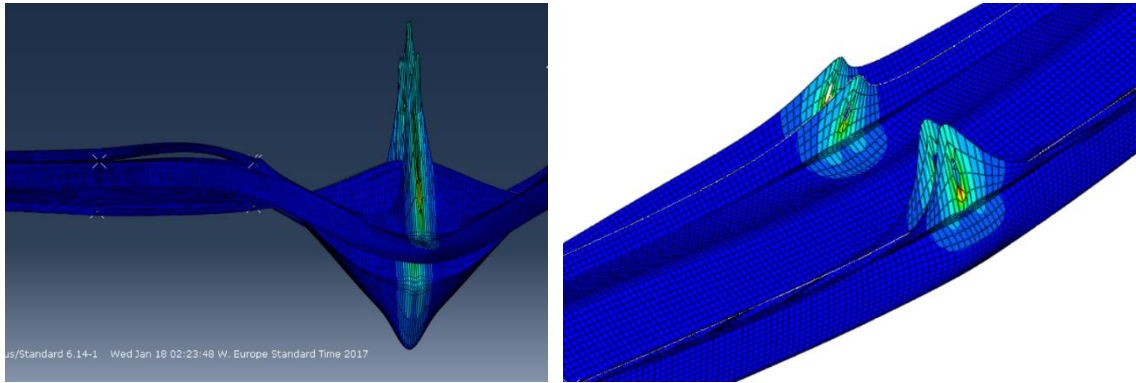
Figure 5.8: Deformation of bolts under rotation
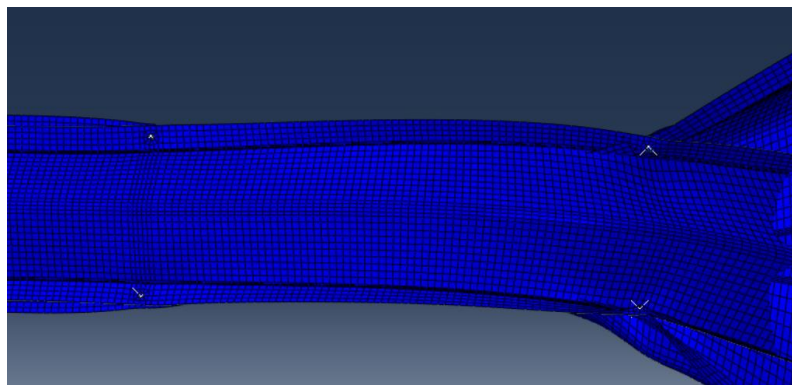
Figure 5.9: Detailed deformation of bolt 2 and 3

Figure 5.8 shows that the pair of bolt 1 and the pair of bolt 3 deform as the direction of loaded rotation; while the pair of bolt 2 deforms to the opposite direction as the rotational load.

5.4 Parametric comparison

Taking k_{11} of translational and rotational reactions, the parametric effects on bolt stiffness are shown as follows:

(1) Diameter

Table 5.12: Comparison of bolt stiffness of sections of different diameter (same bolt spacing ratio b = 3)

d	bolt spacing	t	U (kN)	UR (kNm)
500	1500	11	101.25	148.99
700	2100	11	84.73	151.66
900	2700	11	73.96	195.12
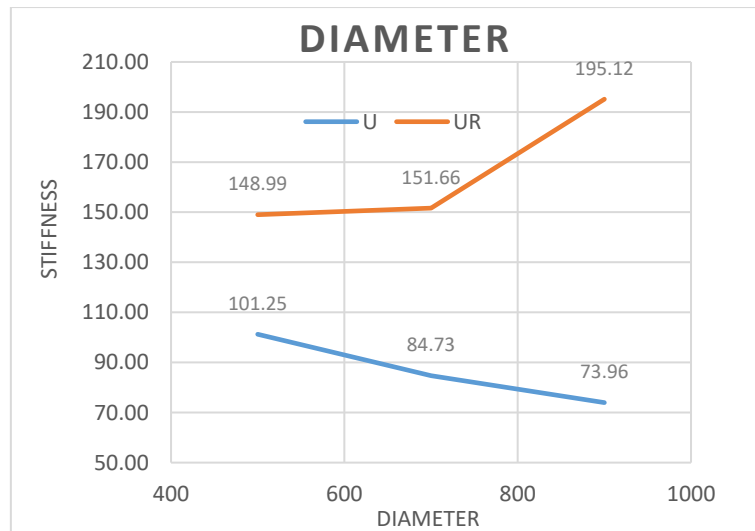
Figure 5.10: Comparison of bolt stiffness of sections of different diameter (same bolt spacing ratio b = 3)

The translational stiffness decreases as long as the diameter increases, while the rotational increases as long as the diameter increases. For same thickness, when diameter increases, the slenderness of cross section increases, which reduces the cross-sectional stiffness to against the translational load, the cross section is easier to deform. However, the closed cross section has benefits on against rotational load, the bigger the cross section, the hard it can be rotated.

(2) Thickness

Table 5.13: Comparison of bolt stiffness of sections of different thickness

d	t	U (kN)	UR (kNm)
700.00	11.00	84.73	151.66
700.00	12.00	101.08	188.20
700.00	13.00	119.71	232.98
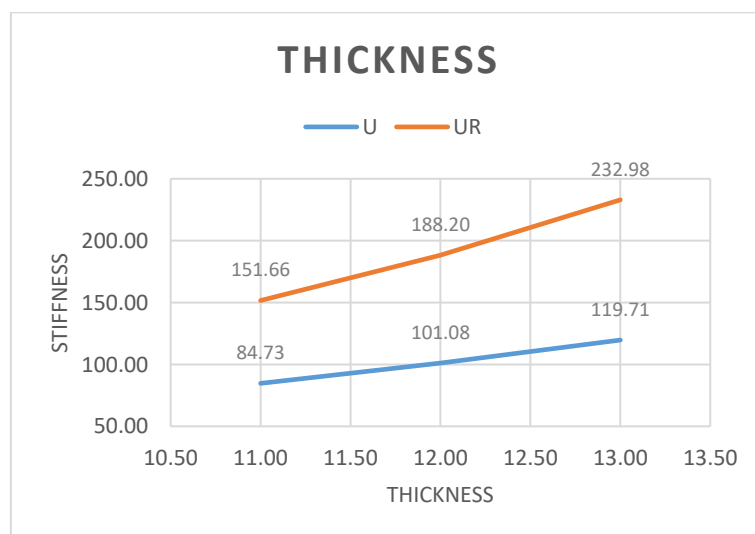
Figure 5.11: Comparison of bolt stiffness of sections of different thickness

Both translational and rotational stiffness increase as long as the thickness increase. The thicker the cross section, the larger the cross-sectional area, the larger the stiffness. Thicker plates have more benefits on against both translational and rotational deformation.

(3) Bolt spacing

Table 5.14: Comparison of bolt stiffness of sections of different bolt spacing

d	t	b	U (kN)	UR (kNm)
700.00	11.00	3.00	84.73	151.66
700.00	11.00	5.00	65.66	135.11
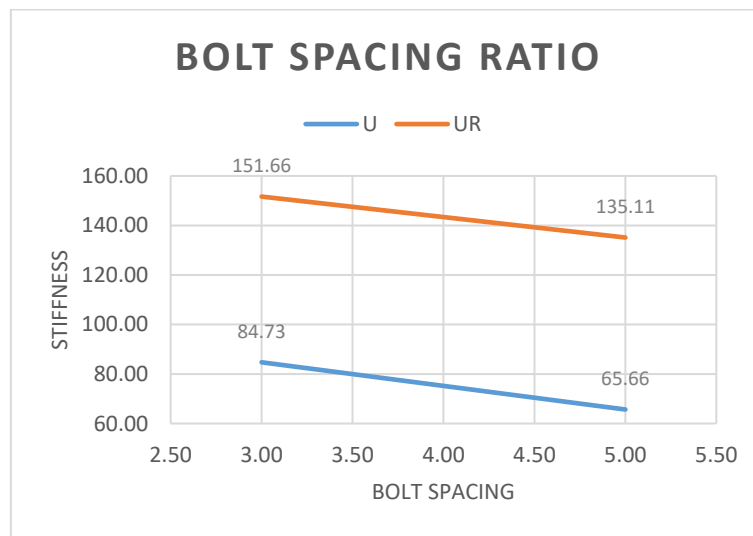
Figure 5.12: Comparison of bolt stiffness of sections of different bolt spacing

Both translational and rotational stiffness decrease as long as the bolt spacing decreases. Larger bolt spacing means smaller the bolt density, which means the stiffness of bolts in a particular length reduces.

6. Results and discussion

In this chapter, the meanings of i, j, k, l and b are shown below:

Table 6.1: i, j, k, l, b

á	Number of corner	1	6
j	diameter	2; 3; 4	500mm; 700mm; 900mm
k	Cross sectional slenderness	3 ;5	90; 110
l	lambda	1; 2; 3	0.65; 1; 1.25
b	Bolt spacing	3; 4; 5	3; 4; 5

6.1. History output from ABAQUS

History outputs for maximum loads and displacements of RIKS models are read by PYTHON (Annex).

6.2. Elastic buckling analysis

Linear elastic buckling analysis is used to check the eigen mode of shape of imperfection for RIKS analysis. The buckling shape mode and eigen values for all the models are shown in Table 6.2. The eigen buckling modes are shown in Annex F. Buckling critical stress is calculated as:

Eigenvalue/A

Table 6.2: Buckling shape and eigen values

i	j	k	l	b	buckling mode	Eigenvalue	A (mm^2)	Buckling critical stress (σ_{cr})
1	2	3	1	3	Distortional	8898760	15699.81	566.81
1	3	3	1	3	Distortional	15768400	29348.14	537.29
1	4	3	1	3	Distortional	24696200	47203.99	523.18
1	2	5	1	3	Distortional	5995460	12298.44	487.50
1	3	5	1	3	Distortional	11899900	24581.75	484.09
1	4	5	1	3	Distortional	19849900	41072.59	483.29
1	2	3	2	3	Flexural	5099450	15699.81	324.81
1	3	3	2	3	Flexural	9486620	29348.14	323.24
1	4	3	2	3	Flexural	15181500	47203.99	321.61
1	2	5	2	3	Flexural	4000870	12298.44	325.32
1	3	5	2	3	Flexural	7932600	24581.75	322.70
1	4	5	2	3	Flexural	13192600	41072.59	321.20
1	2	3	3	3	Flexural	3381900	15699.81	215.41
1	3	3	3	3	Flexural	6300420	29348.14	214.68
1	4	3	3	3	Flexural	10095400	47203.99	213.87
1	2	5	3	3	Flexural	2653540	12298.44	215.76
1	3	5	3	3	Flexural	5271230	24581.75	214.44
1	4	5	3	3	Flexural	8776650	41072.59	213.69
1	2	3	1	4	Distortional	6644620	15699.81	423.23
1	3	3	1	4	Distortional	11605400	29348.14	395.44
1	4	3	1	4	Distortional	17943000	47203.99	380.12
1	2	5	1	4	Distortional	4413400	12298.44	358.86
1	3	5	1	4	Distortional	8682950	24581.75	353.23
1	4	5	1	4	Distortional	14355400	41072.59	349.51
1	2	3	2	4	Flexural	5020520	15699.81	319.78
1	3	3	2	4	Flexural	9332690	29348.14	318.00

1	4	3	2	4	Flexural	14924100	47203.99	316.16
1	2	5	2	4	D+F	3936190	12298.44	320.06
1	3	5	2	4	Flexural	7796940	24581.75	317.18
1	4	5	2	4	Flexural	12956100	41072.59	315.44
1	2	3	3	4	Flexural	3349840	15699.81	213.37
1	3	3	3	4	Flexural	6238580	29348.14	212.57
1	4	3	3	4	Flexural	9991850	47203.99	211.67
1	2	5	3	4	D+F	2628450	12298.44	213.72
1	3	5	3	4	Flexural	5218000	24581.75	212.27
1	4	5	3	4	Flexural	8684710	41072.59	211.45
1	2	3	1	5	Distortional	1848000	15699.81	117.71
1	3	3	1	5	Distortional	9276780	29348.14	316.09
1	4	3	1	5	Distortional	14241900	47203.99	301.71
1	2	5	1	5	Distortional	3540220	12298.44	287.86
1	3	5	1	5	Distortional	6907450	24581.75	281.00
1	4	5	1	5	Distortional	11334700	41072.59	275.97
1	2	3	2	5	Distortional	4888520	15699.81	311.37
1	3	3	2	5	Distortional	8382510	29348.14	285.62
1	4	3	2	5	Distortional	12776600	47203.99	270.67
1	2	5	2	5	Distortional	3181650	12298.44	258.70
1	3	5	2	5	Distortional	6168540	24581.75	250.94
1	4	5	2	5	Distortional	10076400	41072.59	245.33
1	2	3	3	5	Flexural	3307680	15699.81	210.68
1	3	3	3	5	Flexural	6157130	29348.14	209.80
1	4	3	3	5	Flexural	9856750	47203.99	208.81
1	2	5	3	5	D+F	2594100	12298.44	210.93
1	3	5	3	5	Flexural	5146850	24581.75	209.38
1	4	5	3	5	Flexural	8563240	41072.59	208.49

As shown in Table 6.2, there are three buckling modes, which are distortional buckling, flexural buckling and distortional flexural buckling. Figure 6.1 shows the buckling shapes.
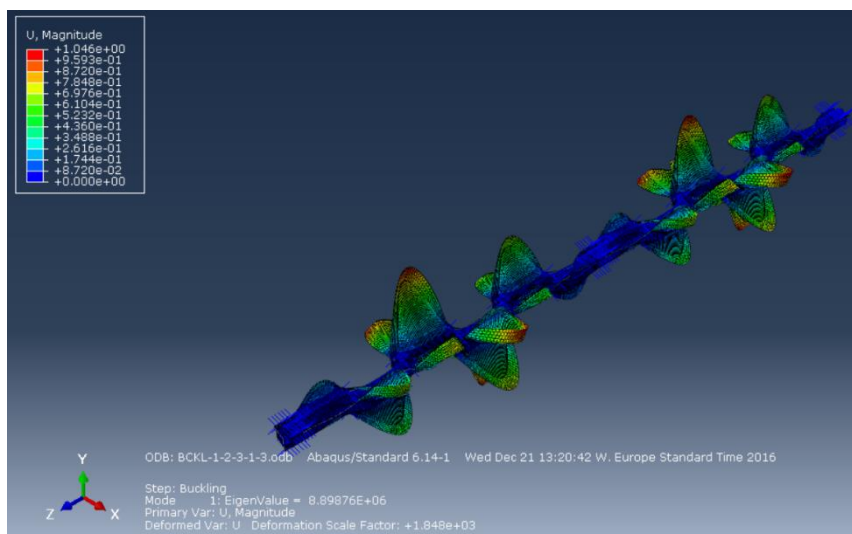
(a) Distortional
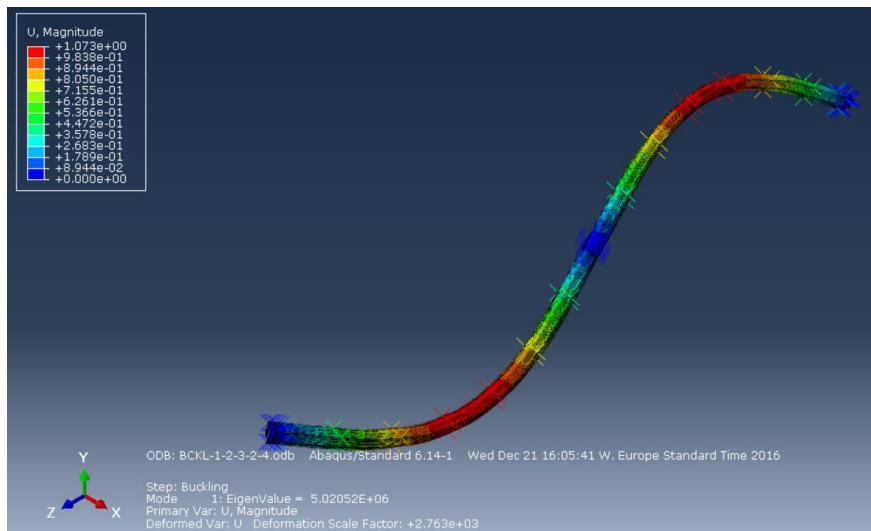
(b) Flexural
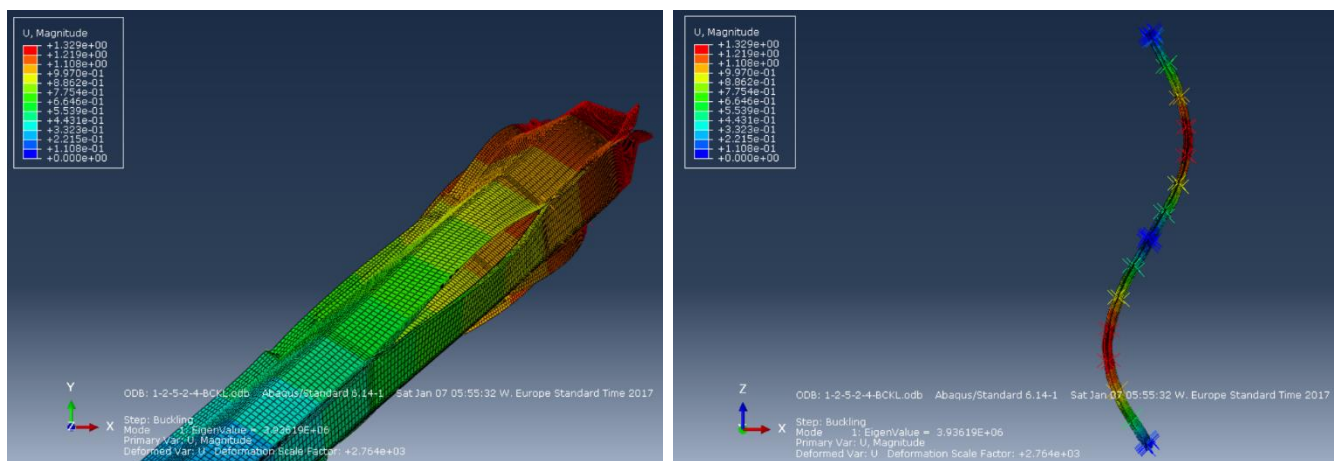
(c) Distortional + flexural
Figure 6.1: Buckling mode

Distortional buckling happens whenever lambda equals to 0.65, and some happen when lambda equals to 1. According to have-wave length method (Figure 6.2), long section tends to have global buckling while shorter section tends to have distortional buckling. Distortional buckling is related to the stiffness of the stiffeners, when the stiffness of the stiffener is low, it is easier to have distortional buckling.
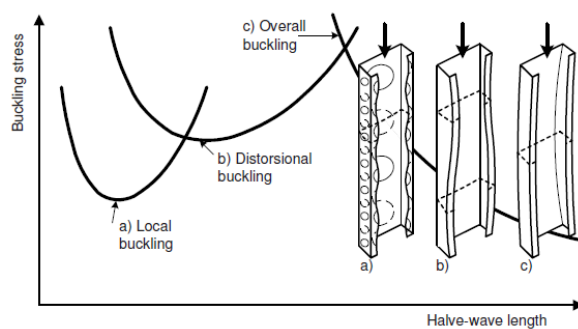
Figure 6.2: Examples of elastic critical stress for various buckling modes as function of half wave length and examples of buckling mode

Lips used to connect the sectors are considered as stiffeners of the sectors. Bolts have benefits on increasing the distortional buckling resistance. Table 6.3 shows the bolt density of all models. As shown in Table 6.3, the bolt density of the models that have distortional buckling is smaller than the models have flexural buckling. The lips of the models have distortional buckling are not stiff to against distortional buckling. For models have flexural buckling, they have enough distortional stiffness, also they have longer section, so the buckling modes tend to become flexural buckling.

Table 6.3 shows the bolt density of the models; bolt density is calculated as:

Bolt density = length of the section/bolt spacing

Table 6.3: Bolt density

i	j	k	l	b	bolt density	buckling mode
1	2	3	1	5	3.32	Distortional
1	3	3	1	5	3.32	Distortional
1	4	3	1	5	3.32	Distortional
1	2	5	1	5	3.32	Distortional
1	3	5	1	5	3.32	Distortional
1	4	5	1	5	3.32	Distortional
1	2	3	1	4	4.15	Distortional
1	3	3	1	4	4.15	Distortional
1	4	3	1	4	4.15	Distortional
1	2	5	1	4	4.15	Distortional
1	3	5	1	4	4.15	Distortional
1	4	5	1	4	4.15	Distortional
1	2	3	2	5	5.10	Distortional
1	3	3	2	5	5.10	Distortional
1	4	3	2	5	5.11	Distortional
1	2	5	2	5	5.11	Distortional
1	3	5	2	5	5.11	Distortional
1	4	5	2	5	5.11	Distortional
1	2	3	1	3	5.53	Distortional
1	3	3	1	3	5.53	Distortional
1	4	3	1	3	5.53	Distortional
1	2	5	1	3	5.53	Distortional
1	3	5	1	3	5.53	Distortional
1	4	5	1	3	5.53	Distortional

i	j	k	l	b	bolt density	buckling mode
1	2	3	2	4	6.38	Flexural
1	3	3	2	4	6.38	Flexural
1	4	3	2	4	6.38	Flexural
1	2	5	2	4	6.38	D+F
1	3	5	2	4	6.38	Flexural
1	4	5	2	4	6.38	Flexural
1	2	3	3	4	7.98	Flexural
1	3	3	3	4	7.98	Flexural
1	4	3	3	4	7.98	Flexural
1	2	5	3	4	7.98	D+F
1	3	5	3	4	7.98	Flexural
1	4	5	3	4	7.98	Flexural
1	2	3	2	3	8.51	Flexural
1	3	3	2	3	8.51	Flexural
1	4	3	2	3	8.51	Flexural
1	2	5	2	3	8.51	Flexural
1	3	5	2	3	8.51	Flexural
1	4	5	2	3	8.51	Flexural
1	2	3	3	3	10.63	Flexural
1	3	3	3	3	10.63	Flexural
1	4	3	3	3	10.64	Flexural
1	2	5	3	3	10.64	Flexural
1	3	5	3	3	10.64	Flexural
1	4	5	3	3	10.64	Flexural
1	2	3	3	5	6.38	Flexural
1	3	3	3	5	6.38	Flexural
1	4	3	3	5	6.38	Flexural
1	2	5	3	5	6.38	D+F
1	3	5	3	5	6.38	Flexural
1	4	5	3	5	6.38	Flexural

6.3. Geometrical data

The geometrical data of the cross sections are shown in Table 6.4. The geometrical data are taken from MATLAB and CFUSM.

Table 6.4: Geometrical data of cross sections

i	j	k	l	b	t (mm)	A (mm^2)	Iy (mm^4)	Iw (mm^6)	It (mm^4)	iy (mm)
1	2	3	1	3	8	15699.81	438338819.35	71719691303900.00	138358568.42	167.09
1	3	3	1	3	12	29348.14	1606289153.77	515533331039000.00	419903046.65	233.95
1	4	3	1	3	15	47203.99	4271198577.77	2267054666730000.00	951581582.26	300.81
1	2	5	1	3	7	12298.44	343729365.05	56424988253800.00	151870831.23	167.18
1	3	5	1	3	10	24581.75	1346405895.86	433130958156000.00	459425007.09	234.04
1	4	5	1	3	12	41072.59	3718528097.50	1977266778180000.00	1033091244.91	300.89
1	2	3	2	3	8	15699.81	438338819.35	71719691303900.00	138358568.42	167.09
1	3	3	2	3	12	29348.14	1606289153.77	515533331039000.00	419903046.65	233.95
1	4	3	2	3	15	47203.99	4271198577.77	2267054666730000.00	951581582.26	300.81
1	2	5	2	3	7	12298.44	343729365.05	56424988253800.00	151870831.23	167.18
1	3	5	2	3	10	24581.75	1346405895.86	433130958156000.00	459425007.09	234.04
1	4	5	2	3	12	41072.59	3718528097.50	1977266778180000.00	1033091244.91	300.89
1	2	3	3	3	8	15699.81	438338819.35	71719691303900.00	138358568.42	167.09
1	3	3	3	3	12	29348.14	1606289153.77	515533331039000.00	419903046.65	233.95
1	4	3	3	3	15	47203.99	4271198577.77	2267054666730000.00	951581582.26	300.81
1	2	5	3	3	7	12298.44	343729365.05	56424988253800.00	151870831.23	167.18
1	3	5	3	3	10	24581.75	1346405895.86	433130958156000.00	459425007.09	234.04
1	4	5	3	3	12	41072.59	3718528097.50	1977266778180000.00	1033091244.91	300.89
1	2	3	1	4	8	15699.81	438338819.35	71719691303900.00	138358568.42	167.09
1	3	3	1	4	12	29348.14	1606289153.77	515533331039000.00	419903046.65	233.95
1	4	3	1	4	15	47203.99	4271198577.77	2267054666730000.00	951581582.26	300.81
1	2	5	1	4	7	12298.44	343729365.05	56424988253800.00	151870831.23	167.18
1	3	5	1	4	10	24581.75	1346405895.86	433130958156000.00	459425007.09	234.04
1	4	5	1	4	12	41072.59	3718528097.50	1977266778180000.00	1033091244.91	300.89
1	2	3	2	4	8	15699.81	438338819.35	71719691303900.00	138358568.42	167.09
1	3	3	2	4	12	29348.14	1606289153.77	515533331039000.00	419903046.65	233.95
1	4	3	2	4	15	47203.99	4271198577.77	2267054666730000.00	951581582.26	300.81
1	2	5	2	4	7	12298.44	343729365.05	56424988253800.00	151870831.23	167.18
1	3	5	2	4	10	24581.75	1346405895.86	433130958156000.00	459425007.09	234.04
1	4	5	2	4	12	41072.59	3718528097.50	1977266778180000.00	1033091244.91	300.89
1	2	3	3	4	8	15699.81	438338819.35	71719691303900.00	138358568.42	167.09
1	3	3	3	4	12	29348.14	1606289153.77	515533331039000.00	419903046.65	233.95
1	4	3	3	4	15	47203.99	4271198577.77	2267054666730000.00	951581582.26	300.81
1	2	5	3	4	7	12298.44	343729365.05	56424988253800.00	151870831.23	167.18
1	3	5	3	4	10	24581.75	1346405895.86	433130958156000.00	459425007.09	234.04
1	4	5	3	4	12	41072.59	3718528097.50	1977266778180000.00	1033091244.91	300.89
1	2	3	1	5	8	15699.81	438338819.35	71719691303900.00	138358568.42	167.09
1	3	3	1	5	12	29348.14	1606289153.77	515533331039000.00	419903046.65	233.95
1	4	3	1	5	15	47203.99	4271198577.77	2267054666730000.00	951581582.26	300.81
1	2	5	1	5	7	12298.44	343729365.05	56424988253800.00	151870831.23	167.18
1	3	5	1	5	10	24581.75	1346405895.86	433130958156000.00	459425007.09	234.04

1	4	5	1	5	12	41072.59	3718528097.50	1977266778180000.00	1033091244.91	300.89
1	2	3	2	5	8	15699.81	438338819.35	71719691303900.00	138358568.42	167.09
1	3	3	2	5	12	29348.14	1606289153.77	515533331039000.00	419903046.65	233.95
1	4	3	2	5	15	47203.99	4271198577.77	2267054666730000.00	951581582.26	300.81
1	2	5	2	5	7	12298.44	343729365.05	56424988253800.00	151870831.23	167.18
1	3	5	2	5	10	24581.75	1346405895.86	433130958156000.00	459425007.09	234.04
1	4	5	2	5	12	41072.59	3718528097.50	1977266778180000.00	1033091244.91	300.89
1	2	3	3	5	8	15699.81	438338819.35	71719691303900.00	138358568.42	167.09
1	3	3	3	5	12	29348.14	1606289153.77	515533331039000.00	419903046.65	233.95
1	4	3	3	5	15	47203.99	4271198577.77	2267054666730000.00	951581582.26	300.81
1	2	5	3	5	7	12298.44	343729365.05	56424988253800.00	151870831.23	167.18
1	3	5	3	5	10	24581.75	1346405895.86	433130958156000.00	459425007.09	234.04
1	4	5	3	5	12	41072.59	3718528097.50	1977266778180000.00	1033091244.91	300.89

6.4. Resistance calculated by ABAQUS

Table 6.5 shows the resistances under different load modes calculated by ABAQUS. Unit of resistance is N.

Table 6.5: Resistance calculated by ABAQUS

i	j	k	l	b	N	N+0.05M	N+0.1M	N+0.15M
1	2	3	1	3	5625706.00	5605363.5	5545844	5466432.5
1	3	3	1	3	10583087.00	10451098	10282754	10116045
1	4	3	1	3	16670033.00	16582636	16390695	16126147
1	2	5	1	3	4132537.75	4123038.25	4092564.75	4058968.75
1	3	5	1	3	8309604.00	8190037.5	8055885	7938304
1	4	5	1	3	13828574.00	13775278	13673367	13559906
1	2	3	2	3	4865734.50	4666121	4520438	4401060
1	3	3	2	3	8974794.00	8689698	8469297	8272490.5
1	4	3	2	3	14330121.00	14622252	14090297	13637780
1	2	5	2	3	3665155.25	3868251	3797848.75	3677001.5
1	3	5	2	3	7105254.50	7334148	6955549.5	6813754
1	4	5	2	3	12124579.00	12608885	12315803	11998239
1	2	3	3	3	3335746.75	3363147.5	3321775.75	3275815.75
1	3	3	3	3	6192938.50	6401776	6215230	6088917.5
1	4	3	3	3	9958434.00	9967404	9732664	9732664
1	2	5	3	3	2606743.50	2682038.5	2615978.75	2565725
1	3	5	3	3	5177700.00	5147440	5090690.5	5037884.5
1	4	5	3	3	8656932.00	8678676	8581120	8464288
1	2	3	1	4	4982469.00	5014146.5	5036568.5	5043992.5
1	3	3	1	4	9053748.00	9129540	9188043	9231048
1	4	3	1	4	14571561.00	14640382	14498077	14491321
1	2	5	1	4	3576702.75	3590678.75	3596110.75	3595793.75
1	3	5	1	4	7358898.00	7341721.5	7270354.5	7169812
1	4	5	1	4	11788016.00	11839698	11871255	11869108
1	2	3	2	4	4554954.50	4690571	4744345	4601612
1	3	3	2	4	8128142.50	8263921.5	8202613	8033411.5
1	4	3	2	4	13158688.00	13515380	13774182	13247309

1	2	5	2	4	3241899.75	3268789.75	3227765.5	3178392.25
1	3	5	2	4	6373936.50	6515841.5	6567193	6461130
1	4	5	2	4	10701573.00	10806273	10639726	10480086
1	2	3	3	4	3269500.75	3306799.5	3269407.25	3219054
1	3	3	3	4	6020514.50	6150010.5	6284756.5	6052439.5
1	4	3	3	4	9777493.00	9806371	9638837	9424572
1	2	5	3	4	2496822.75	2565542	2571958	2512109.25
1	3	5	3	4	4985355.50	5019613	4947741	4872770
1	4	5	3	4	8400347.00	8399798	8293784	8188904
1	2	3	1	5	4531788.50	4508344	4483605	4465950
1	3	3	1	5	8140806.00	8166729.5	8123966	7977142.5
1	4	3	1	5	12630036.00	12678898	12662326	12435650
1	2	5	1	5	3161856.25	3151288.75	3130234.25	3082001.25
1	3	5	1	5	6417545.50	6408448.5	6351252	6090130.5
1	4	5	1	5	10664361.00	10588471	10487240	10408126
1	2	3	2	5	4126211.50	4135203.25	4064987.75	3979550.5
1	3	3	2	5	7400331.50	7346711	7212670	7094293
1	4	3	2	5	11412761.00	11446373	11255507	11059895
1	2	5	2	5	2840899.50	2803881.25	2768924.5	2734765.25
1	3	5	2	5	5661079.00	5593411.5	5520208	5455601
1	4	5	2	5	9216875.00	9074735	8937612	8813193
1	2	3	3	5	3176238.00	3231363.5	3199197.5	3155899
1	3	3	3	5	5901915.50	6029102.5	6401081.5	5909222.5
1	4	3	3	5	9320637.00	9345133	9249142	9135923
1	2	5	3	5	2405325.00	2473606.5	2694520	2420797.75
1	3	5	3	5	4682954.00	4729887	4746525.5	4691815.5
1	4	5	3	5	7913537.00	7874481.5	7772998	7669759

6.5. Parametric studies of ABAQUS results

6.5.1 Diameter
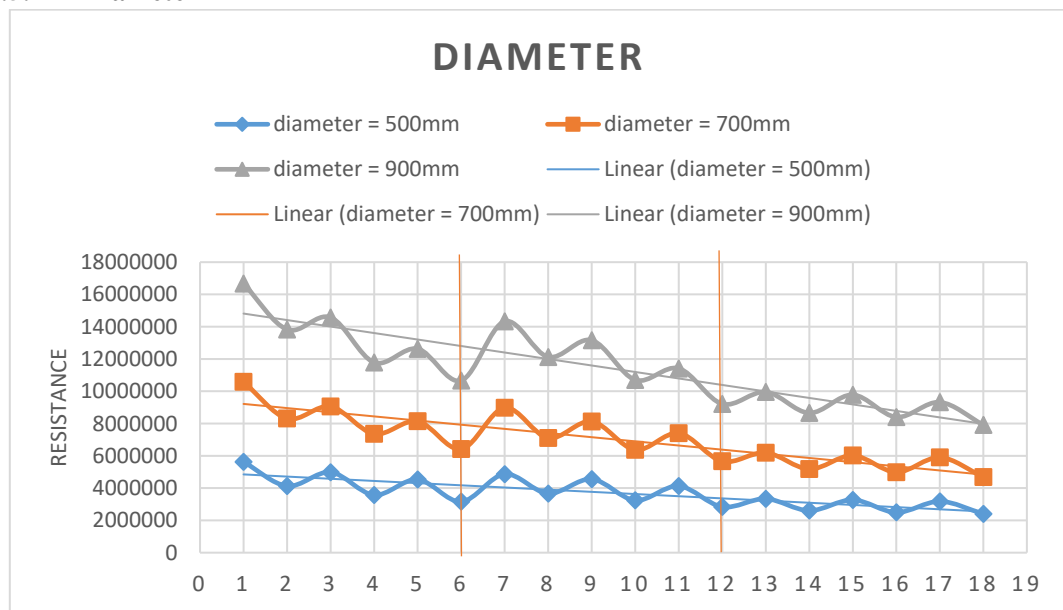
(a) Maximum load
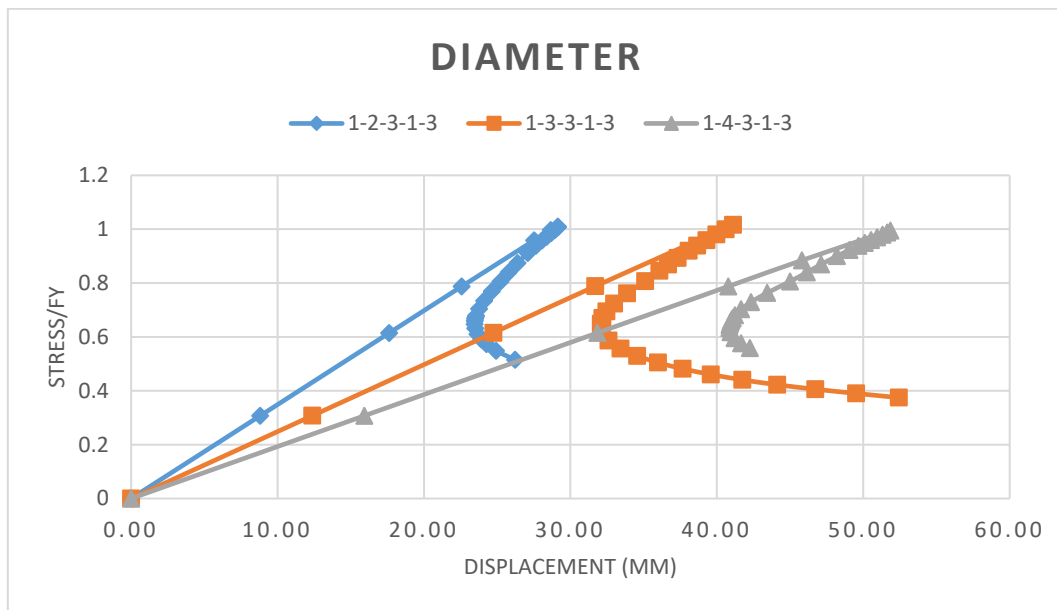
(b) History output

Figure 6.3: Variation of resistance calculated by ABAQUS along diameter

As shown in Figure 6.3 (a), the resistance increases as long as the cross-sectional diameter increases. When cross sectional diameter increases, the cross-sectional area increases, the critical stress decreases.

$$\sigma_{cr} = \frac{\pi^2 EI}{L^2} * \frac{1}{A}$$

In the figure, the trend lines show that the resistance decreases along the x-axis. x-axis represents the xth of models:

$$0 < x \leq 6: lambda = 0.65$$

$$6 < x \leq 12: lambda = 1$$

$$12 < x \leq 18: lambda = 1.25$$

However, when diameter is larger (900mm), the slope is more significant than the others. So, the larger the diameter, the easier the cross section influenced by length of the section. Also, as long as lambda increases, the difference between the resistances caused by different diameters tends to be smaller, which means the longer the section, the smaller the cross section influenced by diameter.

Figure 6.3 (b) shows the history output of displacement-load graphs of models with different diameters. Other parameters are fixed except diameter. As shown in the figure, the maximum loads of all models are closed, however, as long as the diameter decreases, the displacement where the structure reaches to maximum load decreases.

Also, as shown in Figure 6.3 (b), the smaller the cross-sectional diameter, the more sensitive it is to displacement. Small displacement can cause larger change of load.

6.5.2 Bolt spacing
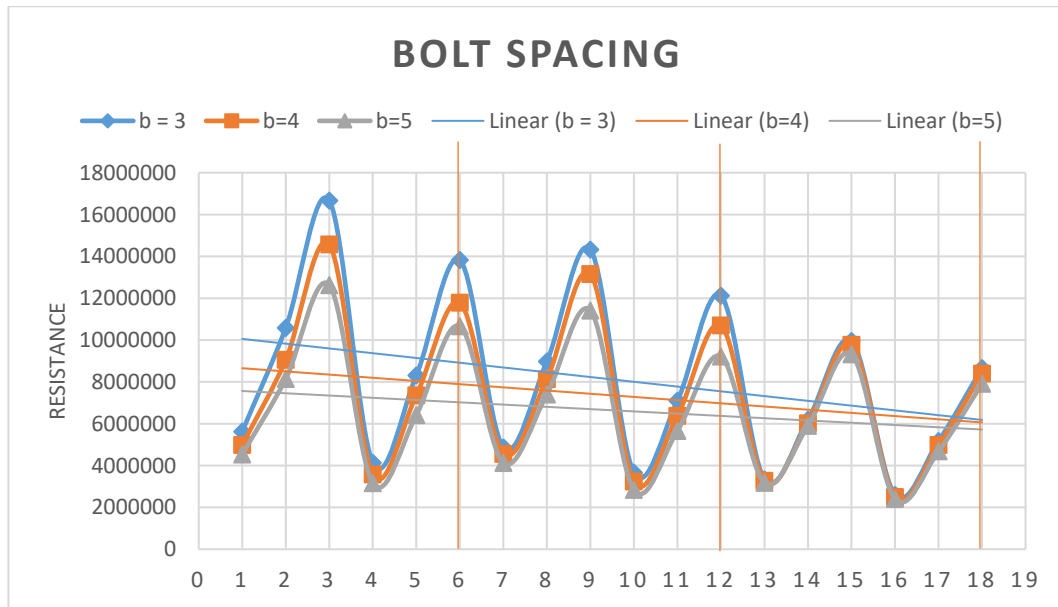
(a) Maximum load
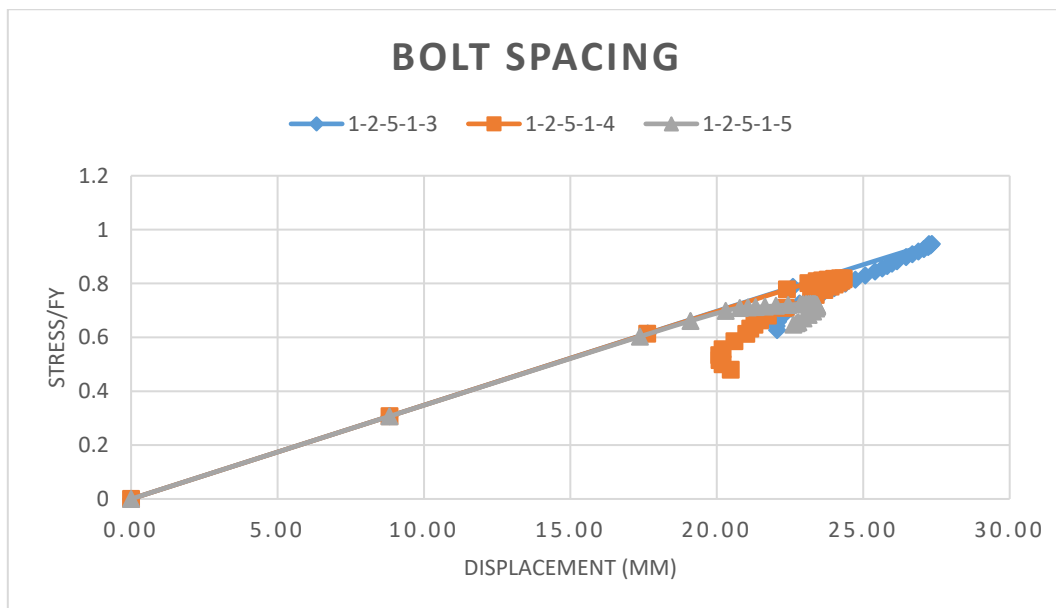
(b) History output

Figure 6.4: Variation of resistance calculated by ABAQUS along bolt spacing

As shown in Figure 6.4 (a), the resistance increases as long as the bolt spacing decreases. Smaller bolt spacing means larger bolt density, which leads to more stiffness of the lips. However, the difference of resistance calculated based on different bolt spacing is not very significant comparing to diameter.

In the figure, the trend lines show that the resistance decreases along the x-axis. x-axis represents the xth of models: $0<x\leq6$: lambda $= 0.65$

$$6<x\leq12: lambda = 1$$

62

$$12<x\leq18: \text{lambda} = 1.25$$

For same bolt spacing, the resistance decreases along the sectional length increases, however, the slope of the trendline is flatter comparing to diameter. So, sectional length has more influence on diameter comparing to bolt spacing. Furthermore, when sectional length increases, the resistances calculated based on different bolt spacing tend to be the same, so, the influence of bolt spacing on resistance is neglectable when the sectional length is beyond a limit.

Figure 6.4 (b) shows that the cross sections with different bolt spacing are not very sensitive to the displacement. The maximum load difference between different bolt spacing is not as significant as diameter.

6.5.3 Lambda
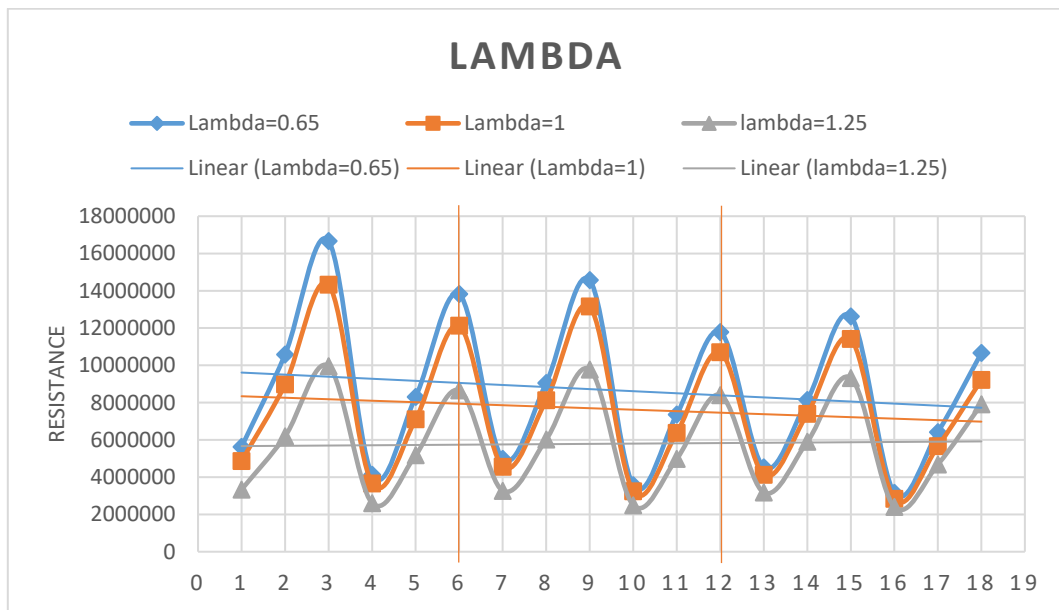
(a) Maximum load
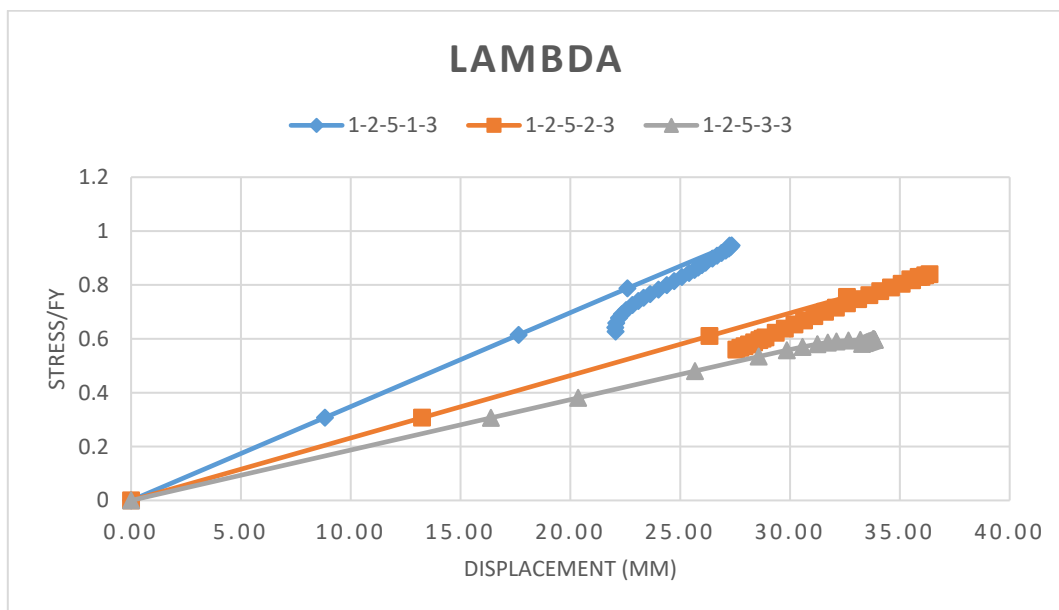
(b) History output

Figure 6.5: Variation of resistance calculated by ABAQUS along length

As shown in Figure 6.5 (a), the sectional slenderness has a significant influence on resistance. The shorter the section, the higher the resistance.

In the figure, the trend lines show that the resistance decreases along the x-axis. x-axis represents the xth of models:

$$0 < x \leq 6: b = 3$$

$$6 < x \leq 12: b = 4$$

$$12 < x \leq 18: b = 5$$

Bolt spacing has a small influence on sectional length when lambda is 0.65 and 1, while it cannot affect the behaviour of the structure when the length is big, as shown in 6.5.2.

According to Figure 6.5 (b), cross sections with difference sectional length are sensitive to variation of displacement. However, when the section is longer, it has less sensibility to the displacement.

6.5.4 Cross sectional slenderness
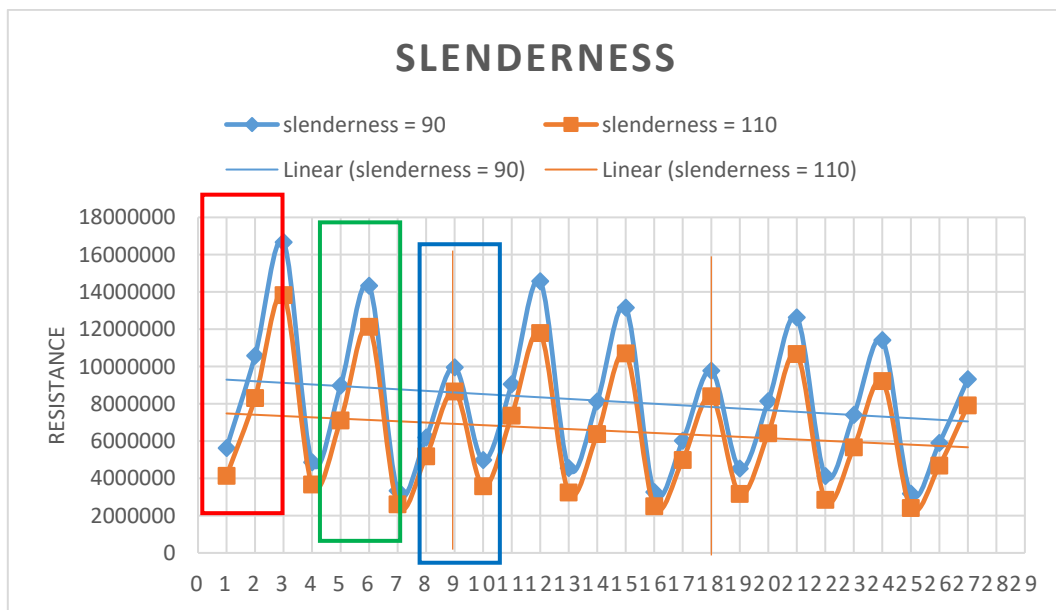
(a) Maximum load
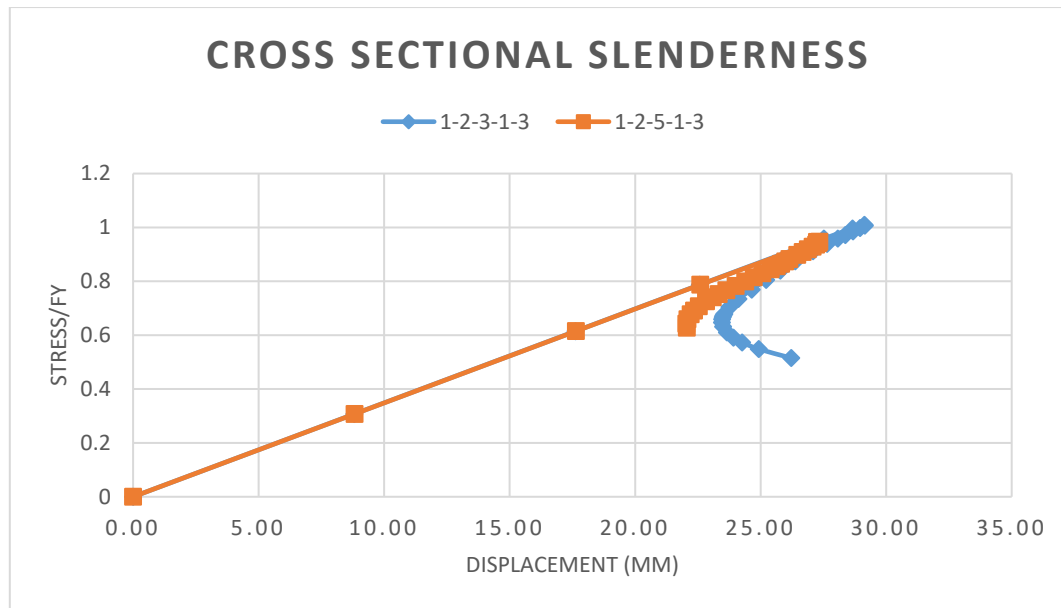
(b) History output

Figure 6.6: Variation of resistance calculated by ABAQUS along cross sectional slenderness

According to Figure 6.6 (a), smaller the cross-sectional slenderness, larger the thickness, larger the resistance the cross section has. The influence of cross-sectional slenderness is not as significant as diameter and sectional length.

In the figure, the trend lines show that the resistance decreases along the x-axis. x-axis represents the xth of models:

$$0<x\leq9: b= 3$$

$$9<x\leq18: b = 4$$

$$18<x\leq27: b = 5$$

And

$$0<x\leq3: l = 0.65$$

$$3<x\leq6: l = 1$$

$$6<x\leq9: l = 1.25$$

The slopes of the trendlines are flat, which means the bolt spacing has small influence on cross-sectional slenderness. Resistance increases as the diameter increases (as shown in the red cycle), however, for the next three x values (sectional length increases, green cycle), the resistance increase caused by diameter is not as significant as when the sectional length is short. This proves that the sectional length has significant influence on diameter, as shown in 6.5.1.

Cross sections with difference slenderness are not sensitive to the change of displacement (Figure 6.6 (b)).

6.5.5 Interaction

According to the analysis in previous sections, the most significant factors that influences the resistance is sectional length. When the section is long enough, the influence of bolt spacing is neglectable and the influence of diameter is less significant. Diameter also has significant influence on the resistance. No matter what else factor changes, resistance increases as long as diameter increases.
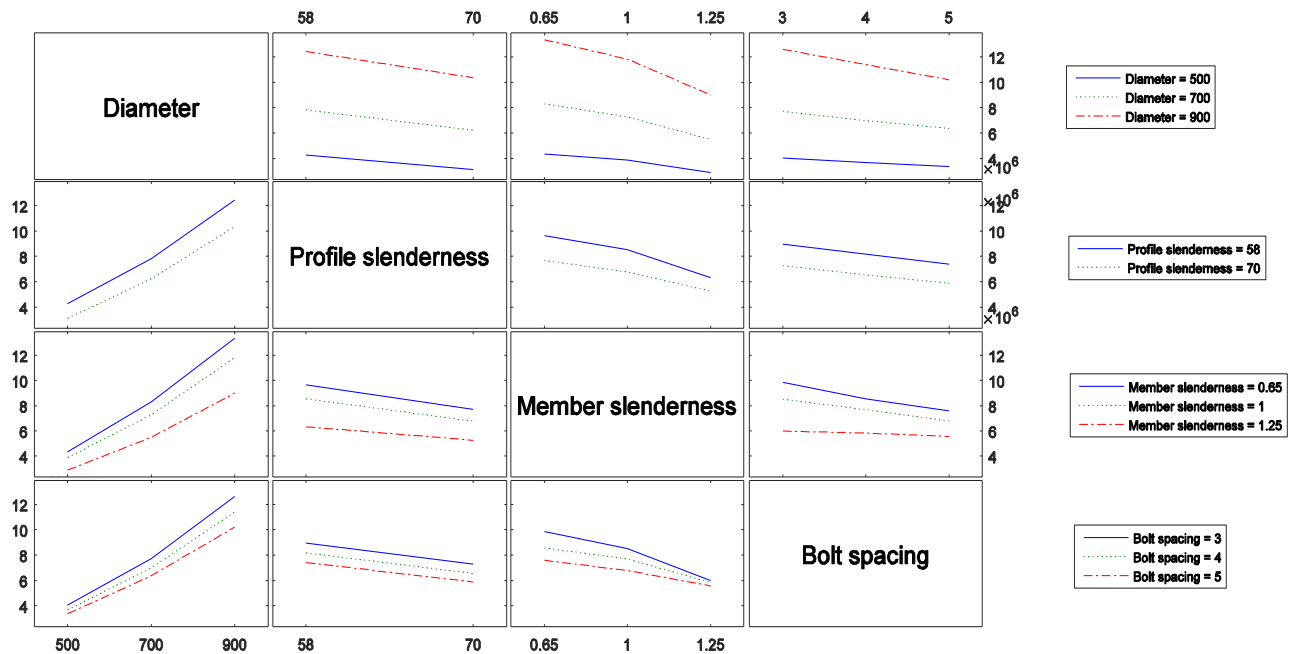
Figure 6.7: Parametric interaction plot of compression
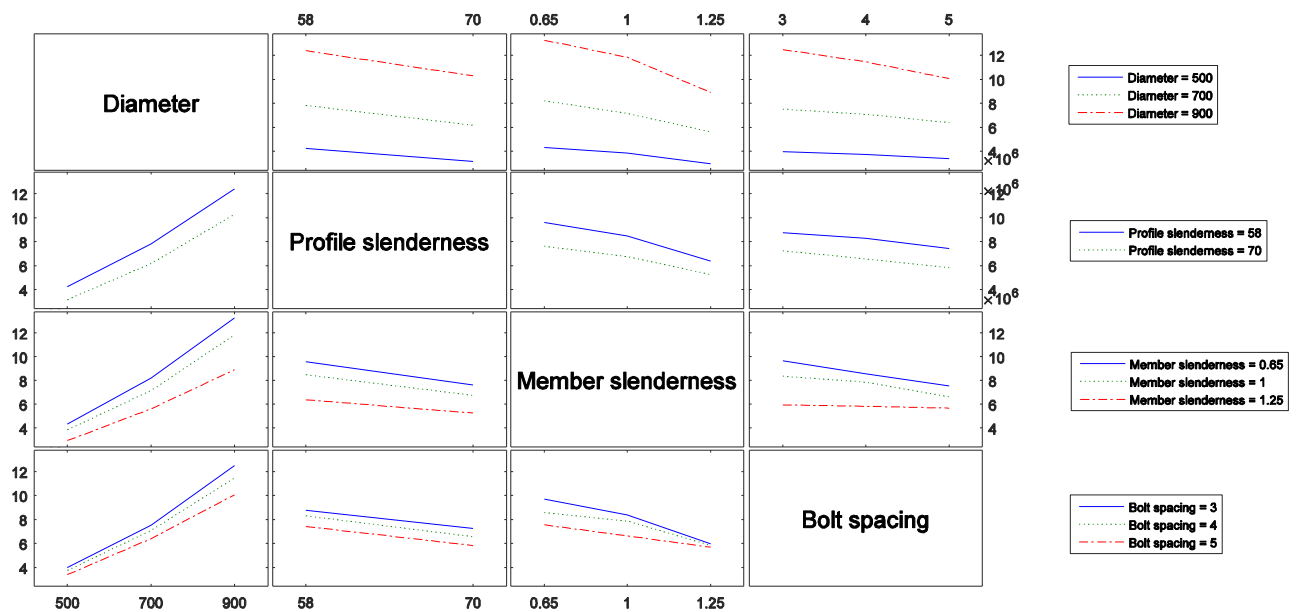
Figure 6.8: Parametric interaction plot of compression and moment

66

Figure 6.7 and 6.8 show the interaction of parametric influences on resistance under compression and compression with moment.

In the interaction plot, the bigger the slope, the more resistance is influenced by the factor. The more parallel the two lines, the less they influence each other. According to the interaction plot, the following results are given:

1. Diameter has the most significant influence on resistance.
2. Sectional length has significant influence on resistance.
3. The most significant interaction is between sectional length and bolt spacing.
4. Sectional length has influence on both diameter and bolt spacing.
5. Influence of bolt spacing becomes very little when sectional length is big.
6. Influence of diameter reduces when sectional length is big.
7. Cross-sectional slenderness and bolt spacing have the least significant influence on resistance.
8. Sectional length has less influence on resistance of cross sections with different slenderness.

6.6 classification

Lips are considered as the edge stiffener of the sector. The notional flat width of the web of the sector is calculated as Figure 6.9 (EN 1993-1-3), take the rounded corner effect into consideration.

$$r_m = r + t/2$$

$$g_r = r_m(\tan\left(\frac{\Phi}{2}\right) - \sin\left(\frac{\Phi}{2}\right))$$
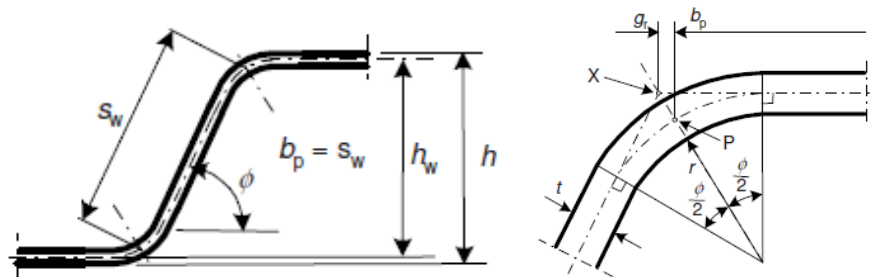
Figure 6.9: Notional flat width

The width of the web is taken as the radius of the cross section as the cross section is hexagonal. So, the notional flat width of the web is shown as follows:

$$h_w = \frac{d}{4} - g_{r\_corner} - g_{r\_lip}$$

$$s_w = h_w/\sin(30)$$

$$g_{r\_lip} = \left(r_{lip} + \frac{t}{2}\right) * (\tan(15) - \sin(15))$$

$$g_{r\_corner} = \left(r_{corner} + \frac{t}{2}\right) * (\tan(15) - \sin(15))$$

$$b_p = h_w/\sin(30)$$

Table 6.4 shows the notional flat width and classification of the webs of all cross sections, based on classification of part subject to compression.

Table 6.4: Classification as plated steel

i	j	k	l	b	r_corner	r_lip	gr_lip	gr_corner	hw	bp	c/t	class	buckling factor	critical stress	λ_p	reduction factor	Aeff
1	2	3	1	3	48	9.6	0.12	0.47	124.40	248.80	31.10	3	4	784.92	0.67	1.00	15708.13
1	3	3	1	3	72	14.4	0.19	0.71	174.10	348.20	29.02	2	4	901.68	0.63	1.00	29348.14
1	4	3	1	3	90	18	0.23	0.89	223.88	447.75	29.85	2	4	852.04	0.65	1.00	47203.99
1	2	5	1	3	42	8.4	0.11	0.42	124.48	248.95	35.56	4	4	600.24	0.77	0.93	11417.04
1	3	5	1	3	60	12	0.16	0.59	174.25	348.50	34.85	4	4	625.09	0.75	0.94	23096.50
1	4	5	1	3	72	14.4	0.19	0.71	224.10	448.20	37.35	4	4	544.21	0.81	0.90	37001.58
1	2	3	2	3	48	9.6	0.12	0.47	124.40	248.80	31.10	3	4	784.92	0.67	1.00	15708.13
1	3	3	2	3	72	14.4	0.19	0.71	174.10	348.20	29.02	2	4	901.68	0.63	1.00	29348.14
1	4	3	2	3	90	18	0.23	0.89	223.88	447.75	29.85	2	4	852.04	0.65	1.00	47203.99
1	2	5	2	3	42	8.4	0.11	0.42	124.48	248.95	35.56	4	4	600.24	0.77	0.93	11417.04
1	3	5	2	3	60	12	0.16	0.59	174.25	348.50	34.85	4	4	625.09	0.75	0.94	23096.50
1	4	5	2	3	72	14.4	0.19	0.71	224.10	448.20	37.35	4	4	544.21	0.81	0.90	37001.58
1	2	3	3	3	48	9.6	0.12	0.47	124.40	248.80	31.10	3	4	784.92	0.67	1.00	15708.13
1	3	3	3	3	72	14.4	0.19	0.71	174.10	348.20	29.02	2	4	901.68	0.63	1.00	29348.14
1	4	3	3	3	90	18	0.23	0.89	223.88	447.75	29.85	2	4	852.04	0.65	1.00	47203.99
1	2	5	3	3	42	8.4	0.11	0.42	124.48	248.95	35.56	4	4	600.24	0.77	0.93	11417.04
1	3	5	3	3	60	12	0.16	0.59	174.25	348.50	34.85	4	4	625.09	0.75	0.94	23096.50
1	4	5	3	3	72	14.4	0.19	0.71	224.10	448.20	37.35	4	4	544.21	0.81	0.90	37001.58
1	2	3	1	4	48	9.6	0.12	0.47	124.40	248.80	31.10	3	4	784.92	0.67	1.00	15708.13
1	3	3	1	4	72	14.4	0.19	0.71	174.10	348.20	29.02	2	4	901.68	0.63	1.00	29348.14
1	4	3	1	4	90	18	0.23	0.89	223.88	447.75	29.85	2	4	852.04	0.65	1.00	47203.99
1	2	5	1	4	42	8.4	0.11	0.42	124.48	248.95	35.56	4	4	600.24	0.77	0.93	11417.04
1	3	5	1	4	60	12	0.16	0.59	174.25	348.50	34.85	4	4	625.09	0.75	0.94	23096.50
1	4	5	1	4	72	14.4	0.19	0.71	224.10	448.20	37.35	4	4	544.21	0.81	0.90	37001.58
1	2	3	2	4	48	9.6	0.12	0.47	124.40	248.80	31.10	3	4	784.92	0.67	1.00	15708.13
1	3	3	2	4	72	14.4	0.19	0.71	174.10	348.20	29.02	2	4	901.68	0.63	1.00	29348.14
1	4	3	2	4	90	18	0.23	0.89	223.88	447.75	29.85	2	4	852.04	0.65	1.00	47203.99
1	2	5	2	4	42	8.4	0.11	0.42	124.48	248.95	35.56	4	4	600.24	0.77	0.93	11417.04
1	3	5	2	4	60	12	0.16	0.59	174.25	348.50	34.85	4	4	625.09	0.75	0.94	23096.50
1	4	5	2	4	72	14.4	0.19	0.71	224.10	448.20	37.35	4	4	544.21	0.81	0.90	37001.58
1	2	3	3	4	48	9.6	0.12	0.47	124.40	248.80	31.10	3	4	784.92	0.67	1.00	15708.13
1	3	3	3	4	72	14.4	0.19	0.71	174.10	348.20	29.02	2	4	901.68	0.63	1.00	29348.14
1	4	3	3	4	90	18	0.23	0.89	223.88	447.75	29.85	2	4	852.04	0.65	1.00	47203.99
1	2	5	3	4	42	8.4	0.11	0.42	124.48	248.95	35.56	4	4	600.24	0.77	0.93	11417.04
1	3	5	3	4	60	12	0.16	0.59	174.25	348.50	34.85	4	4	625.09	0.75	0.94	23096.50
1	4	5	3	4	72	14.4	0.19	0.71	224.10	448.20	37.35	4	4	544.21	0.81	0.90	37001.58
1	2	3	1	5	48	9.6	0.12	0.47	124.40	248.80	31.10	3	4	784.92	0.67	1.00	15708.13
1	3	3	1	5	72	14.4	0.19	0.71	174.10	348.20	29.02	2	4	901.68	0.63	1.00	29348.14
1	4	3	1	5	90	18	0.23	0.89	223.88	447.75	29.85	2	4	852.04	0.65	1.00	47203.99
1	2	5	1	5	42	8.4	0.11	0.42	124.48	248.95	35.56	4	4	600.24	0.77	0.93	11417.04
1	3	5	1	5	60	12	0.16	0.59	174.25	348.50	34.85	4	4	625.09	0.75	0.94	23096.50
1	4	5	1	5	72	14.4	0.19	0.71	224.10	448.20	37.35	4	4	544.21	0.81	0.90	37001.58
1	2	3	2	5	48	9.6	0.12	0.47	124.40	248.80	31.10	3	4	784.92	0.67	1.00	15708.13
1	3	3	2	5	72	14.4	0.19	0.71	174.10	348.20	29.02	2	4	901.68	0.63	1.00	29348.14
1	4	3	2	5	90	18	0.23	0.89	223.88	447.75	29.85	2	4	852.04	0.65	1.00	47203.99
1	2	5	2	5	42	8.4	0.11	0.42	124.48	248.95	35.56	4	4	600.24	0.77	0.93	11417.04
1	3	5	2	5	60	12	0.16	0.59	174.25	348.50	34.85	4	4	625.09	0.75	0.94	23096.50
1	4	5	2	5	72	14.4	0.19	0.71	224.10	448.20	37.35	4	4	544.21	0.81	0.90	37001.58
1	2	3	3	5	48	9.6	0.12	0.47	124.40	248.80	31.10	3	4	784.92	0.67	1.00	15708.13
1	3	3	3	5	72	14.4	0.19	0.71	174.10	348.20	29.02	2	4	901.68	0.63	1.00	29348.14
1	4	3	3	5	90	18	0.23	0.89	223.88	447.75	29.85	2	4	852.04	0.65	1.00	47203.99
1	2	5	3	5	42	8.4	0.11	0.42	124.48	248.95	35.56	4	4	600.24	0.77	0.93	11417.04
1	3	5	3	5	60	12	0.16	0.59	174.25	348.50	34.85	4	4	625.09	0.75	0.94	23096.50
1	4	5	3	5	72	14.4	0.19	0.71	224.10	448.20	37.35	4	4	544.21	0.81	0.90	37001.58

6.7 Resistance calculation based on EN 1993-1-3

Since the geometric data are calculated by CUFSM, the reduction of area and moment of inertia due to rounded corner is not taken into consideration.

Take model 1-3-3-1-3 as the calculation example for distortional buckling reduction.

$d = 700mm$; $t = 12mm$; $A = 29348.14mm^2$; $I = 1606289153.77mm^4$

Step 1: Effective area due to class 4 cross section

Calculation of notional flat width:

$$r_{corner} = 6 * 12 = 72mm$$

$$r_{lip} = \frac{1}{5} * 72 = 14.4mm$$

$$g_{r\_lip} = (14.4 + 12/2) * (\tan(15) - \sin(15)) = 0.186$$

$$g_{r\_corner} = (72 + 12/2) * (\tan(15) - \sin(15)) = 0.71$$

$$h_w = \frac{700}{4} - 0.19 - 0.71 = 174.1mm$$

$$b_p = \frac{174.1}{\sin(30)} = 348.2$$

Step 2: Reduction due to distortional buckling (EN 1993-1-3)

$$c = l_{lip} = 0.1 * 700 = 70mm$$

$$b_{p,c} = 70 - (\frac{0.186}{\sin(30)}) = 69.63mm$$

Reduction of stiffener (lip):

$$\frac{b_{p,c}}{b_p} = 0.2 < 0.35$$

$$\therefore k_\sigma = 0.5$$

$$\lambda_p = \frac{69.63/12}{28.4 * 0.81 * \sqrt{0.5}} = 0.36$$

$$\rho = 1$$

$$c_{eff} = 69.62mm$$

$$b_{e1} = b_{e2} = \frac{348.2 * 1}{2} = 174.1mm$$

$$A_s = (b_{e1} + c_{eff}) * t = (174.1 + 69.63) * 12 = 2924.7mm^2$$

$$I_s = \left(\frac{1}{12} * 12 * 69.63^3\right) + \left(\frac{1}{12} * 12^3 * 174.1\right) = 362623.9mm^4$$

Resistance of Polygonal Cross Section of Lattice Wind Tower

$$b_1 = 177mm$$

$$K = \frac{210000 * 12^3}{4 * (1 - 0.3^2)} * \frac{1}{177^2 * 174.1 + 177^3 + 0.5 * 177 * 177 * 1} = 3.22$$

$$\sigma_{cr,s} = \frac{2 * \sqrt{3.22 * 210000 * 362623.9}}{2924.7} = 338.44 N/mm^2$$

$$\overline{\lambda_d} = \sqrt{355/338.44} = 1.02$$

$$\chi_d = 1.47 - 1.02 * 0.723 = 0.73$$

So, the reduction factor for stiffness is 0.73.

Effective stiffener area is $2924.7*0.73 = 2135.031mm^2$

The total reduced area of stiffener is calculated as:

$$(2924.7\text{-}2135.031) * 6 = 4738.014$$

The effective cross-sectional area is:

$$29348.14\text{-}4738.014 = 24610.126mm^2$$

The resistance is calculated as:

$$24610.126*355 = 8736594.73N$$

Step 3: Reduction due to flexural buckling (EN 1993-1-1)

Take model 1-2-3-2-3 as the example.

$d = 500mm$; $t = 8mm$; $A = 15699.81mm^2$; $A_{eff} = 15699.81\ mm^2$; $I = 438338819.35mm^4$; $L = 12760.95mm$

$$N_{cr} = \frac{\pi^2 * 210000 * 438338819.35}{12760.95^2} = 3327469.239N$$

$$\bar{\lambda} = \sqrt{15699.81 * \frac{355}{3327469.239}} = 1$$

$$\Phi = 0.5 * (1 + 0.34 * (1 - 0.2) + 1^2) = 1.136$$

$$\chi = \frac{1}{1.136 + \sqrt{1.136^2 - 1^2}} = 0.6$$

Table 6.5 shows the distortional resistance calculated based on EN 1993-1-3 for all cross sections. Table 6.6 shows the flexural resistance calculated based on EN 1993-1-1 for all cross sections.

Resistance of Polygonal Cross Section of Lattice Wind Tower

Table 6.5: Distortional resistance calculated based on EN 1993-1-3

i	j	k	l	b	l_lip	bp,c	be1	bpc/bp	buckling factor	stiffener λ_p	Reduction factor	ceff	As	Is	b1	K	Critical stress	λ_d	Xd	stiffener Aeff	Reduced area	total Aeff	Distortional Ncr,d	
1	2	3	1	3	50	49.8	124	0.20	0.5	0.38	1	49.75	1393.22	87405.59	176.88	2.60	313.45	1.06	0.70	976.06	417.17	13196.82	4684869.61	Distortional
1	3	3	1	3	70	69.6	174	0.20	0.5	0.36	1	69.63	2924.75	362623.91	246.97	3.22	338.44	1.02	0.73	2133.66	791.09	24601.62	8733575.70	Distortional
1	4	3	1	3	90	89.5	224	0.20	0.5	0.37	1	89.53	4701.17	960144.95	317.87	2.95	327.99	1.04	0.72	3374.61	1326.56	39244.64	13931847.87	Distortional
1	2	5	1	3	50	49.8	116	0.20	0.5	0.44	1	49.78	1157.36	75273.08	177.92	1.71	284.48	1.12	0.66	766.57	390.79	9072.29	3220661.55	Distortional
1	3	5	1	3	70	69.7	164	0.20	0.5	0.43	1	69.69	2334.12	295691.10	248.85	1.83	288.52	1.11	0.67	1559.24	774.88	18447.19	6548752.58	Distortional
1	4	5	1	3	90	89.6	202	0.20	0.5	0.46	1	89.63	3498.20	749057.62	321.01	1.47	275.12	1.14	0.65	2269.37	1228.83	29628.60	10518154.36	Distortional
1	2	3	1	4	50	49.8	124	0.20	0.5	0.38	1	49.75	1393.22	87405.59	176.88	2.60	313.45	1.06	0.70	976.06	417.17	13196.82	4684869.61	Distortional
1	3	3	1	4	70	69.6	174	0.20	0.5	0.36	1	69.63	2924.75	362623.91	246.97	3.22	338.44	1.02	0.73	2133.66	791.09	24601.62	8733575.70	Distortional
1	4	3	1	4	90	89.5	224	0.20	0.5	0.37	1	89.53	4701.17	960144.95	317.87	2.95	327.99	1.04	0.72	3374.61	1326.56	39244.64	13931847.87	Distortional
1	2	5	1	4	50	49.8	116	0.20	0.5	0.44	1	49.78	1157.36	75273.08	177.92	1.71	284.48	1.12	0.66	766.57	390.79	9072.29	3220661.55	Distortional
1	3	5	1	4	70	69.7	164	0.20	0.5	0.43	1	69.69	2334.12	295691.10	248.85	1.83	288.52	1.11	0.67	1559.24	774.88	18447.19	6548752.58	Distortional
1	4	5	1	4	90	89.6	202	0.20	0.5	0.46	1	89.63	3498.20	749057.62	321.01	1.47	275.12	1.14	0.65	2269.37	1228.83	29628.60	10518154.36	Distortional
1	2	5	2	4	50	49.8	116	0.20	0.5	0.44	1	49.78	1157.36	75273.08	177.92	1.71	284.48	1.12	0.66	766.57	390.79	9072.29	3220661.55	D+F
1	2	5	3	4	50	49.8	116	0.20	0.5	0.44	1	49.78	1157.36	75273.08	177.92	1.71	284.48	1.12	0.66	766.57	390.79	9072.29	3220661.55	D+F
1	2	3	1	5	50	49.8	124	0.20	0.5	0.38	1	49.75	1393.22	87405.59	176.88	2.60	313.45	1.06	0.70	976.06	417.17	13196.82	4684869.61	Distortional
1	3	3	1	5	70	69.6	174	0.20	0.5	0.36	1	69.63	2924.75	362623.91	246.97	3.22	338.44	1.02	0.73	2133.66	791.09	24601.62	8733575.70	Distortional
1	4	3	1	5	90	89.5	224	0.20	0.5	0.37	1	89.53	4701.17	960144.95	317.87	2.95	327.99	1.04	0.72	3374.61	1326.56	39244.64	13931847.87	Distortional
1	2	5	1	5	50	49.8	116	0.20	0.5	0.44	1	49.78	1157.36	75273.08	177.92	1.71	284.48	1.12	0.66	766.57	390.79	9072.29	3220661.55	Distortional
1	3	5	1	5	70	69.7	164	0.20	0.5	0.43	1	69.69	2334.12	295691.10	248.85	1.83	288.52	1.11	0.67	1559.24	774.88	18447.19	6548752.58	Distortional
1	4	5	1	5	90	89.6	202	0.20	0.5	0.46	1	89.63	3498.20	749057.62	321.01	1.47	275.12	1.14	0.65	2269.37	1228.83	29628.60	10518154.36	Distortional
1	2	3	2	5	50	49.8	124	0.20	0.5	0.38	1	49.75	1393.22	87405.59	176.88	2.60	313.45	1.06	0.70	976.06	417.17	13196.82	4684869.61	Distortional
1	3	3	2	5	70	69.6	174	0.20	0.5	0.36	1	69.63	2924.75	362623.91	246.97	3.22	338.44	1.02	0.73	2133.66	791.09	24601.62	8733575.70	Distortional
1	4	3	2	5	90	89.5	224	0.20	0.5	0.37	1	89.53	4701.17	960144.95	317.87	2.95	327.99	1.04	0.72	3374.61	1326.56	39244.64	13931847.87	Distortional
1	2	5	2	5	50	49.8	116	0.20	0.5	0.44	1	49.78	1157.36	75273.08	177.92	1.71	284.48	1.12	0.66	766.57	390.79	9072.29	3220661.55	Distortional
1	3	5	2	5	70	69.7	164	0.20	0.5	0.43	1	69.69	2334.12	295691.10	248.85	1.83	288.52	1.11	0.67	1559.24	774.88	18447.19	6548752.58	Distortional
1	4	5	2	5	90	89.6	202	0.20	0.5	0.46	1	89.63	3498.20	749057.62	321.01	1.47	275.12	1.14	0.65	2269.37	1228.83	29628.60	10518154.36	Distortional
1	2	5	3	5	50	49.9	116	0.20	0.5	0.44	1	49.78	1157.36	75273.08	177.92	1.71	284.48	1.12	0.66	766.57	390.79	9072.29	3220661.55	D+F

71

Table 6.6: Flexural resistance calculated based on EN 1993-1-3

	i	j	k	l	b	Ncr	λ	Φ	χ	Flexural Aeff	Flexural resistance
Flexural	1	2	3	2	3	5573433.81	1.00	1.14	0.60	9375.48	3328294.43
Flexural	1	3	3	2	3	10418589.57	1.00	1.14	0.60	17521.52	6220139.59
Flexural	1	4	3	2	3	16757417.57	1.00	1.14	0.60	28181.88	10004566.92
Flexural	1	2	5	2	3	4365947.88	0.96	1.09	0.62	7082.30	2514217.19
Flexural	1	3	5	2	3	8726522.14	0.97	1.10	0.62	14241.22	5055632.37
Flexural	1	4	5	2	3	14580768.65	0.95	1.08	0.63	23294.20	8269442.12
Flexural	1	2	3	3	3	3566997.64	1.25	1.46	0.45	7093.36	2518141.52
Flexural	1	3	3	3	3	6667897.32	1.25	1.46	0.45	13257.79	4706513.87
Flexural	1	4	3	3	3	10724747.25	1.25	1.46	0.45	21324.02	7570028.33
Flexural	1	2	5	3	3	2794206.64	1.20	1.40	0.48	5431.74	1928268.86
Flexural	1	3	5	3	3	5584974.17	1.21	1.41	0.47	10897.96	3868776.43
Flexural	1	4	5	3	3	9331691.94	1.19	1.37	0.49	17965.82	6377866.45
Flexural	1	2	3	2	4	5573433.81	1.00	1.14	0.60	9375.48	3328294.43
Flexural	1	3	3	2	4	10418589.57	1.00	1.14	0.60	17521.52	6220139.59
Flexural	1	4	3	2	4	16757417.57	1.00	1.14	0.60	28181.88	10004566.92
D+F	1	2	5	2	4	4365947.88	0.96	1.09	0.62	7082.30	2428301.79
Flexural	1	3	5	2	4	8726522.14	0.97	1.10	0.62	14241.22	5055632.37
Flexural	1	4	5	2	4	14580768.65	0.95	1.08	0.63	23294.20	8269442.12
Flexural	1	2	3	3	4	3566997.64	1.25	1.46	0.45	7093.36	2518141.52
Flexural	1	3	3	3	4	6667897.32	1.25	1.46	0.45	13257.79	4706513.87
Flexural	1	4	3	3	4	10724747.25	1.25	1.46	0.45	21324.02	7570028.33
D+F	1	2	5	3	4	2794206.64	1.20	1.40	0.48	5431.74	1862376.39
Flexural	1	3	5	3	4	5584974.17	1.21	1.41	0.47	10897.96	3868776.43
Flexural	1	4	5	3	4	9331691.94	1.19	1.37	0.49	17965.82	6377866.45
Flexural	1	2	3	3	5	3566997.64	1.25	1.46	0.45	7093.36	2518141.52
Flexural	1	3	3	3	5	6667897.32	1.25	1.46	0.45	13257.79	4706513.87
Flexural	1	4	3	3	5	10724747.25	1.25	1.46	0.45	21324.02	7570028.33
D+F	1	2	5	3	5	2794206.64	1.20	1.40	0.48	5431.74	1862376.39
Flexural	1	3	5	3	5	5584974.17	1.21	1.41	0.47	10897.96	3868776.43
Flexural	1	4	5	3	5	9331691.94	1.19	1.37	0.49	17965.82	6377866.45

6.8 Comparison between EN1993-1-3 and ABAQUS

Table 6.7 and Figure 6.7 shows the comparison between resistances calculated based on EN 1993-1-3 and ABAQUS.

Table 6.7: Comparison between resistances calculated based on EN 1993-1-3 and ABAQUS

i	j	k	l	b	EN	ABAQUS	Difference (%)	Difference	
1	2	3	1	3	4684869.61	5625706	16.72	-940836.39	Distortional
1	3	3	1	3	8733575.70	10583087	17.48	-1849511.30	Distortional
1	4	3	1	3	13931847.87	16670033	16.43	-2738185.13	Distortional
1	2	5	1	3	3220661.55	4132537.75	22.07	-911876.20	Distortional
1	3	5	1	3	6548752.58	8309604	21.19	-1760851.42	Distortional
1	4	5	1	3	10518154.36	13828574	23.94	-3310419.64	Distortional
1	2	3	2	3	3327469.24	4865734.5	31.61	-1538265.26	Flexural
1	3	3	2	3	6220139.59	8974794	30.69	-2754654.41	Flexural
1	4	3	2	3	10004566.92	14330121	30.19	-4325554.08	Flexural
1	2	5	2	3	2514217.19	3665155.25	31.40	-1150938.06	Flexural
1	3	5	2	3	5055632.37	7105254.5	28.85	-2049622.13	Flexural
1	4	5	2	3	8269442.12	12124579	31.80	-3855136.88	Flexural
1	2	3	3	3	2517753.80	3335746.75	24.52	-817992.95	Flexural
1	3	3	3	3	4706513.87	6192938.5	24.00	-1486424.63	Flexural
1	4	3	3	3	7570028.33	9958434	23.98	-2388405.67	Flexural
1	2	5	3	3	1928268.86	2606743.5	26.03	-678474.64	Flexural
1	3	5	3	3	3868776.43	5177700	25.28	-1308923.57	Flexural
1	4	5	3	3	6377866.45	8656932	26.33	-2279065.55	Flexural
1	2	3	1	4	4684869.61	4982469	5.97	-297599.39	Distortional
1	3	3	1	4	8733575.70	9053748	3.54	-320172.30	Distortional
1	4	3	1	4	13931847.87	14571561	4.39	-639713.13	Distortional
1	2	5	1	4	3220661.55	3576702.75	9.95	-356041.20	Distortional
1	3	5	1	4	6548752.58	7358898	11.01	-810145.42	Distortional
1	4	5	1	4	10518154.36	11788016	10.77	-1269861.64	Distortional
1	2	3	2	4	3327469.24	4554954.5	26.95	-1227485.26	Flexural
1	3	3	2	4	6220139.59	8128142.5	23.47	-1908002.91	Flexural
1	4	3	2	4	10004566.92	13158688	23.97	-3154121.08	Flexural
1	2	5	2	4	1997863.942	3241899.75	38.37	-1244035.81	D+F
1	3	5	2	4	5055632.367	6373936.5	20.68	-1318304.13	Flexural
1	4	5	2	4	8269442.121	10701573	22.73	-2432130.88	Flexural
1	2	3	3	4	2517753.802	3269500.75	22.99	-751746.95	Flexural
1	3	3	3	4	4706513.866	6020514.5	21.83	-1314000.63	Flexural
1	4	3	3	4	7570028.329	9777493	22.58	-2207464.67	Flexural
1	2	5	3	4	1532253.793	2496822.75	38.63	-964568.96	D+F
1	3	5	3	4	3868776.426	4985355.5	22.40	-1116579.07	Flexural
1	4	5	3	4	6377866.446	8400347	24.08	-2022480.55	Flexural
1	2	3	**1**	**5**	4684869.613	4531788.5	3.38	**153081.11**	Distortional
1	3	3	**1**	**5**	8733575.699	8140806	7.28	**592769.70**	Distortional
1	4	3	**1**	**5**	13931847.87	12630036	10.31	**1301811.87**	Distortional
1	2	5	**1**	**5**	3220661.549	3161856.25	1.86	**58805.30**	Distortional

73

1	3	5	**1**	**5**	6548752.58	6417545.5	2.04	**131207.08**	Distortional
1	4	5	**1**	**5**	10518154.36	10664361	1.37	-146206.64	Distortional
1	2	3	**2**	**5**	4684869.613	4126211.5	13.54	**558658.11**	Distortional
1	3	3	**2**	**5**	8733575.699	7400331.5	18.02	**1333244.20**	Distortional
1	4	3	**2**	**5**	13931847.87	11412761	22.07	**2519086.87**	Distortional
1	2	5	**2**	**5**	3220661.549	2840899.5	13.37	**379762.05**	Distortional
1	3	5	**2**	**5**	6548752.58	5661079	15.68	**887673.58**	Distortional
1	4	5	**2**	**5**	10518154.36	9216875	14.12	**1301279.36**	Distortional
1	2	3	3	5	2517753.802	3176238	20.73	-658484.20	Flexural
1	3	3	3	5	4706513.866	5901915.5	20.25	-1195401.63	Flexural
1	4	3	3	5	7570028.329	9320637	18.78	-1750608.67	Flexural
1	2	5	3	5	1532253.793	2405325	36.30	-873071.21	D+F
1	3	5	3	5	3868776.426	4682954	17.39	-814177.57	Flexural
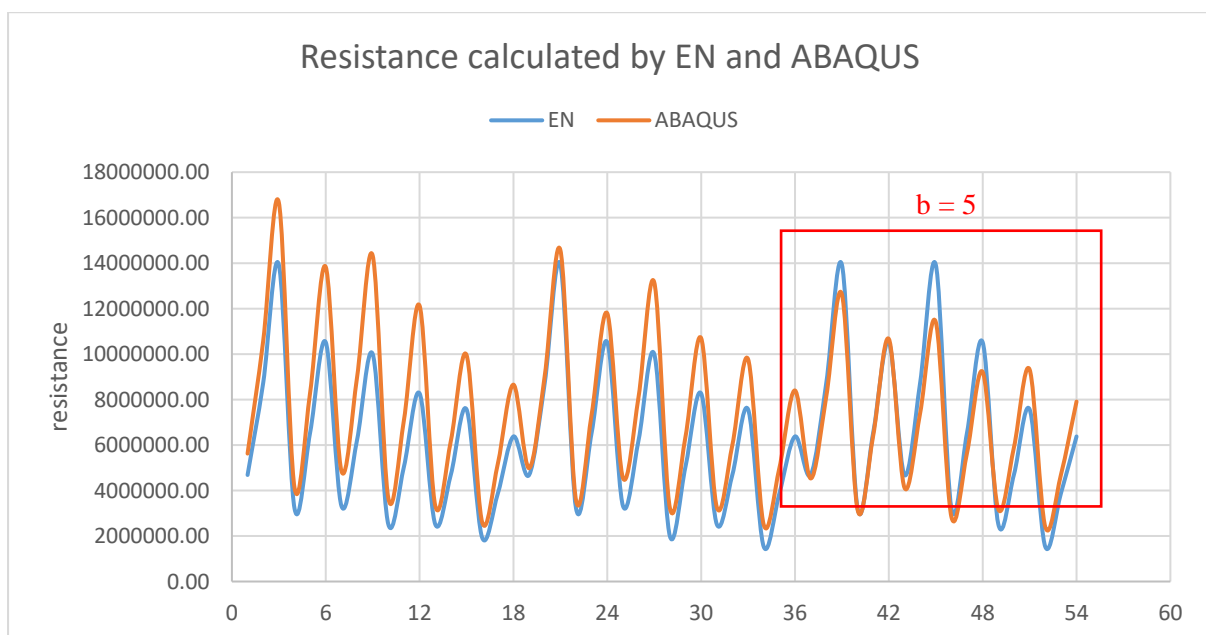
Figure 6.11: Comparison between resistance calculated based on EN 1993-1-3 and ABAQUS

6.8.1   Models in unsafe region

Generally, the resistance calculated based on Eurocode is supposed to be lower than the resistance calculated by numerical method, however, as shown in Figure 6.11, there are some models have resistances calculated by EN 1993-1-3 higher than the ones calculated by ABAQUS. According to Figure 6.11, it seems that the models are in unsafe regions have large bolt spacing (b=5). So, the differences between resistances calculated based on EN 1993-1-3 and ABAQUS under different values of sectional length and bolt spacing are compared as shown in Figure 6.12 and 6.13.
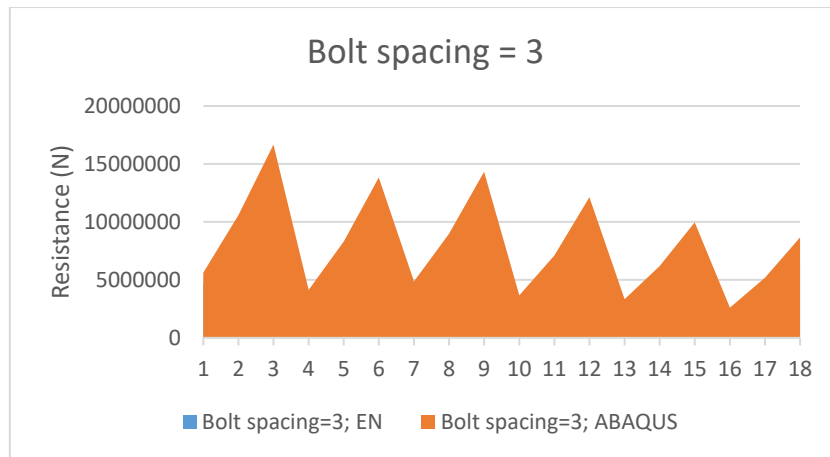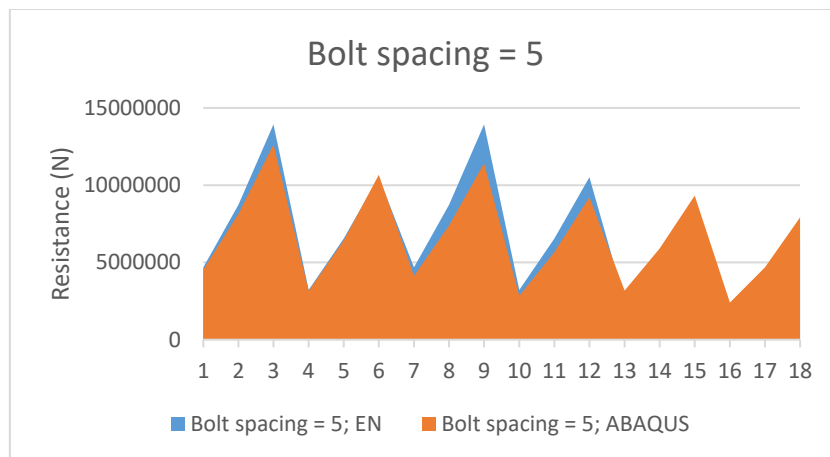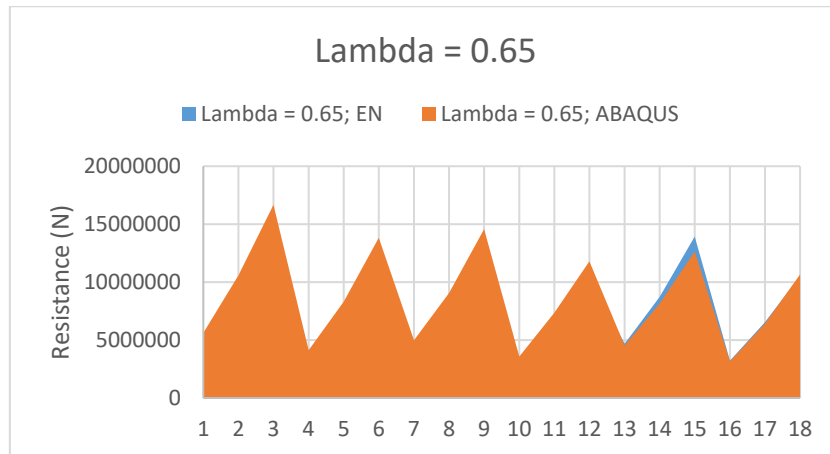
(a) b = 3
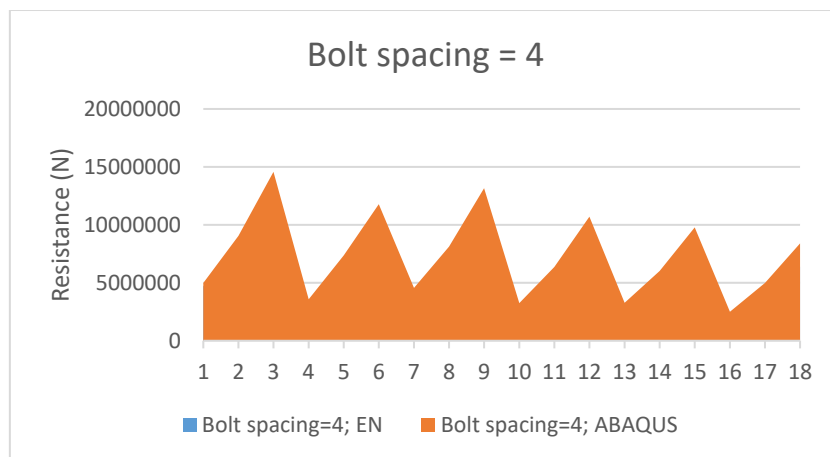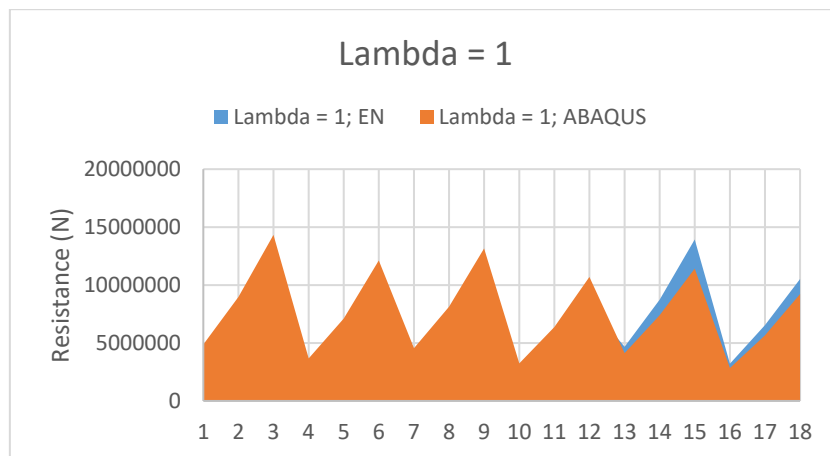

(b) b = 4

(c) b = 5

Figure 6.12: Comparison between resistances calculated based on EN 1993-1-3 and ABAQUS under different bolt spacing

Resistance of Polygonal Cross Section of Lattice Wind Tower
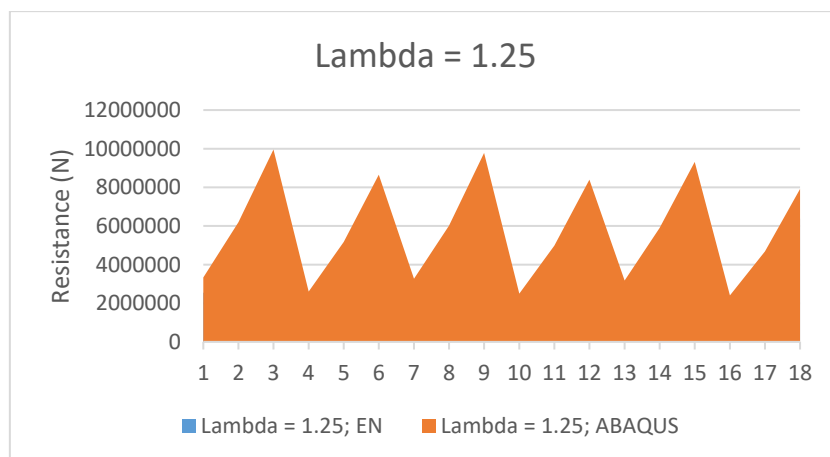
According to Figure 6.12, when bolt spacing increases (b = 5), there are more models in unsafe regions.

(a) Lambda = 0.65

(b) Lambda = 1

(c) Lambda = 1.25

Figure 6.13: Comparison between resistances calculated based on EN 1993-1-3 and ABAQUS under different sectional length

Resistance of Polygonal Cross Section of Lattice Wind Tower

According to Figure 6.13, when sectional length is shorter (lambda = 0.65 and 1), there are more models in unsafe region.

Table 6.8: Models in unsafe region

i	j	k	l	b	EN	ABAQUS	Difference (%)	Difference		Bolt density
1	2	3	1	5	4684869.613	4531788.5	3.38	153081.11	Distortional	3.32
1	3	3	1	5	8733575.699	8140806	7.28	592769.70	Distortional	3.32
1	4	3	1	5	13931847.87	12630036	10.31	1301811.87	Distortional	3.32
1	2	5	1	5	3220661.549	3161856.25	1.86	58805.30	Distortional	3.32
1	3	5	1	5	6548752.58	6417545.5	2.04	131207.08	Distortional	3.32
1	2	3	2	5	4684869.613	4126211.5	13.54	558658.11	Distortional	5.10
1	3	3	2	5	8733575.699	7400331.5	18.02	1333244.20	Distortional	5.10
1	4	3	2	5	13931847.87	11412761	22.07	2519086.87	Distortional	5.11
1	2	5	2	5	3220661.549	2840899.5	13.37	379762.05	Distortional	5.11
1	3	5	2	5	6548752.58	5661079	15.68	887673.58	Distortional	5.11
1	4	5	2	5	10518154.36	9216875	14.12	1301279.36	Distortional	5.11

Table 6.9: Models of distortional buckling which are in safe region

i	j	k	l	b	EN	ABAQUS	Difference (%)	Difference		Bolt density
1	2	3	1	3	4684869.61	5625706	16.72	-940836.39	Distortional	5.53
1	3	3	1	3	8733575.70	10583087	17.48	-1849511.30	Distortional	5.53
1	4	3	1	3	13931847.87	16670033	16.43	-2738185.13	Distortional	5.53
1	2	5	1	3	3220661.55	4132537.8	22.07	-911876.20	Distortional	5.53
1	3	5	1	3	6548752.58	8309604	21.19	-1760851.42	Distortional	5.53
1	4	5	1	3	10518154.36	13828574	23.94	-3310419.64	Distortional	5.53
1	2	3	1	4	4684869.61	4982469	5.97	-297599.39	Distortional	4.15
1	3	3	1	4	8733575.70	9053748	3.54	-320172.30	Distortional	4.15
1	4	3	1	4	13931847.87	14571561	4.39	-639713.13	Distortional	4.15
1	2	5	1	4	3220661.55	3576702.8	9.95	-356041.20	Distortional	4.15
1	3	5	1	4	6548752.58	7358898	11.01	-810145.42	Distortional	4.15
1	4	5	1	4	10518154.36	11788016	10.77	-1269861.64	Distortional	4.15

The resistance calculated based on Eurocode considers the perfect cross section, and consider the whole section as the rigid body (the entire lips are rigid body constrained). However, in ABAQUS, only the bolted areas are rigid body constrained, which causes the distortional stiffness strongly depends on the bolt spacing (as the size of the bolt remains the same). When the bolts cannot provide enough distortional stiffness, the section has low resistance.

The tables above show all the distortional buckling models. As shown in Table 6.8, all models that are in unsafe region have distortional buckling mode. Comparing to the models in safe region, which are shown in Table 6.9, when the sectional length remains the same, the larger the bolt spacing, the smaller the bolt density, the smaller the resistance calculated by ABAQUS, which causes the models unsafe. For the same cross section, the lower the stiffness, the lower the critical stress of stiffener, the lower the resistance.

$$\sigma_{cr} = \frac{2\sqrt{EIK}}{A}$$

However, as shown in Table 6.8, when section is longer, even though the bolt density is large, the models are still in unsafe region. When section is longer, it tends to have flexural buckling. Due to the interaction of distortional and flexural buckling, the resistance calculated by ABAQUS is reduced. When EN 1993-1-3 is used, it's hard to see the interaction manually, which causes the larger calculation difference.

As results we can say that the length of the section has a dominant influence on the resistance calculated by ABAQUS (also shown in section 6.5). Bolt spacing does not have significant influence on resistance when the section is long. One reasonable reason is that when section is longer, the section tends to have flexural distortional buckling mode.

6.8.2 parametric influences on difference calculated by EN 1993-1-3 and ABAQUS

Figure 6.11 shows that when bolt spacing and sectional length are big, the calculation difference is big. Figure 6.15 shows the relationship between calculation difference (%) and the parameters for all cross sections.
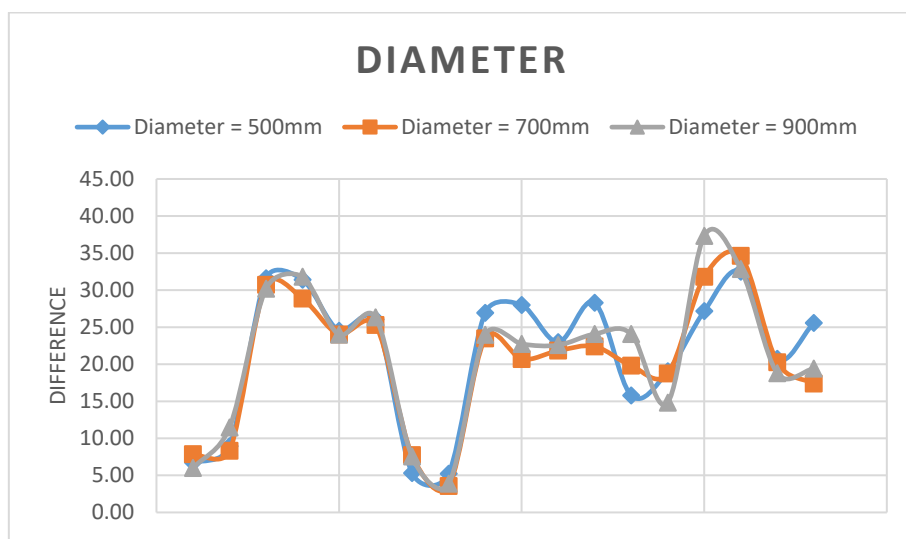
(a) Diameter
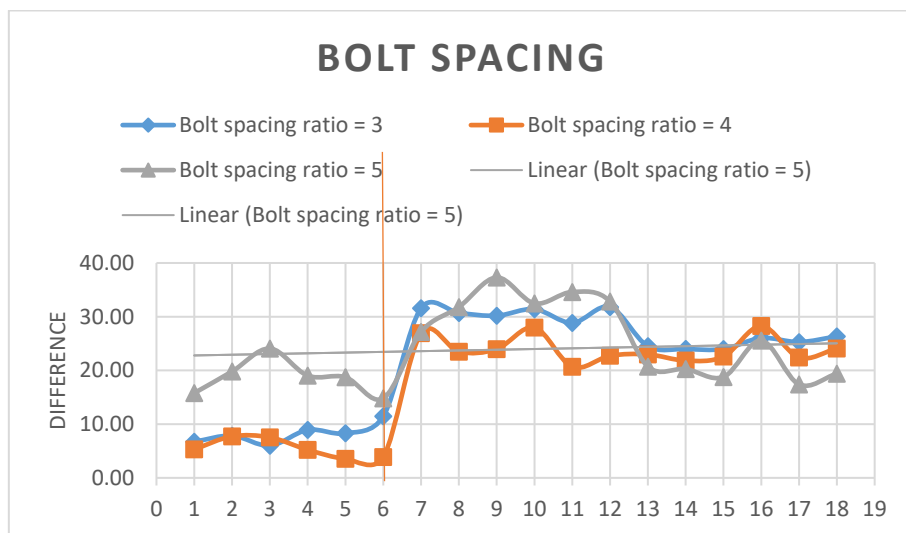
(b) Bolt spacing
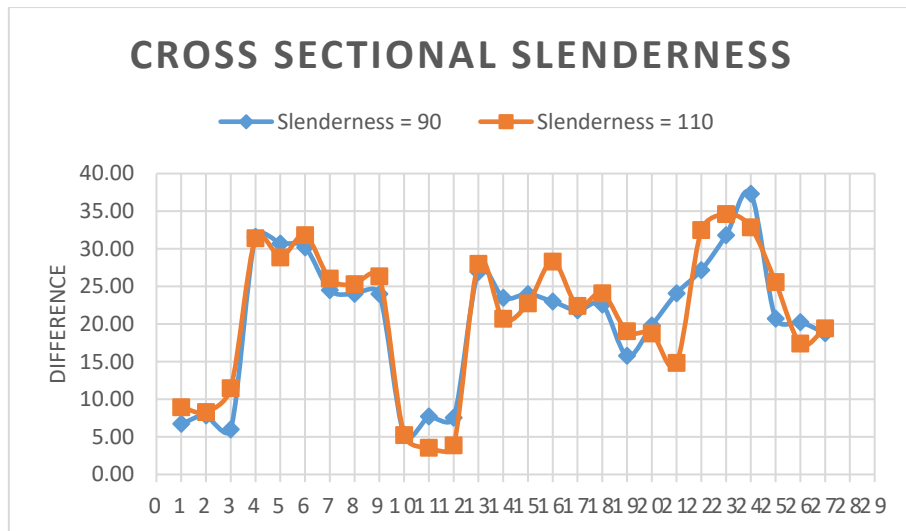
(c) Cross-sectional slenderness
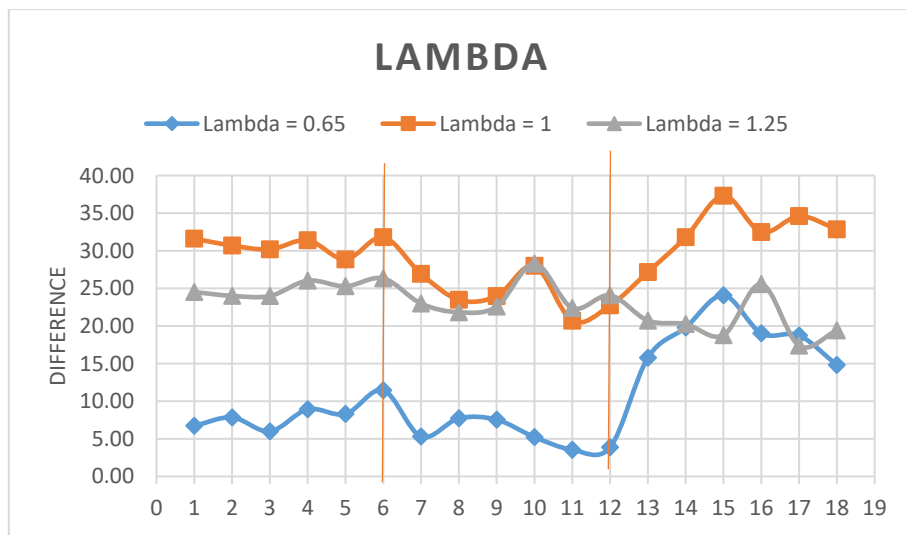
(d) Sectional length

Figure 6.14: Relationship between the calculation difference and parameters

Table 6.10: Resistance calculation difference when resistances calculated by EN 1993-1-3 are smaller than ABAQUS values

i	j	k	l	b	EN	ABAQUS	Difference (%)	Difference		Bolt density
1	2	3	1	3	4684869.61	5625706	16.72	-940836.39	Distortional	5.53
1	3	3	1	3	8733575.70	10583087	17.48	-1849511.30	Distortional	5.53
1	4	3	1	3	13931847.87	16670033	16.43	-2738185.13	Distortional	5.53
1	2	5	1	3	3220661.55	4132537.75	22.07	-911876.20	Distortional	5.53
1	3	5	1	3	6548752.58	8309604	21.19	-1760851.42	Distortional	5.53
1	4	5	1	3	10518154.36	13828574	23.94	-3310419.64	Distortional	5.53
1	2	3	2	3	3327469.24	4865734.5	31.61	-1538265.26	Flexural	8.51
1	3	3	2	3	6220139.59	8974794	30.69	-2754654.41	Flexural	8.51
1	4	3	2	3	10004566.92	14330121	30.19	-4325554.08	Flexural	8.51
1	2	5	2	3	2514217.19	3665155.25	31.40	-1150938.06	Flexural	8.51

79

1	3	5	2	3	5055632.37	7105254.5	28.85	-2049622.13	Flexural	8.51
1	4	5	2	3	8269442.12	12124579	31.80	-3855136.88	Flexural	8.51
1	2	3	3	3	2517753.80	3335746.75	24.52	-817992.95	Flexural	10.63
1	3	3	3	3	4706513.87	6192938.5	24.00	-1486424.63	Flexural	10.63
1	4	3	3	3	7570028.33	9958434	23.98	-2388405.67	Flexural	10.64
1	2	5	3	3	1928268.86	2606743.5	26.03	-678474.64	Flexural	10.64
1	3	5	3	3	3868776.43	5177700	25.28	-1308923.57	Flexural	10.64
1	4	5	3	3	6377866.45	8656932	26.33	-2279065.55	Flexural	10.64
1	2	3	1	4	4684869.61	4982469	5.97	-297599.39	Distortional	4.15
1	3	3	1	4	8733575.70	9053748	3.54	-320172.30	Distortional	4.15
1	4	3	1	4	13931847.87	14571561	4.39	-639713.13	Distortional	4.15
1	2	5	1	4	3220661.55	3576702.75	9.95	-356041.20	Distortional	4.15
1	3	5	1	4	6548752.58	7358898	11.01	-810145.42	Distortional	4.15
1	4	5	1	4	10518154.36	11788016	10.77	-1269861.64	Distortional	4.15
1	2	3	2	4	3327469.24	4554954.5	26.95	-1227485.26	Flexural	6.38
1	3	3	2	4	6220139.59	8128142.5	23.47	-1908002.91	Flexural	6.38
1	4	3	2	4	10004566.92	13158688	23.97	-3154121.08	Flexural	6.38
1	2	5	2	4	1997863.942	3241899.75	38.37	-1244035.81	D+F	6.38
1	3	5	2	4	5055632.367	6373936.5	20.68	-1318304.13	Flexural	6.38
1	4	5	2	4	8269442.121	10701573	22.73	-2432130.88	Flexural	6.38
1	2	3	3	4	2517753.802	3269500.75	22.99	-751746.95	Flexural	7.98
1	3	3	3	4	4706513.866	6020514.5	21.83	-1314000.63	Flexural	7.98
1	4	3	3	4	7570028.329	9777493	22.58	-2207464.67	Flexural	7.98
1	2	5	3	4	1532253.793	2496822.75	38.63	-964568.96	D+F	7.98
1	3	5	3	4	3868776.426	4985355.5	22.40	-1116579.07	Flexural	7.98
1	4	5	3	4	6377866.446	8400347	24.08	-2022480.55	Flexural	7.98
1	4	5	1	5	10518154.36	10664361	1.37	-146206.64	Distortional	3.32
1	2	3	3	5	2517753.802	3176238	20.73	-658484.20	Flexural	6.38
1	3	3	3	5	4706513.866	5901915.5	20.25	-1195401.63	Flexural	6.38
1	4	3	3	5	7570028.329	9320637	18.78	-1750608.67	Flexural	6.38
1	2	5	3	5	1532253.793	2405325	36.30	-873071.21	D+F	6.38
1	3	5	3	5	3868776.426	4682954	17.39	-814177.57	Flexural	6.38
1	4	5	3	5	6377866.446	7913537	19.41	-1535670.55	Flexural	6.38

As shown in Figure 6.14, diameter and cross-sectional slenderness do not have influence on the calculation difference. While bolt spacing and sectional length have significant influences on the calculation difference. In figure 6.14 (b),

$$0<x\leq6: l = 0.65$$

$$6<x\leq12: l = 1$$

$$12<x\leq18: l = 1.25$$

In Figure 6.15 (d),

$$0<x\leq6: b = 3$$

$$6<x\leq12: b = 4$$

$$12 < x \leq 18: b = 5$$

According to Figure 6.14 (b) and (d), when lambda = 0.65 and bolt spacing = 5, the calculation difference is larger. When lambda equals to 1 and 1.25, bolt spacing does not have significant influence on the calculation difference, also, the calculation difference is not every significant.

The calculation difference is analysed separately for distortional and flexural buckling mode, under safe region (Table 6.10).

- Distortional

For models in unsafe region, the calculation difference is big when the models have longer section (lambda = 1). The big calculation difference is due to distortional and flexural interaction.

For models in safe region, the shorter the bolt spacing, the larger the calculation difference. When bolt spacing is shorter, the bolt density is larger, the sections have more stiffness provided by bolts to against distortional buckling. While the resistance calculated by EN does not consider the stiffness provided by bolt, so when the EN calculated value remains the same, larger the resistance calculated by ABAQUS, larger the difference.

- Flexural
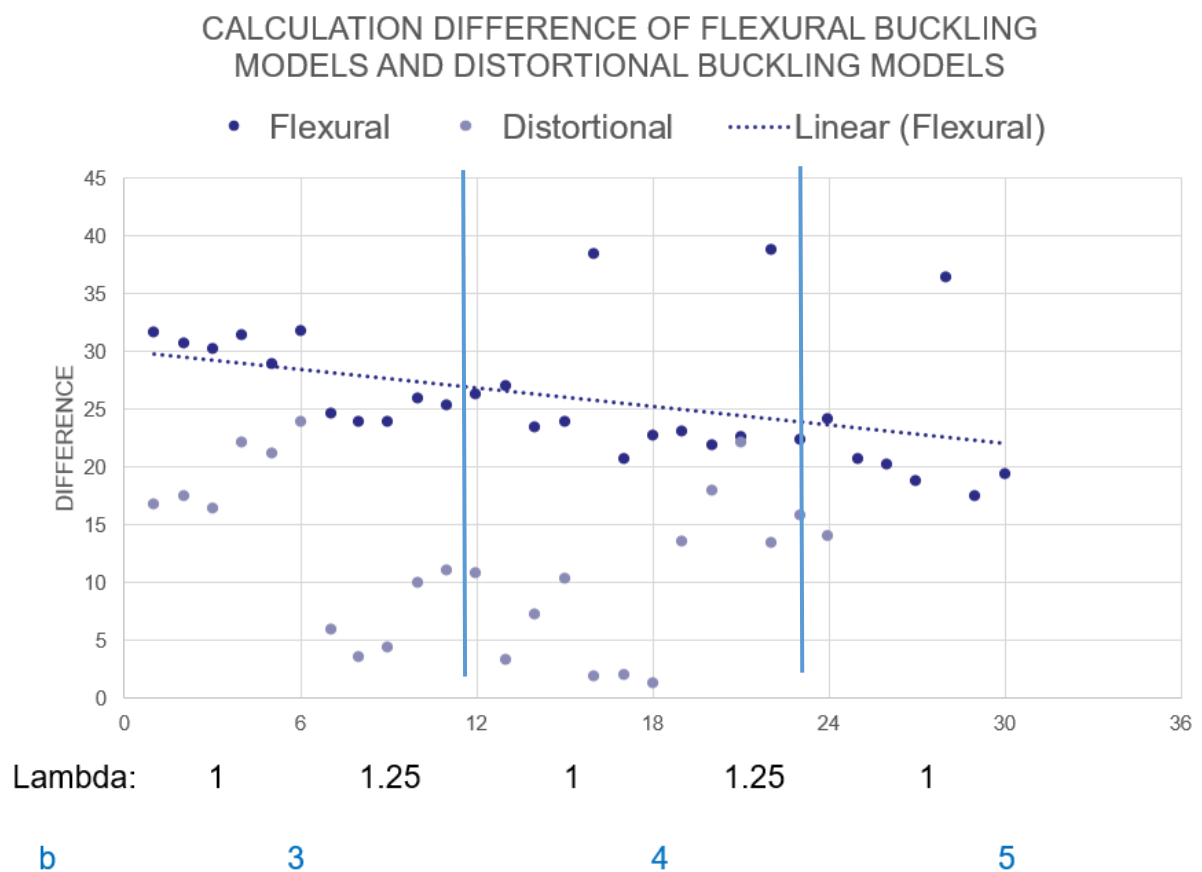
Figure 6.15: Calculation difference for models have flexural buckling mode

All models of flexural buckling mode are in safe region. As shown in Figure 6.15, the calculation difference for distortional buckling models is smaller than the calculation difference for flexural buckling models. All sections with lambda equals to 0.65 are in distortional buckling mode. Flexural buckling happens when lambda equals to 1 and 1.25.

81

The calculation differences for all flexural buckling models are high. The calculation difference decreases as long as the sectional length increases, in other words, the resistance calculated by ABAQUS is more closed to the EN resistance when section is long. The calculation difference decreases as long as the bolt spacing increases (lambda = 1), however, the influence is less significant when section is longer (lambda = 1.25).

So, it gives following results:

- In general, both sectional length and bolt spacing have significant influence on the calculation difference.
- The bolt spacing has less significant influence when section is long.
- The large calculation difference for the models which have distortional buckling modes in unsafe region is due to distortional flexural interaction.
- The large calculation difference for the models which have distortional buckling modes in safe region is due to the bolt stiffness.
- All calculation difference for models have flexural buckling mode is large.
- Both bolt spacing and sectional length have influence on the calculation difference of flexural buckling models, however, when the section is long, the influence by bolt spacing is not significant.
- When section is longer, the calculation difference is smaller, in other words, the ABAQUS results are more closed to EN.
- Bolt stiffness might have influence on flexural buckling resistance.

6.9 N+M interaction

In axial-moment interaction diagram, y-axis represents the ratio between loaded moment and moment resistance which is M_{Ed}/M_{Rd}; M_{Ed}, $0.05*M_{Ed}$, $0.1*M_{Ed}$ and $0.15*M_{Ed}$ are taken as the loaded moment. x-axis represents P/P_{Rd}; P is the maximum load calculated from ABAQUS corresponding to the loaded moment and P_{Rd} is the compressive resistance.

(a)
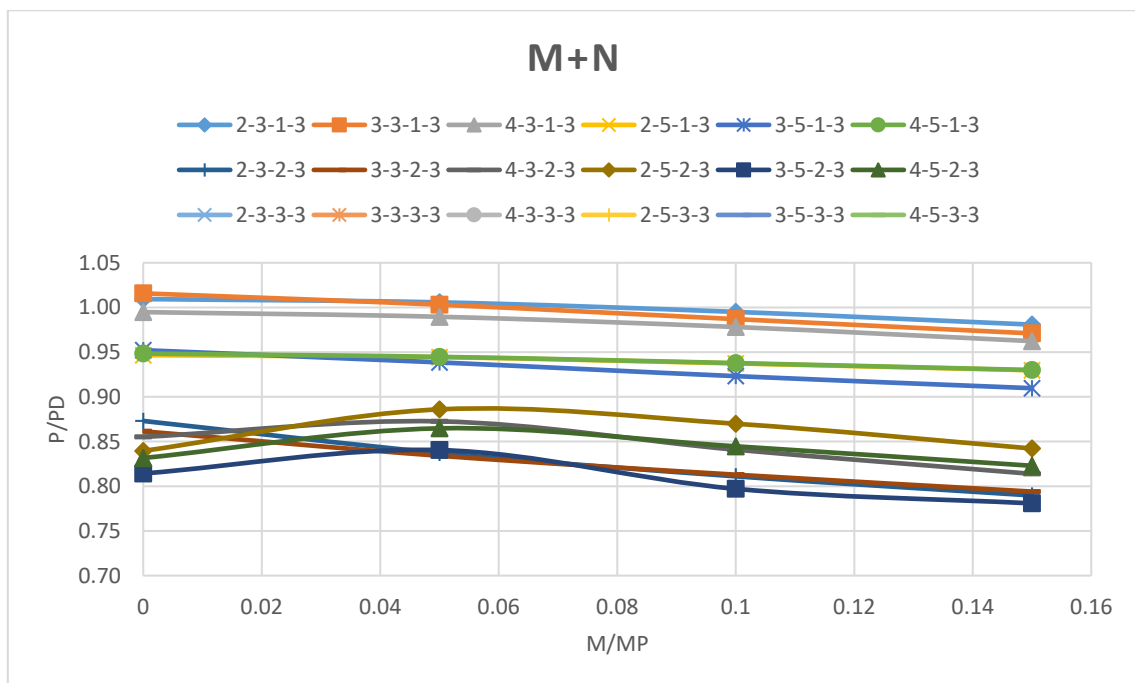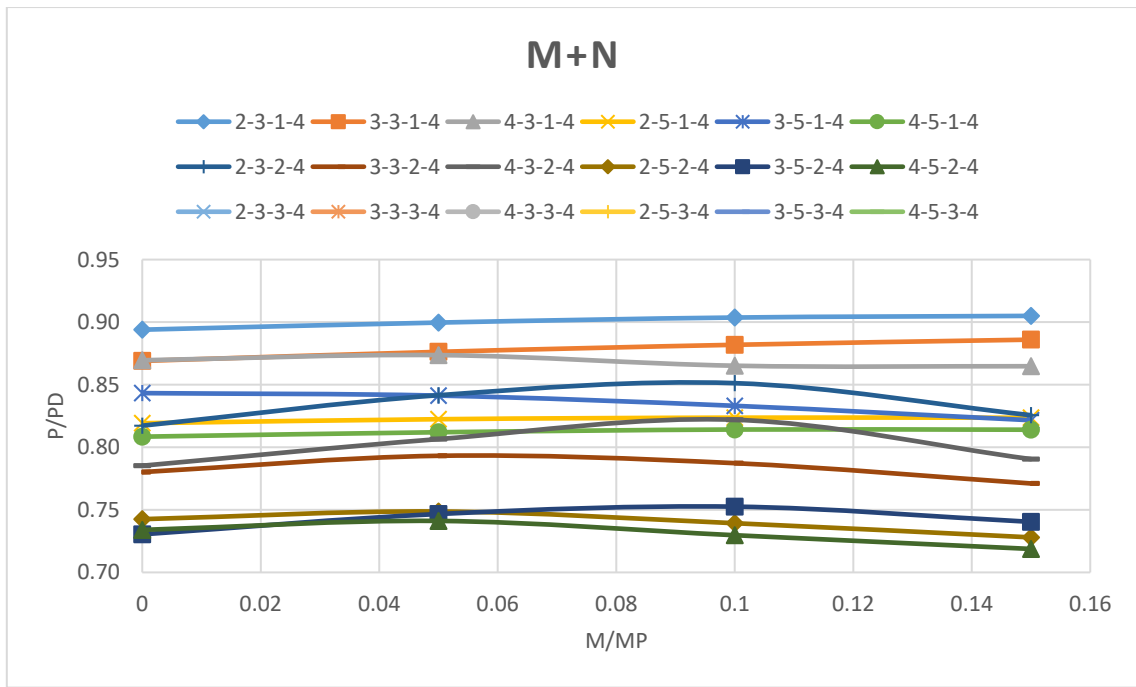
(b)
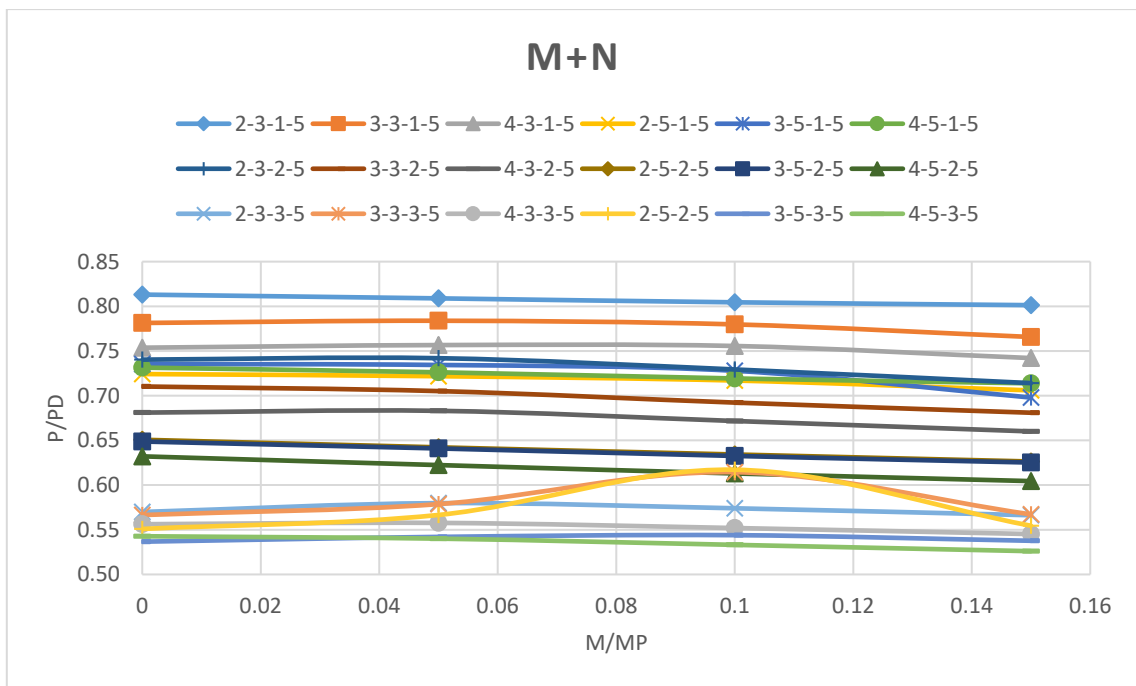
(c)

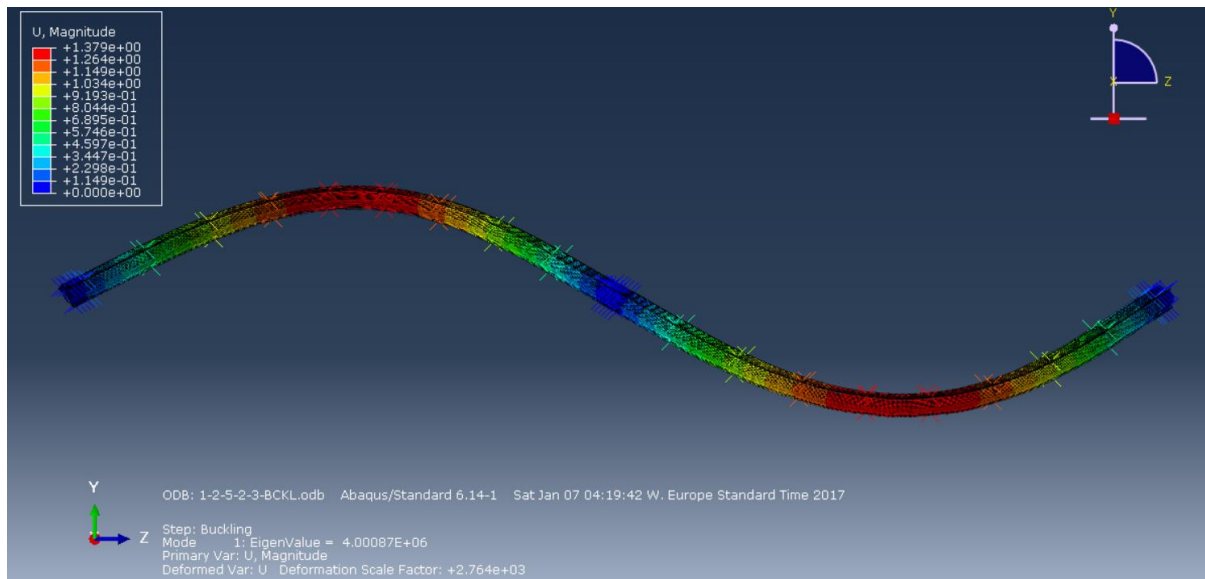**Figure 6.16: M+N interaction diagram of all models**

Figure 6.17: Buckling shape of model 1-2-5-2-3

Since the moments applied on the sections are quite small (0.05, 0.1 and 0.15 of the moment resistance), the moment compression interaction diagrams show that the moments do not have significant influences on the compressive resistance (Figure 6.16).

As noticed, there are some models have higher compressive resistance when moment is applied. Take model 1-2-5-2-3 as example, when the section buckles on the opposite direction as moment (Figure 6.17), the moment stabilizes the buckling structure. However, it seems no regular pattern that when it occurs.

6.10 Strength to weight ratio

The specific strength is a material's strength divided by its weight, which is also known as strength-to-weight ratio. Generally, steel has a higher strength to weight ratio than other materials. The steel construction requires less materials, which reduces the costs and environmental impacts of the building. For a unit of weight, the material has higher weight to strength ratio has more strength. Table 6.10 shows the strength to weight ratio of all cross sections.

Table 6.10: Strength to weight ratio

i	j	k	l	b	A (mm^2)	l (m)	Volume (mm^3)	weight (kg)	N (kN)	Strength to weight ratio
1	2	3	1	3	15699.81	8.29	0.13	1022.26	5625.71	5.50
1	3	3	1	3	29348.14	11.61	0.34	2675.53	10583.09	3.96
1	4	3	1	3	47203.99	14.93	0.70	5533.15	16670.03	3.01
1	2	5	1	3	12298.44	8.30	0.10	801.20	4132.54	5.16
1	3	5	1	3	24581.75	11.62	0.29	2241.83	8309.60	3.71
1	4	5	1	3	41072.59	14.94	0.61	4815.81	13828.57	2.87
1	2	3	2	3	15699.81	12.76	0.20	1572.70	4865.73	3.09
1	3	3	2	3	29348.14	17.87	0.52	4116.20	8974.79	2.18
1	4	3	2	3	47203.99	22.97	1.08	8512.54	14330.12	1.68
1	2	5	2	3	12298.44	12.77	0.16	1232.62	3665.16	2.97
1	3	5	2	3	24581.75	17.87	0.44	3448.97	7105.25	2.06
1	4	5	2	3	41072.59	22.98	0.94	7408.94	12124.58	1.64
1	2	3	3	3	15699.81	15.95	0.25	1965.88	3335.75	1.70

Resistance of Polygonal Cross Section of Lattice Wind Tower

|										
1	3	3	3	3	29348.14	22.33	0.66	5145.26	6192.94	1.20
1	4	3	3	3	47203.99	28.72	1.36	10640.67	9958.43	0.94
1	2	5	3	3	12298.44	15.96	0.20	1540.77	2606.74	1.69
1	3	5	3	3	24581.75	22.34	0.55	4311.21	5177.70	1.20
1	4	5	3	3	41072.59	28.72	1.18	9261.18	8656.93	0.93
1	2	3	1	4	15699.81	8.29	0.13	1022.26	4982.47	4.87
1	3	3	1	4	29348.14	11.61	0.34	2675.53	9053.75	3.38
1	4	3	1	4	47203.99	14.93	0.70	5533.15	14571.56	2.63
1	2	5	1	4	12298.44	8.30	0.10	801.20	3576.70	4.46
1	3	5	1	4	24581.75	11.62	0.29	2241.83	7358.90	3.28
1	4	5	1	4	41072.59	14.94	0.61	4815.81	11788.02	2.45
1	2	3	2	4	15699.81	12.76	0.20	1572.70	4554.95	2.90
1	3	3	2	4	29348.14	17.87	0.52	4116.20	8128.14	1.97
1	4	3	2	4	47203.99	22.97	1.08	8512.54	13158.69	1.55
1	2	5	2	4	12298.44	12.77	0.16	1232.62	3241.90	2.63
1	3	5	2	4	24581.75	17.87	0.44	3448.97	6373.94	1.85
1	4	5	2	4	41072.59	22.98	0.94	7408.94	10701.57	1.44
1	2	3	3	4	15699.81	15.95	0.25	1965.88	3269.50	1.66
1	3	3	3	4	29348.14	22.33	0.66	5145.26	6020.51	1.17
1	4	3	3	4	47203.99	28.72	1.36	10640.67	9777.49	0.92
1	2	5	3	4	12298.44	15.96	0.20	1540.77	2496.82	1.62
1	3	5	3	4	24581.75	22.34	0.55	4311.21	4985.36	1.16
1	4	5	3	4	41072.59	28.72	1.18	9261.18	8400.35	0.91
1	2	3	1	5	15699.81	8.29	0.13	1022.26	4531.79	4.43
1	3	3	1	5	29348.14	11.61	0.34	2675.53	8140.81	3.04
1	4	3	1	5	47203.99	14.93	0.70	5533.15	12630.04	2.28
1	2	5	1	5	12298.44	8.30	0.10	801.20	3161.86	3.95
1	3	5	1	5	24581.75	11.62	0.29	2241.83	6417.55	2.86
1	4	5	1	5	41072.59	14.94	0.61	4815.81	10664.36	2.21
1	2	3	2	5	15699.81	12.76	0.20	1572.70	4126.21	2.62
1	3	3	2	5	29348.14	17.87	0.52	4116.20	7400.33	1.80
1	4	3	2	5	47203.99	22.97	1.08	8512.54	11412.76	1.34
1	2	5	2	5	12298.44	12.77	0.16	1232.62	2840.90	2.30
1	3	5	2	5	24581.75	17.87	0.44	3448.97	5661.08	1.64
1	4	5	2	5	41072.59	22.98	0.94	7408.94	9216.88	1.24
1	2	3	3	5	15699.81	15.95	0.25	1965.88	3176.24	1.62
1	3	3	3	5	29348.14	22.33	0.66	5145.26	5901.92	1.15
1	4	3	3	5	47203.99	28.72	1.36	10640.67	9320.64	0.88
1	2	5	3	5	12298.44	15.96	0.20	1540.77	2405.33	1.56
1	3	5	3	5	24581.75	22.34	0.55	4311.21	4682.95	1.09
1	4	5	3	5	41072.59	28.72	1.18	9261.18	7913.54	0.85

(1) Lambda
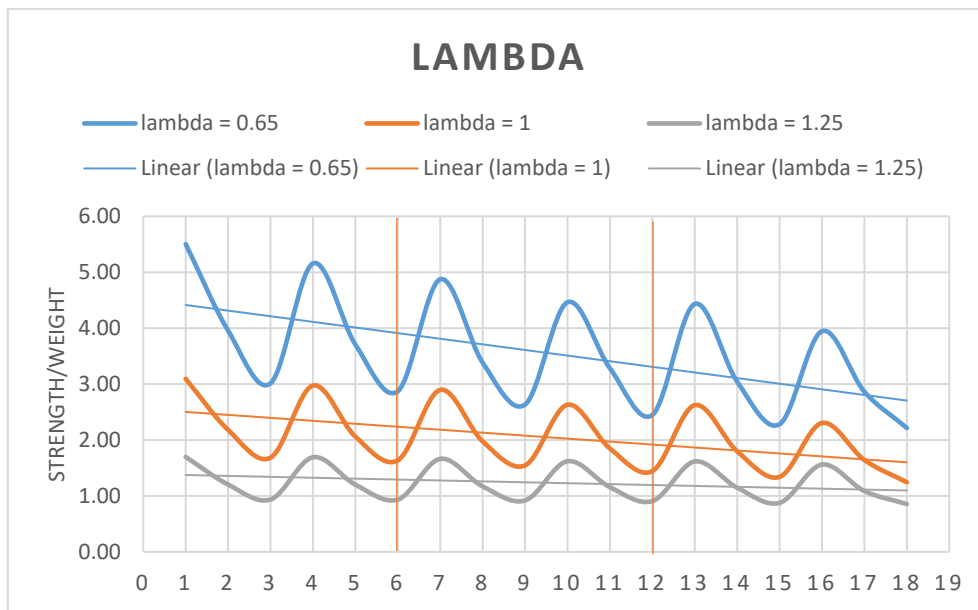
Figure 6.18: Strength to weight ratio under difference lambda

As shown in Figure 6.18, the higher then lambda, the higher the length of the section, the lower the strength to weight ratio. In the figure, x-axis represents the xth of models:

$$0<x\leq6: \text{bolt spacing ratio} = 3$$

$$6<x\leq12: \text{bolt spacing} =4$$

$$12<x\leq18: \text{bolt spacing} = 5$$

All trendlines shown in the graph are going downwards along the increase of bolt spacing, the bolt spacing has a negative effect on strength to weight ratio. However, it's shown that when section is longer (lambda = 1 and 1.25), the slope of the trendline is smaller, the bolt spacing has less significant influence on strength to weight ratio.

(2) Bolt spacing
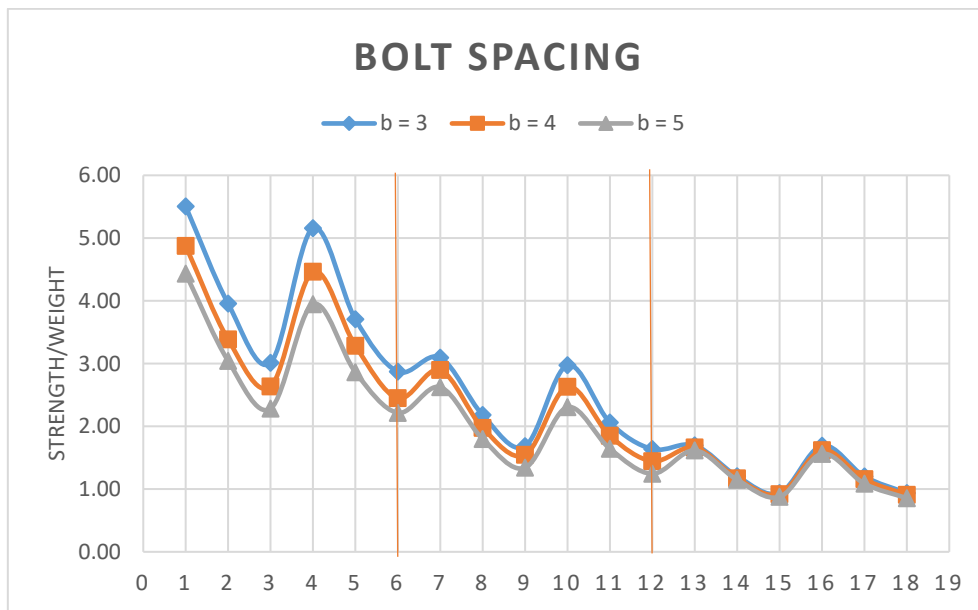
Figure 6.19: Strength to weight ratio under difference bolt spacing

Within a range of length, the higher the bolt spacing, the lower the strength to weight ratio. In the figure, x-axis represents the xth of models: $0 < x \leq 6$: lambda = 0.65

$$6 < x \leq 12: \text{lambda} = 1$$

$$12 < x \leq 18: \text{lambda} = 1.25$$

As shown in Figure 6.19, when the section is short, the influence of bolt spacing is larger; however, when lambda equals to 1.25, the bolt spacing has no effect on strength to weight ratio at all.

(3) Cross sectional slenderness
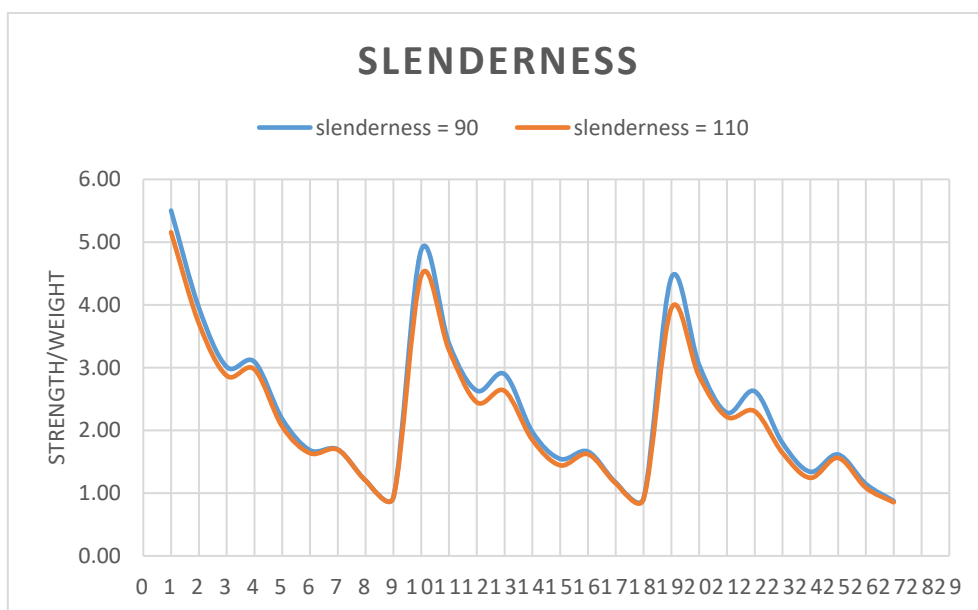
Figure 6.20: Strength to weight ratio under difference cross sectional slenderness

As shown in Figure 6.20, cross sectional slenderness does not have significant influence on strength to weight ratio.

(4) Diameter
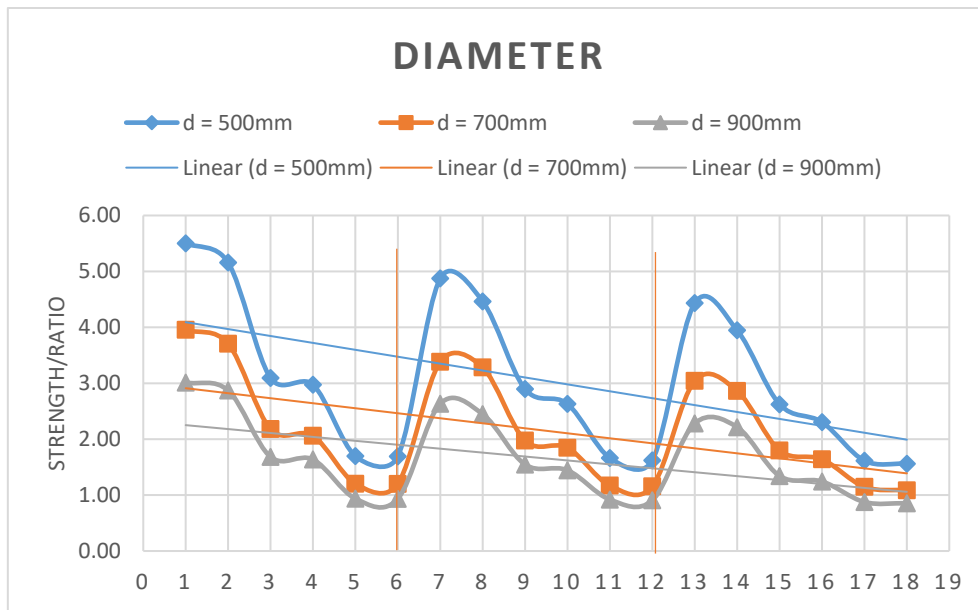
Figure 6.21: Strength to weight ratio under difference diameter

As shown in Figure 6.21, the higher the diameter, the lower the strength to weight ratio.

In the figure, x-axis represents the xth of models:

$$0<x\leq3: lambda = 0.65$$

$$3<x\leq5: lambda = 1$$

$$5<x\leq7: lambda = 1.25$$

(same mode for range 6-12 and 12-18)

The large drop between 1-6; 6-12 and 12-18 is caused by the increase of length. Also, the difference among the strength to weight ratios due to different diameters is not very significant when the section is long (lambda = 1.25).

According to the graphs shown above, the length of the section and diameter have the most significant influences on the strength to weight ratio, while bolt spacing does not have such obvious influence on it; cross sectional slenderness has no influence on strength to weight ratio. It results in that a polygonal section with small cross-sectional diameter and short length has better specific strength. When polygonal section is long enough, the influence of bolt spacing on the strength to weight ratio is neglectable; and the influence of diameter becomes small.

6.11 Resistance calculated based on EN 1993-1-6

Table 6.10 shows the resistance of cross sections calculated based on EN 1993-1-6 shell structure, and the difference between it and ABAQUS result.

Table 6.10: Resistance calculated by EN 1993-1-6

i	j	k	l	b	EN1-6	ABAQUS	difference (%)	EN 1-3	difference (%)	
1	2	3	1	3	4602260.86	5625706.00	0.18	5247088.13	12.29	Distortional
1	3	3	1	3	8554844.33	10583087.00	0.19	9753081.05	12.29	Distortional
1	4	3	1	3	13714013.61	16670033.00	0.18	15670631.51	12.49	Distortional
1	2	5	1	3	3495434.95	4132537.75	0.15	3763544.13	7.12	Distortional
1	3	5	1	3	7005237.86	8309604.00	0.16	7620020.24	8.07	Distortional
1	4	5	1	3	11721678.44	13828574.00	0.15	12244317.05	4.27	Distortional
1	2	3	2	3	4602260.86	4865734.50	0.05	3328294.43	38.28	Flexural
1	3	3	2	3	8554844.33	8974794.00	0.05	6220139.59	37.53	Flexural
1	4	3	2	3	13714013.61	14330121.00	0.04	10004566.92	37.08	Flexural
1	2	5	2	3	3495434.95	3665155.25	0.05	2514217.19	39.03	Flexural
1	3	5	2	3	7005237.86	7105254.50	0.01	5055632.37	38.56	Flexural
1	4	5	2	3	11721678.44	12124579.00	0.03	8269442.12	41.75	Flexural
1	2	3	3	3	4602260.86	3335746.75	0.38	2518141.52	82.76	Flexural
1	3	3	3	3	8554844.33	6192938.50	0.38	4706513.87	81.77	Flexural
1	4	3	3	3	13714013.61	9958434.00	0.38	7570028.33	81.16	Flexural
1	2	5	3	3	3495434.95	2606743.50	0.34	1928268.86	81.27	Flexural
1	3	5	3	3	7005237.86	5177700.00	0.35	3868776.43	81.07	Flexural
1	4	5	3	3	11721678.44	8656932.00	0.35	6377866.45	83.79	Flexural
1	2	3	1	4	4602260.86	4982469.00	0.08	5247088.13	12.29	Distortional
1	3	3	1	4	8554844.33	9053748.00	0.06	9753081.05	12.29	Distortional
1	4	3	1	4	13714013.61	14571561.00	0.06	15670631.51	12.49	Distortional
1	2	5	1	4	3495434.95	3576702.75	0.02	3763544.13	7.12	Distortional
1	3	5	1	4	7005237.86	7358898.00	0.05	7620020.24	8.07	Distortional
1	4	5	1	4	11721678.44	11788016.00	0.01	12244317.05	4.27	Distortional
1	2	3	2	4	4602260.86	4554954.50	0.01	3328294.43	38.28	Flexural
1	3	3	2	4	8554844.33	8128142.50	0.05	6220139.59	37.53	Flexural
1	4	3	2	4	13714013.61	13158688.00	0.04	10004566.92	37.08	Flexural
1	2	5	2	4	3495434.95	3241899.75	0.08	2334628.77	49.72	D+F
1	3	5	2	4	7005237.86	6373936.50	0.10	5055632.37	38.56	Flexural
1	4	5	2	4	11721678.44	10701573.00	0.10	8269442.12	41.75	Flexural
1	2	3	3	4	4602260.86	3269500.75	0.41	2518141.52	82.76	Flexural
1	3	3	3	4	8554844.33	6020514.50	0.42	4706513.87	81.77	Flexural
1	4	3	3	4	13714013.61	9777493.00	0.40	7570028.33	81.16	Flexural
1	2	5	3	4	3495434.95	2496822.75	0.40	1790534.24	95.22	D+F
1	3	5	3	4	7005237.86	4985355.50	0.41	3868776.43	81.07	Flexural
1	4	5	3	4	11721678.44	8400347.00	0.40	6377866.45	83.79	Flexural
1	2	3	1	5	4602260.86	4531788.50	0.02	5247088.13	12.29	Distortional
1	3	3	1	5	8554844.33	8140806.00	0.05	9753081.05	12.29	Distortional
1	4	3	1	5	13714013.61	12630036.00	0.09	15670631.51	12.49	Distortional
1	2	5	1	5	3495434.95	3161856.25	0.11	3763544.13	7.12	Distortional
1	3	5	1	5	7005237.86	6417545.50	0.09	7620020.24	8.07	Distortional

1	4	5	1	5	11721678.44	10664361.00	0.10	12244317.05	4.27	Distortional
1	2	3	2	5	4602260.86	4126211.50	0.12	5247088.13	12.29	Distortional
1	3	3	2	5	8554844.33	7400331.50	0.16	9753081.05	12.29	Distortional
1	4	3	2	5	13714013.61	11412761.00	0.20	15670631.51	12.49	Distortional
1	2	5	2	5	3495434.95	2840899.50	0.23	3763544.13	7.12	Distortional
1	3	5	2	5	7005237.86	5661079.00	0.24	7620020.24	8.07	Distortional
1	4	5	2	5	11721678.44	9216875.00	0.27	12244317.05	4.27	Distortional
1	2	3	3	5	4602260.86	3176238.00	0.45	2518141.52	82.76	Flexural
1	3	3	3	5	8554844.33	5901915.50	0.45	4706513.87	81.77	Flexural
1	4	3	3	5	13714013.61	9320637.00	0.47	7570028.33	81.16	Flexural
1	2	5	3	5	3495434.95	2405325.00	0.45	1790534.24	95.22	D+F
1	3	5	3	5	7005237.86	4682954.00	0.50	3868776.43	81.07	Flexural
1	4	5	3	5	11721678.44	7913537.00	0.48	6377866.45	83.79	Flexural

Figure 6.22 shows the resistances calculated based on EN 1993-1-6 and ABAQUS.
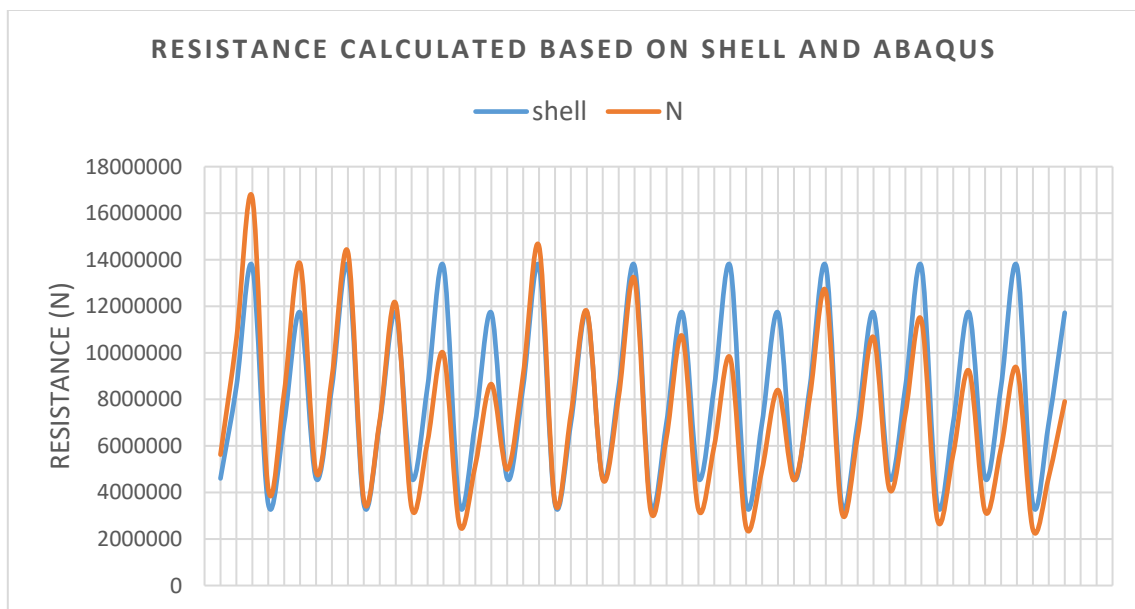
Figure 6.22: Resistances calculated based on EN 1993-1-6 and ABAQUS

Figure 6.23 shows the difference of resistances calculated based on EN 1993-1-3 and EN 1993-1-6 under difference lambda values. According to the figure, the resistance calculated by EN 1993-1-6 and EN 1993-1-3 do not have significant difference when the section is shorter. Shell structure is more sensitive to the length of the section, when the section tends to be longer, shell structure requires more resistance, which means more strength materials or thicker the structure, than polygonal cross sectional structure. So, when longer structure is provided, polygonal cross section is a better choice.
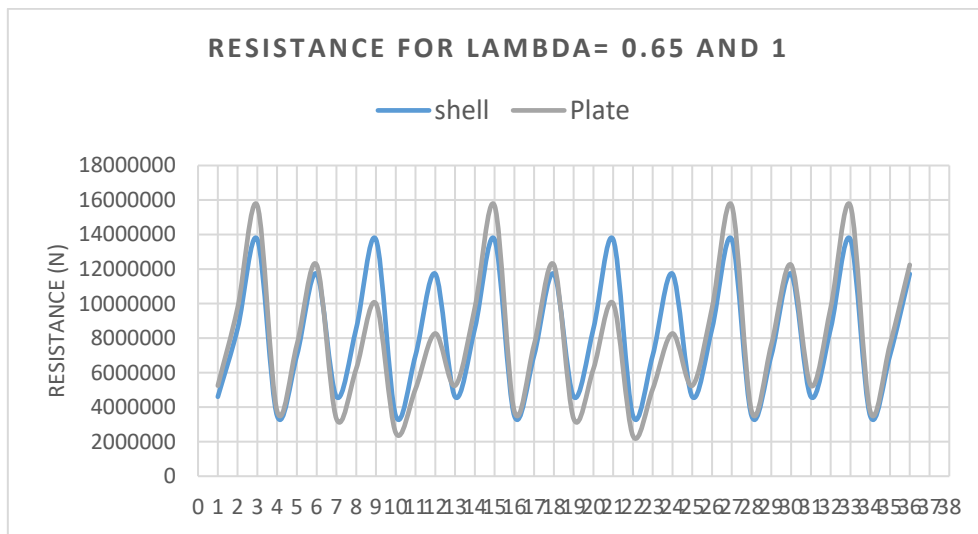
(a) Lambda = 0.65 and 1
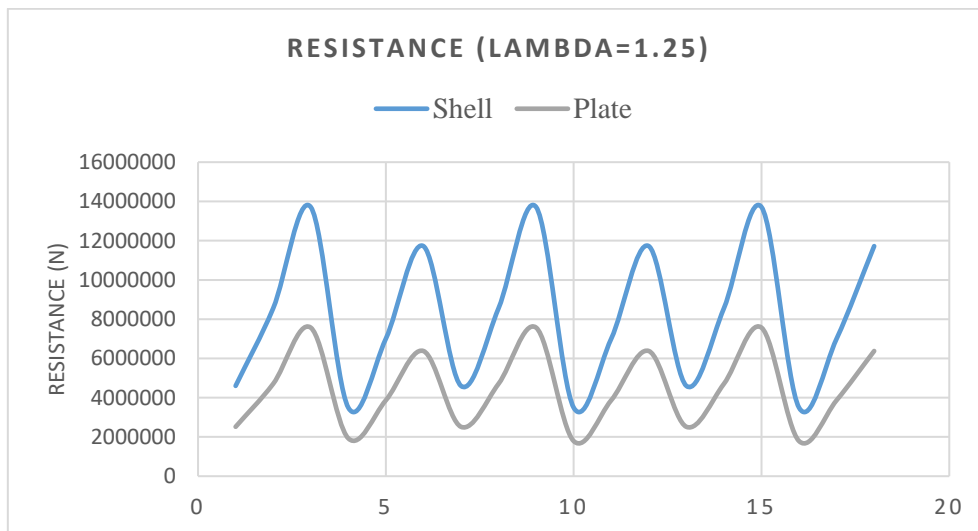
(b) Lambda = 1.25

Figure 6.23: Resistance differences under different lambda

7. Conclusion

The result of this thesis has following conclusions:

- Diameter and the sectional slenderness have the most significant influences on polygonal cross sectional resistance.
- Bolt spacing and sectional length have the most significant interaction.
- Bolted connected and stiffened polygonal cross section that axially loaded showed a good agreement between numerical and EN 1993-1-3 calculations within a length limit (lambda = 0.65).
- Within a limit of sectional length, the bolt density matters to the resistance; however, when section is long enough, the bolt spacing no long matters to resistance.
- The stiffness of the lips has influence on flexural resistance.
- Translational stiffness of bolts increases as long as the thickness increases; decreases as long as either the cross-sectional diameter or bolt spacing increases; rotational stiffness of bolts increases when either thickness or cross-sectional increases, decreases when bolt spacing increases.
- Moment stabilizes the structure when the bucking shape deforms on the opposite direction as the moment's direction.
- Length of the section and diameter are the most important factors that affect the strength to weight ratio of polygonal section. Small diameter and short section are better.
- When the section tends to be built longer, polygonal cross section is better than cylinder shell structure.

References

[1] Norwegian wind, 2017. [Online]. Available: http://zephyr.no

[2] Energy from renewable sources, 2016. [Online]. Available: http://ec.europa.eu/eurostat/statistics-explained/index.php/Energy_from_renewable_sources

[3] Wind in power, 2015 European statistics, 2016. [Online]. Available: https://windeurope.org/wp-content/uploads/files/about-wind/statistics/EWEA-Annual-Statistics-2015.pdf

[4] Wind power roadmap, 2013. [Online]. Available: https://www.ieawind.org/index_page_postings/ieawind_paris/IEA%20Wind%20Roadmap%20launch_CWP2013_final.pdf

[5] Heistermann, C., Husson, W., & Veljkovic, M. (2009). Flange connection vs. friction connection in towers for wind turbines. In Proc. of Nordic steel and construction conference (NSCC 2009) (pp. 296-303).

[6] Hassanzadeh, M. (2012). Cracks in onshore wind power foundations (pp. 2012-01). Tech. rep. Elforsk.

[7] Muskulus, M. (2012). The full-height lattice tower concept. Energy Procedia, 24, 371-377.

[8] M.Ragheb. (2012). Structural Towers. [Online]. Available: http://mragheb.com/NPRE%20475%20Wind%20Power%20Systems/Structural%20Towers.pdf

[9] Engström, S., Lyrner, T., Hassanzadeh, M., Stalin, T., & Johansson, J. (2010). Tall towers for large wind turbines. Report from Vindforsk project, 342, 50.

[10] Michelle Froese. (2016). Nordex installs the world's tallest wind turbine. [Online]. Available: http://www.windpowerengineering.com/featured/business-news-projects/nordex-installs-worlds-tallest-wind-turbine/

[11] [Online.] Available: https://www.revolvy.com/main/index.php?s=Fuhrl%C3%A4nder%20Wind%20Turbine%20Laasow&item_type=topic

[12] Punmia, B. C., Jain, A. K., & Jain, A. K. (1998). Comprehensive design of steel structures. Firewall Media.

[13] Madugula, M. K. (Ed.). (2001). Dynamic response of lattice towers and guyed masts. ASCE Publications.

[14] Baniotopoulos, Charalambos, Claudio Borri, and Theodore Stathopoulos, eds. Environmental wind engineering and design of wind energy structures. Vol. 531. Springer Science & Business Media, 2011.

[15] Lee, Y. H., Tan, C. S., Mohammad, S., Md Tahir, M., & Shek, P. N. (2014). Review on Cold-formed steel Connections. The Scientific World Journal, 2014.

[16] Yu, C., & Panyanouvong, M. X. (2013). Bearing strength of cold-formed steel bolted connections with a gap. Thin-Walled Structures, 67, 110-115.

[17] Vaghe, V. M., Belgaonkar, S. L., Kharade, A. S., & Bhosale, A. S. (2013). Experimental Study on Connections, By Using Light Gauge Channel Sections and Packing Plates/Stiffener Plate at the Joints. International Journal of Engineering and Innovative Technology (IJEIT) Volume, 2.

[18] Chen, W. F., & Atsuta, T. (2007). Theory of beam-columns, volume 2: space behavior and design (Vol. 2) Chap. 13. J. Ross Publishing.

[19] Zeinoddini, V., & Schafer, B. W. (2010). Impact of corner radius on cold-formed steel member strength.

[20] Schafer, B.W. (2002). "Local, Distortional, and Euler Buckling in Thin-walled Columns." ASCE, Journal of Structural Engineering. 128 (3) 289-299.

[21]

[22] Pietraszkiewicz, W., & Gorski, J. (Eds.). (2013). Shell Structures: Theory and Applications (Vol. 3). CRC Press.

[23] European Commission. (1993). Interaction Diagrams between Axial Load N Bending Moment M for Columns Submitted to Buckling

[24] Dubina, Dan, Raffaele Landolfo, and Viorel Ungureanu. Design of cold-formed steel structures.: Eurocode 3: design of steel structures. Part 1-3, Design of cold-formed steel structures. Eccs, 2012.

[25] Schafer, B. W. (2000). Distoritonal buckling of cold-formed steel columns.

[26] Satishkumar, S. R., & Kumar, A. R. (2014). Design of Steel Structures II.

[27] Ellobody, E. (2014). Finite Element Analysis and Design of Steel and Steel–Concrete Composite Bridges. Butterworth-Heinemann.

[28] [Online.] Available: http://www.javelin-tech.com/blog/2012/10/shell-vs-solid-elements/#.WHfF1vkrJEY

[29] Manual, A. U. S. (2010). Version 6.10. ABAQUS Inc.

[30] Manual, A. U. S. (2012). Version 6.12. Dassault Systémes Simulia Corp., Providence, RI.

[31] Hibbitt, H., Karlsson, B., & Sorensen, P. (2011). Abaqus analysis user's manual version 6.10. Dassault Systèmes Simulia Corp.: Providence, RI, USA.

Annex A MATLAB code for cross-sectional coordinates

```
function [x_out, y_out, t, tg, l_lip] = pcoords(n, d, slend, fy, rcoef, nbend, l_ratio, t_ratio)
% Return x, y coords of points of a 1/3 of folded polygonal cross section.
% input args: number of corners, CS diameter, slenderness, yield strength,
% bending arc radius r/t, no. of points along the bending arcs,lip length
% to diameter ratio, gusset plate thickness to sector thickness ratio.
% output: [x, y], sector thickness, gussetplate thickness


%% Input (recomended values)
% % Number of corners (entire polygon, only 3*m)
% n = 9;
%
% % Polygon diameter
% d = 500;
%
% % Yield strength
% fy = 355;
%
% % Bending radius to thickness ratio
% % (r/t = rcoef)
% rcoef = 6;
%
% % Number of points along the bend
% nbend = 6;
%
% % extension length to diameter ratio
% l_ratio = 0.1;
%
% % Thickness of the gusset plate to sector thickness ratio
% t_ratio = 1.20;
%
% % Slenderness
% slend = 90;



% Calculated characteristics
R = d/2;
epsilon = sqrt(fy/235);
t = (epsilon^2 * d / slend);
tg = (t_ratio*t);
l_lip = l_ratio*d;

%% Polygon sector
% Angle corresponding to one edge of the polygon
theta = 2*pi/n;

% Angles of radii (measured from x-axis)
phi=5*pi/6:-theta:pi/6;

% xy coords of the polygon's corners
x = R*cos(phi);
y = R*sin(phi);

%% Bends
% Bending radius
rbend = rcoef*t;
```

Resistance of Polygonal Cross Section of Lattice Wind Tower

```
% Distance between bending centre and corner
lc = rbend/cos(theta/2);


% Centers of bending arcs
xc  = (x(2:end-1) - lc*cos(phi(2:end-1)));
yc  = (y(2:end-1) - lc*sin(phi(2:end-1)));


% Bending arc angle
theta_b = pi - theta;


% Angles of the edges' midlines (measured from x-axis)
phi_mids = phi(1:end-1) - theta/2 ;


% xy coords of the arc's points
for i = 1:n/3 -1;
    for j = 1:nbend+1;
        xarc(i, j) = xc(i) + rbend*cos(phi_mids(i)-(j-1)*(theta/nbend));
        yarc(i, j) = yc(i) + rbend*sin(phi_mids(i)-(j-1)*(theta/nbend));
    end;
end;


%% Start-end extensions
% Bending radius
rs = rbend/5;


% First bend
v1 = phi_mids(1)-pi/2;
v2 = (phi(1)+phi_mids(1)-pi/2)/2;
l1 = (t+tg)/(2*cos(phi(1)-phi_mids(1)));
l2 = rs/sin(v2-phi_mids(1)+pi/2);
x1 = x(1)+l1*cos(v1);
y1 = y(1)+l1*sin(v1);


% First bend centre coords
xcs(1) = x1+l2*cos(v2);
ycs(1) = y1+l2*sin(v2);


% Last bend
v1 = phi_mids(end)+pi/2;
v2 = (v1+phi(end))/2;
l1 = (t+tg)/(2*cos(v1-phi(end)-pi/2));
l2 = rs/sin(v2-phi(end));
x1 = x(end)+l1*cos(v1);
y1 = y(end)+l1*sin(v1);


% Last bend centre coords
xcs(2) = x1+l2*cos(v2);
ycs(2) = y1+l2*sin(v2);


% First and last bend arc points coords
for j = 1:nbend+1;
    xsarc(1, j) = xcs(1) + rs*cos(4*pi/3+(j-1)*((phi_mids(1)-pi/3)/nbend));
    ysarc(1, j) = ycs(1) + rs*sin(4*pi/3+(j-1)*((phi_mids(1)-pi/3)/nbend));
    xsarc(2, j) = xcs(2) + rs*cos(phi_mids(end)+pi+(j-1)*((phi(end)+pi/2-phi_mids(end))/nbend));
    ysarc(2, j) = ycs(2) + rs*sin(phi_mids(end)+pi+(j-1)*((phi(end)+pi/2-phi_mids(end))/nbend));
end;
```

```matlab
%% Points of the lips
% First lip
xstart = [xsarc(1, 1) + l_lip*cos(phi(1)), xsarc(1, 1) + l_lip*cos(phi(1))/2];
ystart = [ysarc(1, 1) + l_lip*sin(phi(1)), ysarc(1, 1) + l_lip*sin(phi(1))/2];



% Last point
xend = [xsarc(2, end) + l_lip*cos(phi(end))/2, xsarc(2, end) + l_lip*cos(phi(end))];
yend = [ysarc(2, end) + l_lip*sin(phi(end))/2, ysarc(2, end) + l_lip*sin(phi(end))];

%% Collect the x, y values in a sorted 2xn array
xarc = xarc';
yarc = yarc';

x_out = [xstart, xsarc(1, :), xarc(:)', xsarc(2, :), xend];
y_out = [ystart, ysarc(1, :), yarc(:)', ysarc(2, :), yend];

%Plot result
plot(x_out, y_out);
```

Annex B MATLAB code for parametric range

```matlab
function [profiles, meta] = polygoner(nrange, drange, slendrange, fy, rcoef, nbend, l_ratio, t_ratio, lambda);
% Return a cell array with the points of all the profiles within a range of
% values.
% input args: numbers of corners, CS diameters, slenderness', yield strength,
% bending arc radius r/t, no. of points along the bending arcs, end
% extensions length, gusset plate thickness.
% profiles output  : [x; y], [diameter; plate thicness; gusset plate thickness; fy]
% meta outpur      : d; t; tg; fy; A; Ixx; Izz; Ixz

% Example input
nrange = [6];
drange = [500];
slendrange = [90];
lambda = [0.65];
%
fy = 355;
rcoef = 6;
nbend = 4;
l_ratio = 0.1;
t_ratio = 1.2;

E = 210000;

% Initialise a cell array to host the profiles' xy values
profiles = cell(length(nrange), length(drange), length(slendrange));

% Initialise a cell array to host the profile metadata
meta = cell(length(nrange), length(drange), length(slendrange), length(lambda));

% Loop through the values within the given ranges
for i = 1:length(nrange);
  for j = 1:length(drange);
    for k = 1:length(slendrange);

        % Call pcoords to get data for a profile
        [x, y, t, tg] = pcoords(nrange(i), drange(j), slendrange(k), fy, rcoef, nbend, l_ratio, t_ratio);

        % Collect the xy values in a database
        profiles{i, j, k} = [x; y];

        % Metadata of the profiles
        % Crate node and elem arrays for the profile appropriate for
        % input to cutwp_prop2 function which returns cs properties

        % Current profile xy
        c_prof1 = profiles{i, j, k}';

        % Number of vertices on the current profile
        l_prof = length(c_prof1);

        % Construct the 2 extra parts by rotating the imported one
        R2 = [cos(-2*pi/3), -sin(-2*pi/3); sin(-2*pi/3), cos(-2*pi/3)];
        R3 = [cos(2*pi/3), -sin(2*pi/3); sin(2*pi/3), cos(2*pi/3)];
        for a = 1:l_prof;
```

```
    c_prof2(a, :) = (R2*c_prof1(a, :)')';
    c_prof3(a, :) = (R3*c_prof1(a, :)')';
end;


% A column of ones
col1 = ones(l_prof', 1);


% Construct the 'node' array
node = [c_prof1(:, 1), c_prof1(:, 2);
    c_prof2(:, 1), c_prof2(:, 2);
    c_prof3(:, 1), c_prof3(:, 2)];


% Construct the 'elem' array
elem = [(1:l_prof-1)', (2:l_prof)', t*ones(l_prof-1', 1);
    l_prof, l_prof+1, 0.1;
    l_prof+(1:l_prof-1)', l_prof+(2:l_prof)', t*ones(l_prof-1', 1);
    2*l_prof, 2*l_prof+1, 0.1;
    2*l_prof+(1:l_prof-1)', 2*l_prof+(2:l_prof)', t*ones(l_prof-1', 1);
    3*l_prof, 1, 0.1];


% Return cs properties using cutwp
[A, ~, ~, Iyy, Izz] = cutwp_prop2(node, elem);


% Current profile area and moment of inertia
I = min(Iyy, Izz);


% find the element properties on the current profile
nele = size(elem,1);
for v = 1:nele;
    sn = elem(v,1); fn = elem(v,2);
    % thickness of the element
    tk(v,1) = t;
    % compute the coordinate of the mid point of the element
    xm(v) = mean(node([sn fn],1));
    ym(v) = mean(node([sn fn],2));
    % compute the dimension of the element
    xd(v) = diff(node([sn fn],1));
    yd(v) = diff(node([sn fn],2));
    % compute the length of the element
    L(v,1) = norm([xd(v) yd(v)]);
    Ao(v,1) = L(v)*tk(v);
end


% Calculating cross-sectional class and effective area if needed:
for v = 1:nele;
    Ep = [Ao L tk];
    epsilon=sqrt(235/fy); Ep2=zeros(nele,2); lambdap=zeros(nele,1); ro=zeros(nele,1);
    if Ep(v,1) == eps
        Ep2(v,:)=[0 123];
    else
        %EC3-1-5 Part 4.4
        lambdap(v)=(Ep(v,2)/Ep(v,3))/(28.4*epsilon*2);
        ro(v)=abs((lambdap(v)-0.055*4)/lambdap(v)^2);
        if ro(v)>1
            ro(v)=1;
        end
        %EC3-1-1 Table 5.2
        if Ep(v,2)/Ep(v,3) <= 42*epsilon
```

99

```matlab
                    Ep2(v,1)=Ep(v,1);
                    Ep2(v,2)=3;
                else
                    Ep2(v,1)=Ep(v,1)*ro(v);
                    Ep2(v,2)=4;
                end
            end
        end
        % compute the effective cross section area
        Aeff = sum(Ep2(:,1))-3*(tg+t)*t;
        Class = max(Ep2(:,2));


        % Classification according to EC3 1-1
        max_side = max(sqrt(diff(node(:, 2)).^2+diff(node(:, 1)).^2))
        if max_side/t <= 42*epsilon
            Class = 3;
        else
            Class = 4;
        end

        % Loop through the different member slendernesses. The 'meta'
        % array has one more dimension (4D)
        for l = 1:length(lambda);

            % Current profile length
            len = lambda*pi*sqrt(E*I/(A*fy));

            % Store the metadata in a cell array
            meta{i, j, k, l} = [drange(j); t; tg; fy; A; Iyy; Izz; len(l); Aeff; Class];
        end
    end
  end
end

disp(A);
disp(Iyy);
disp(Izz);
% Plot result
% plot(x, y);

% Save the profile database and metadata to the current directory as .mat
save('profiles.mat', 'profiles');
save('meta.mat', 'meta');
```

Annex C Python script for ABAQUS models

```python
 import numpy as np
import string
import sys
import os
from part import *
from material import *
from section import *
from assembly import *
from step import *
from interaction import *
from load import *
from mesh import *
from optimization import *
from job import *
from sketch import *
#from visualization import *
from connectorBehavior import *
session.journalOptions.setValues(replayGeometry=COORDINATE, recoverGeometry=COORDINATE)
# Import profiles database and profile metadata ------------------------------------------------------------

# Import pickle to load the .pkl database
import pickle

# Define a method to get the block number of a specific string in the keywords

def GetBlockPosition(model,blockPrefix):
    pos = 0
    for block in model.keywordBlock.sieBlocks:
        if string.lower(block[0:len(blockPrefix)])==string.lower(blockPrefix):
            return pos
        pos=pos+1
    return -1

# Open and read the database
profiles_file = open("./profiles.pkl",'rb')
profiles = pickle.load(profiles_file)
profiles_file.close()

profiles_file = open("./meta.pkl",'rb')
profiles_meta = pickle.load(profiles_file)
profiles_file.close()

# number of corners
#i = int(sys.argv[-5])
i = 0

# diameter of the profile
#j = int(sys.argv[-4])
j = 0

# Profile slenderness
#k = int(sys.argv[-3])
k = 0

# Member slenderness
#l = int(sys.argv[-2])
l = 0
```

101

Resistance of Polygonal Cross Section of Lattice Wind Tower

```python
# bolt spacing to diameter ratio (s/d)
#b = int(sys.argv[-1])
b = 6

# Variables holding information of the current profile
buckle_model = 'BCKL-'+str(i+1)+'-'+str(j+1)+'-'+str(k+1)+'-'+str(l+1)
current_d = float(profiles_meta[i][j][k][l][0][0])
current_t = float(profiles_meta[i][j][k][l][1][0])
current_tg = float(profiles_meta[i][j][k][l][2][0])
current_fy = float(profiles_meta[i][j][k][l][3][0])
current_l = float(profiles_meta[i][j][k][l][7][0])
current_llip = sqrt((profiles[i][j][k][0][0]-profiles[i][j][k][0][2])**2+(profiles[i][j][k][1][0]-
profiles[i][j][k][1][2])**2)
area = profiles_meta[i][j][k][l][4][0]
current_Iy = float(profiles_meta[i][j][k][l][5][0])

# Buckling model
++++++++++++++++++++++++++++++++++++++++++++++++++++++++++++++++++++++++++++++++++++++++++++
+++++++++++++++++++++++++++++++++++++++

mdb.Model(modelType=STANDARD_EXPLICIT, name=buckle_model)
c_model = mdb.models[buckle_model]


# Delete initial model
del mdb.models['Model-1']

# Create Parts ------------------------------------------------------------------------------------------------------------
-

# Sector

# -Profile sketch for sector
sector_sketch = c_model.ConstrainedSketch(name='sector', sheetSize=1200.0)

# -Sketch sector lines
for n in range(profiles[i][j][k].shape[1]-1):
    sector_sketch.Line(
        point1=(profiles[i][j][k][0][n], profiles[i][j][k][1][n]),
        point2=(profiles[i][j][k][0][n+1], profiles[i][j][k][1][n+1])
        )

# -Extrude sector part
l_tot = 2*current_l + 3*current_d
sector_part = c_model.Part(
    dimensionality=THREE_D,
    name='sector',
    type=DEFORMABLE_BODY
    )
sector_part.BaseShellExtrude(
    depth=l_tot,
    sketch=sector_sketch
    )
# Calculate bolt positions

# -Distance on the width
bolts_w = current_llip/2

# -Distances on the length
```

```python
current_b =  b
s = current_b*current_d

#4
(n0, s0) = divmod(current_l, s)
s1 = (s0 + s)/2

bolts_z1 = np.concatenate([[bolts_w], bolts_w + ((current_d - current_llip)/5) * np.linspace(1, 4, 4), [current_d - bolts_w]])
bolts_z2 = np.concatenate([[current_d + s1], s1 + current_d + (s * np.linspace(1, n0-1, n0-1))])
bolts_z3 = bolts_z1 + (current_l + current_d)
bolts_z4 = bolts_z2 + (current_l + current_d)
bolts_z5 = bolts_z3 + (current_l + current_d)

bolts_z = np.concatenate([bolts_z1, bolts_z2, bolts_z3, bolts_z4, bolts_z5])

# Washer diameter
d_washer = 30

# Initiate list to store datum planes
datum_p=[]

# Make holes

for o in range(int(bolts_z.shape[0])):

    sector_part.HoleBlindFromEdges(
        depth=1.0,
        diameter=d_washer,
        distance1=bolts_z[o],
        distance2=bolts_w,
        edge1=sector_part.edges.getClosest(coordinates=((profiles[i][j][k][0][1], profiles[i][j][k][1][1], 0),))[0][0],
        edge2=sector_part.edges.getClosest(coordinates=((profiles[i][j][k][0][0], profiles[i][j][k][1][0], 1),))[0][0],
        plane=sector_part.faces.getClosest(coordinates=((profiles[i][j][k][0][0], profiles[i][j][k][1][0], 0),))[0][0],
        planeSide=SIDE1
        )

    sector_part.HoleBlindFromEdges(
        depth=1.0,
        diameter=d_washer,
        distance1=bolts_z[o],
        distance2=bolts_w,
        edge1=sector_part.edges.getClosest(coordinates=((profiles[i][j][k][0][-2], profiles[i][j][k][1][-2], 0),))[0][0],
        edge2=sector_part.edges.getClosest(coordinates=((profiles[i][j][k][0][-1], profiles[i][j][k][1][-1], 1),))[0][0],
        plane=sector_part.faces.getClosest(coordinates=((profiles[i][j][k][0][-1], profiles[i][j][k][1][-1], 0),))[0][0],
        planeSide=SIDE1
        )

    # Create datum planes to be used for partitioning the sector

    datum1=sector_part.DatumPlaneByPrincipalPlane(
        offset=bolts_z[o]-bolts_w,
        principalPlane=XYPLANE
        )
    datum2=sector_part.DatumPlaneByPrincipalPlane(
        offset=bolts_z[o]+bolts_w,
        principalPlane=XYPLANE
```

```python
    )
  datum_p.append(datum1)
  datum_p.append(datum2)

# Partition the sector

# -Number of datum planes
n_dat = int(len(sector_part.datums))

# cut all the faces using the datum planes

for o in range((n_dat-2)):
#for o in range(2):
  sector_part.PartitionFaceByDatumPlane(
    datumPlane=sector_part.datums.items()[o+1][1],
    faces=sector_part.faces[:]
    )

# Gusset

# -Profile sketch for gusset
gusset_sketch=c_model.ConstrainedSketch(name='__profile__', sheetSize=1200.0)

# -Sketch gusset lines
# First point of the first sector
x0 = profiles[i][j][k][0][0]
y0 = profiles[i][j][k][1][0]

# Angle of the first gusset fin
phi = pi*5/6

# Calculate the end point of the gusset's first fin as an orthogonal projection of the sector's first point on the line
of the gusset plate
gp1 = np.array([(x0*cos(phi)+y0*sin(phi))*cos(phi), (x0*cos(phi)+y0*sin(phi))*sin(phi)])

# Rotation matrix to multiply the previous point in order to get the points of the other 2 gusset fins
Rmat = np.array([[cos(-2*pi/3), -sin(-2*pi/3)], [sin(-2*pi/3), cos(-2*pi/3)]])

# Calculate the end points of the other 2 gusset fins by multiplying with the 120 degrees rotation matrix
gp2 = gp1.dot(Rmat)
gp3 = gp2.dot(Rmat)

# Draw lines for the sketch of the gusset plate between 0, 0 and the calculated points gp1, gp2, gp3
gusset_sketch.Line(
  point1=(0.0, 0.0),
  point2=(gp1[0], gp1[1])
  )
gusset_sketch.Line(
  point1=(0.0, 0.0),
  point2=(gp2[0], gp2[1])
  )
gusset_sketch.Line(
  point1=(0.0, 0.0),
  point2=(gp3[0], gp3[1])
  )

# -Extrude gusset part
gusset_part=c_model.Part(
  dimensionality=THREE_D,
```

```python
    name='gusset',
    type=DEFORMABLE_BODY
    )
gusset_part.BaseShellExtrude(
    depth=current_d,
    sketch=gusset_sketch
    )

# -Holes
for o in range(int(bolts_z1.shape[0])):
    gusset_part.HoleBlindFromEdges(
        depth=1.0,
        diameter=d_washer,
        distance1=bolts_z1[o],
        distance2=bolts_w,
        edge1=gusset_part.edges.getClosest(coordinates=((gp1[0]/2, gp1[1]/2, 0),))[0][0],
        edge2=gusset_part.edges.getClosest(coordinates=((gp1[0], gp1[1], 1),))[0][0],
        plane=gusset_part.faces.getClosest(coordinates=((gp1[0], gp1[1], 0),))[0][0],
        planeSide=SIDE1
        )

    gusset_part.HoleBlindFromEdges(
        depth=1.0,
        diameter=d_washer,
        distance1=bolts_z1[o],
        distance2=bolts_w,
        edge1=gusset_part.edges.getClosest(coordinates=((gp2[0]/2, gp2[1]/2, 0),))[0][0],
        edge2=gusset_part.edges.getClosest(coordinates=((gp2[0], gp2[1], 1),))[0][0],
        plane=gusset_part.faces.getClosest(coordinates=((gp2[0], gp2[1], 0),))[0][0],
        planeSide=SIDE1
        )

    gusset_part.HoleBlindFromEdges(
        depth=1.0,
        diameter=d_washer,
        distance1=bolts_z1[o],
        distance2=bolts_w,
        edge1=gusset_part.edges.getClosest(coordinates=((gp3[0]/2, gp3[1]/2, 0),))[0][0],
        edge2=gusset_part.edges.getClosest(coordinates=((gp3[0], gp3[1], 1),))[0][0],
        plane=gusset_part.faces.getClosest(coordinates=((gp3[0], gp3[1], 0),))[0][0],
        planeSide=SIDE1
        )

# Partition gusset

gusset_part.DatumPointByCoordinate((gp1[0]-current_llip*cos(5*pi/6), gp1[1]-current_llip*sin(5*pi/6), 0),)
gusset_part.DatumPointByCoordinate((gp1[0]-current_llip*cos(5*pi/6), gp1[1]-current_llip*sin(5*pi/6), current_d),)

gusset_part.PartitionFaceByShortestPath(
    faces=gusset_part.faces.getClosest(coordinates=((gp1[0], gp1[1], 0),))[0][0],
    point1=gusset_part.datum.items()[0][1],
    point2=gusset_part.datum.items()[1][1],
    )

gusset_part.DatumPointByCoordinate((gp2[0]-current_llip*cos(-pi/2), gp2[1]-current_llip*sin(-pi/2), 0),)
gusset_part.DatumPointByCoordinate((gp2[0]-current_llip*cos(-pi/2), gp2[1]-current_llip*sin(-pi/2), current_d),)
```

```
gusset_part.PartitionFaceByShortestPath(
    faces=gusset_part.faces.getClosest(coordinates=((gp2[0], gp2[1], 0),))[0][0],
    point1=gusset_part.datum.items()[2][1],
    point2=gusset_part.datum.items()[3][1],
    )

gusset_part.DatumPointByCoordinate((gp3[0]-current_llip*cos(pi/6), gp3[1]-current_llip*sin(pi/6), 0),)
gusset_part.DatumPointByCoordinate((gp3[0]-current_llip*cos(pi/6), gp3[1]-current_llip*sin(pi/6), current_d),)

gusset_part.PartitionFaceByShortestPath(
    faces=gusset_part.faces.getClosest(coordinates=((gp3[0], gp3[1], 0),))[0][0],
    point1=gusset_part.datum.items()[4][1],
    point2=gusset_part.datum.items()[5][1],
    )

# Material ----------------------------------------------------------------------------------------------------

c_model.Material(name='optim355')
c_model.materials['optim355'].Elastic(table=((210000.0, 0.3), ))

# Create sections ----------------------------------------------------------------------------------------------

# -for sector
c_model.HomogeneousShellSection(
    idealization=NO_IDEALIZATION,
    integrationRule=SIMPSON,
    material='optim355',
    name='sector',
    numIntPts=5,
    poissonDefinition=DEFAULT,
    preIntegrate=OFF,
    temperature=GRADIENT,
    thickness=current_t,
    thicknessField='',
    thicknessModulus=None,
    thicknessType=UNIFORM,
    useDensity=OFF
    )

# -for gusset
c_model.HomogeneousShellSection(
    idealization=NO_IDEALIZATION,
    integrationRule=SIMPSON,
    material='optim355',
    name='gusset',
    numIntPts=5,
    poissonDefinition=DEFAULT,
    preIntegrate=OFF,
    temperature=GRADIENT,
    thickness=current_tg,
    thicknessField='',
    thicknessModulus=None,
    thicknessType=UNIFORM,
    useDensity=OFF
    )

# Assign sections ----------------------------------------------------------------------------------------------

# -for sector
```

```
sector_part.Set(
    faces=sector_part.faces[:],
    name='AllSectorFaces'
    )
sector_part.SectionAssignment(
    offset=0.0,
    offsetField='',
    offsetType=MIDDLE_SURFACE,
    region=sector_part.sets['AllSectorFaces'],
    sectionName='sector',
    thicknessAssignment=FROM_SECTION
    )

# -for gusset
gusset_part.Set(
    faces=gusset_part.faces[:],
    name='AllGussetFaces')
gusset_part.SectionAssignment(
    offset=0.0,
    offsetField='',
    offsetType=MIDDLE_SURFACE,
    region=gusset_part.sets['AllGussetFaces'],
    sectionName='gusset',
    thicknessAssignment=FROM_SECTION
    )

# Meshing --------------------------------------------------------------------------------------------------------------

# Global seeding in mm
seedsize = 30

# -Sector
sector_part.setMeshControls(
    algorithm=MEDIAL_AXIS,
    elemShape=QUAD,
    regions=sector_part.faces[:]
    )
sector_part.seedPart(
    deviationFactor=0.1,
    minSizeFactor=0.1,
    size=seedsize
    )
sector_part.generateMesh()

# -Gusset
gusset_part.setMeshControls(
    algorithm=MEDIAL_AXIS,
    elemShape=QUAD,
    regions=gusset_part.faces[:]
    )
gusset_part.seedPart(
    deviationFactor=0.1,
    minSizeFactor=0.1,
    size=seedsize
    )
gusset_part.generateMesh()

# Create assembly -------------------------------------------------------------------------------------------------
```

```python
c_assembly=c_model.rootAssembly
c_assembly.DatumCsysByDefault(CARTESIAN)

# -Sectors
s1_instance=c_assembly.Instance(
    dependent=ON,
    name='sector-1',
    part=sector_part
    )
c_assembly.DatumAxisByPrincipalAxis(
    principalAxis=ZAXIS
    )
s3_instance=c_assembly.RadialInstancePattern(
    axis=(0.0, 0.0, 1.0),
    instanceList=('sector-1', ),
    number=3, point=(0.0, 0.0, 0.0),
    totalAngle=240.0
    )

s2_instance=s3_instance[0]
s3_instance=s3_instance[1]

s_instance = (s1_instance,s2_instance ,s3_instance)

# -Gusset plate

# --Create the instances
g1_instance=c_assembly.Instance(
    dependent=ON,
    name='gusset-1',
    part=gusset_part
    )
g2_instance=c_assembly.Instance(
    dependent=ON,
    name='gusset-2',
    part=gusset_part
    )
g3_instance=c_assembly.Instance(
    dependent=ON,
    name='gusset-3',
    part=gusset_part
    )

# --Translate them to the right position
g2_instance.translate(
    vector=(0.0, 0.0, (current_l + current_d))
    )
g3_instance.translate(
    vector=(0.0, 0.0, 2*(current_l + current_d))
    )

# Interactions ------------------------------------------------------------------------------------------------------

# Create sets node regions to be used for the tie and coupling constraints
# initiate variables to store points for findAt

holes11=()
holes12=()
holes21=()
```

```python
holes22=()
holes31=()
holes32=()
gholes1=()
gholes2=()
gholes3=()

# Position of the holes on the cross-section
sh11 = np.array([profiles[i][j][k][0][1], profiles[i][j][k][1][1]])
sh12 = np.array([profiles[i][j][k][0][-2], profiles[i][j][k][1][-2]])

gh1 = (gp1[0]-bolts_w*cos(5*pi/6), gp1[1]-bolts_w*sin(5*pi/6))
gh2 = (gp2[0]-bolts_w*cos(-pi/2), gp2[1]-bolts_w*sin(-pi/2))
gh3 = (gp3[0]-bolts_w*cos(pi/6), gp3[1]-bolts_w*sin(pi/6))

gh=(gh1, gh2, gh3)

# Rotation matrix to multiply the previous point in order to get the points of the other 2 gusset fins
Rmat = np.array([[cos(-2*pi/3), -sin(-2*pi/3)], [sin(-2*pi/3), cos(-2*pi/3)]])

# Calculate the end points of the other 2 gusset fins by multiplying with the 120 degrees rotation matrix
sh21 = sh11.dot(Rmat)
sh22 = sh12.dot(Rmat)

sh31 = sh21.dot(Rmat)
sh32 = sh22.dot(Rmat)

sh = ((sh11, sh12), (sh21, sh22), (sh31, sh32))

# Create reference points for the bolt ridig body couplings

# Create the necessary sets and the tie constraints for all the bolts

# End 1 connection
for oo in (range(3)):
    ii=1
    for o in tuple(bolts_z1):

        c_assembly.ReferencePoint((gh[oo-3][0], gh[oo-3][1], float(o)))

        c_assembly.Set(
            edges=s_instance[oo-3].edges.findAt(((sh[oo-3][0][0], sh[oo-3][0][1], float(o)-d_washer/2), ), )+\
            s_instance[oo-2].edges.findAt(((sh[oo-2][1][0], sh[oo-2][1][1], float(o)-d_washer/2), ), )+\
            g1_instance.edges.findAt(((gh[oo-3][0], gh[oo-3][1], float(o)-d_washer/2), ), ),
            name='b'+str(ii)+str(oo)+'set1'
            )

        c_model.RigidBody(
            name='b1'+str(ii)+str(oo)+'joint1',
            refPointRegion=Region(referencePoints=(c_assembly.referencePoints.findAt((gh[oo-3][0], gh[oo-3][1],
float(o))), )),
            tieRegion=c_assembly.sets['b'+str(ii)+str(oo)+'set1']
            )

        ii+=1

# Span 1

for oo in (range(3)):
```

```python
    ii=1
    for o in tuple(bolts_z2):

        c_assembly.ReferencePoint((gh[oo-3][0], gh[oo-3][1], float(o)))

        c_assembly.Set(
            edges=s_instance[oo-3].edges.findAt(((sh[oo-3][0][0], sh[oo-3][0][1], float(o)-d_washer/2), ), )+\
            s_instance[oo-2].edges.findAt(((sh[oo-2][1][0], sh[oo-2][1][1], float(o)-d_washer/2), ), ),
            name='b'+str(ii)+str(oo)+'-set2'
            )

        c_model.RigidBody(
            name='b1'+str(ii)+str(oo)+'span1',
            refPointRegion=Region(referencePoints=(c_assembly.referencePoints.findAt((gh[oo-3][0], gh[oo-3][1],
float(o))), )),
            tieRegion=c_assembly.sets['b'+str(ii)+str(oo)+'-set2']
            )

        ii+=1

# middle connection


for oo in (range(3)):
    ii=1
    for o in tuple(bolts_z3):

        c_assembly.ReferencePoint((gh[oo-3][0], gh[oo-3][1], float(o)))

        c_assembly.Set(
            edges=s_instance[oo-3].edges.findAt(((sh[oo-3][0][0], sh[oo-3][0][1], float(o)-d_washer/2), ), )+\
            s_instance[oo-2].edges.findAt(((sh[oo-2][1][0], sh[oo-2][1][1], float(o)-d_washer/2), ), )+\
            g2_instance.edges.findAt(((gh[oo-3][0], gh[oo-3][1], float(o)-d_washer/2), ), ),
            name='b'+str(ii)+str(oo)+'set3'
            )

        c_model.RigidBody(
            name='b1'+str(ii)+str(oo)+'joint2',
            refPointRegion=Region(referencePoints=(c_assembly.referencePoints.findAt((gh[oo-3][0], gh[oo-3][1],
float(o))), )),
            tieRegion=c_assembly.sets['b'+str(ii)+str(oo)+'set3']
            )

        ii+=1

# Span 2

for oo in (range(3)):
    ii=1
    for o in tuple(bolts_z4):

        c_assembly.ReferencePoint((gh[oo-3][0], gh[oo-3][1], float(o)))

        c_assembly.Set(
            edges=s_instance[oo-3].edges.findAt(((sh[oo-3][0][0], sh[oo-3][0][1], float(o)-d_washer/2), ), )+\
            s_instance[oo-2].edges.findAt(((sh[oo-2][1][0], sh[oo-2][1][1], float(o)-d_washer/2), ), ),
            name='b'+str(ii)+str(oo)+'-set4'
            )
```

```python
    c_model.RigidBody(
        name='b1'+str(ii)+str(oo)+'span2',
        refPointRegion=Region(referencePoints=(c_assembly.referencePoints.findAt((gh[oo-3][0], gh[oo-3][1],
float(o))), )),
        tieRegion=c_assembly.sets['b'+str(ii)+str(oo)+'-set4']
        )

    ii+=1

# End 2 connection
for oo in (range(3)):
    ii=1
    for o in tuple(bolts_z5):

        c_assembly.ReferencePoint((gh[oo-3][0], gh[oo-3][1], float(o)))

        c_assembly.Set(
            edges=s_instance[oo-3].edges.findAt(((sh[oo-3][0][0], sh[oo-3][0][1], float(o)-d_washer/2), ), )+\
            s_instance[oo-2].edges.findAt(((sh[oo-2][1][0], sh[oo-2][1][1], float(o)-d_washer/2), ), )+\
            g3_instance.edges.findAt(((gh[oo-3][0], gh[oo-3][1], float(o)-d_washer/2), ), ),
            name='b'+str(ii)+str(oo)+'set5'
            )

        c_model.RigidBody(
            name='b1'+str(ii)+str(oo)+'joint3',
            refPointRegion=Region(referencePoints=(c_assembly.referencePoints.findAt((gh[oo-3][0], gh[oo-3][1],
float(o))), )),
            tieRegion=c_assembly.sets['b'+str(ii)+str(oo)+'set5']
            )

        ii+=1

# Create reference points for BCs/loads.

# -RPs for the faces at the two ends of the columns
c_assembly.ReferencePoint((0.0, 0.0, 0.0))
c_assembly.ReferencePoint((0.0, 0.0, (2*current_l + 3*current_d)))

# - RP at the middle
c_assembly.ReferencePoint((0.0, 0.0, (current_l + 1.5*current_d)))


# - End face couplings to reference points

# End 1
c_assembly.Set(
    name='RP-1-set',
    referencePoints=(c_assembly.referencePoints.findAt((0, 0, 0)), )
    )

c_assembly.Set(
    edges=g1_instance.edges.getByBoundingBox(-current_d,-current_d,0,current_d,current_d,0)+\
    s_instance[0].edges.getByBoundingBox(-current_d,-current_d,0,current_d,current_d,0)+\
    s_instance[1].edges.getByBoundingBox(-current_d,-current_d,0,current_d,current_d,0)+\
    s_instance[2].edges.getByBoundingBox(-current_d,-current_d,0,current_d,current_d,0),
    name='end1-face',
    )

c_model.Coupling(
```

```python
    controlPoint=c_assembly.sets['RP-1-set'],
    couplingType=KINEMATIC,
    influenceRadius=WHOLE_SURFACE,
    localCsys=None,
    name='end1-coupling',
    surface=c_assembly.sets['end1-face'],
    u1=ON, u2=ON, u3=ON, ur1=ON, ur2=ON, ur3=ON
    )

# End 2

c_assembly.Set(
    name='RP-2-set',
    referencePoints=(c_assembly.referencePoints.findAt((0, 0, 2*(current_l+1.5*current_d))), )
    )

c_assembly.Set(
    edges=g3_instance.edges.getByBoundingBox(-current_d,-
current_d,2*(current_l+1.5*current_d),current_d,current_d,2*(current_l+1.5*current_d))+\
    s_instance[0].edges.getByBoundingBox(-current_d,-
current_d,2*(current_l+1.5*current_d),current_d,current_d,2*(current_l+1.5*current_d))+\
    s_instance[1].edges.getByBoundingBox(-current_d,-
current_d,2*(current_l+1.5*current_d),current_d,current_d,2*(current_l+1.5*current_d))+\
    s_instance[2].edges.getByBoundingBox(-current_d,-
current_d,2*(current_l+1.5*current_d),current_d,current_d,2*(current_l+1.5*current_d)),
    name='end2-face'
    )

c_model.Coupling(
    controlPoint=c_assembly.sets['RP-2-set'],
    couplingType=KINEMATIC, influenceRadius=WHOLE_SURFACE,
    localCsys=None,
    name='end2-coupling',
    surface=c_assembly.sets['end2-face'],
    u1=ON, u2=ON, u3=ON, ur1=ON, ur2=ON, ur3=ON
    )

# Middle

c_assembly.Set(
    name='RP-Mid-set',
    referencePoints=(c_assembly.referencePoints.findAt((0.0, 0.0, (current_l + 1.5*current_d))), )
    )

c_assembly.Set(
    edges=g2_instance.edges.findAt(((0, 0, (current_l + 1.5*current_d)), ), ),
    name='gusset-fin-interface',
    )

c_model.Coupling(
    controlPoint=c_assembly.sets['RP-Mid-set'],
    couplingType=KINEMATIC,
    influenceRadius=WHOLE_SURFACE,
    localCsys=None,
    name='Mid-coupling',
    surface=c_assembly.sets['gusset-fin-interface'],
    u1=ON, u2=ON, u3=ON, ur1=ON, ur2=ON, ur3=ON
    )
```

Resistance of Polygonal Cross Section of Lattice Wind Tower

```python
# Step ----------------------------------------------------------------------

c_model.BuckleStep(
    maxIterations=300,
    name='Buckling',
    numEigen=4,
    previous='Initial',
    vectors=10
    )


# Boundary Conditions -------------------------------------------------------

# BCs
end1_BC=c_model.DisplacementBC(
    amplitude=UNSET,
    createStepName='Initial',
    distributionType=UNIFORM,
    fieldName='',
    localCsys=None,
    name='fix-end1',
    region=Region(referencePoints=(c_assembly.referencePoints.findAt((0, 0, 0)), )),
    u1=SET, u2=SET, u3=SET, ur1=UNSET, ur2=UNSET, ur3=SET
    )

end2_BC=c_model.DisplacementBC(
    amplitude=UNSET,
    createStepName='Initial',
    distributionType=UNIFORM,
    fieldName='',
    localCsys=None,
    name='fix-end2',
    region=Region(referencePoints=(c_assembly.referencePoints.findAt((0, 0, 2*(current_l+1.5*current_d))), )),
    u1=SET, u2=SET, u3=UNSET, ur1=UNSET, ur2=UNSET, ur3=SET
    )

middle_BC=c_model.DisplacementBC(
    amplitude=UNSET,
    createStepName='Initial',
    distributionType=UNIFORM,
    fieldName='',
    localCsys=None,
    name='fix-middle',
    region=Region(referencePoints=(c_assembly.referencePoints.findAt((0, 0, current_l+1.5*current_d)), )),
    u1=SET, u2=SET, u3=UNSET, ur1=UNSET, ur2=UNSET, ur3=UNSET
    )


# Load ----------------------------------------------------------------------

c_model.ConcentratedForce(
    cf3=-1.0,
    createStepName='Buckling',
    distributionType=UNIFORM,
    field='',
    localCsys=None,
    name='compression',
    region=c_assembly.sets['RP-2-set']
    )
```

Resistance of Polygonal Cross Section of Lattice Wind Tower

```
# Create the job -----------------------------------------------------------

c_job=mdb.Job(
    atTime=None,
    contactPrint=OFF,
    description='',
    echoPrint=OFF,
    explicitPrecision=SINGLE,
    getMemoryFromAnalysis=True,
    historyPrint=OFF,
    memory=90,
    memoryUnits=PERCENTAGE,
    model=buckle_model,
    modelPrint=OFF,
    multiprocessingMode=DEFAULT,
    name=buckle_model,
    nodalOutputPrecision=SINGLE,
    numCpus=1,
    numGPUs=0,
    queue=None,
    resultsFormat=ODB,
    scratch='',
    type=ANALYSIS,
    userSubroutine='',
    waitHours=0,
    waitMinutes=0
    )

# Edit the keywords to output translations on the output file
c_model.keywordBlock.synchVersions(storeNodesAndElements=False)
c_model.keywordBlock.insert(GetBlockPosition(c_model,'*End Step')-1, '*NODE FILE\nU')

# Write the input file
mdb.jobs[buckle_model].writeInput()

# RIKS model, Only axial
++++++++++++++++++++++++++++++++++++++++++++++++++++++++++++++++++++++++++++++++++
++++++++++++++++++++++++++++

riks_model_N = 'RIKS-N-'+str(i+1)+'-'+str(j+1)+'-'+str(k+1)+'-'+str(l+1)

# Copy model from buckling analysis
r_model_N=mdb.Model(
    name=riks_model_N,
    objectToCopy=c_model
    )

# Delete buckling step
del r_model_N.steps['Buckling']

# Create RIKS step
r_model_N.StaticRiksStep(
    name='RIKS',
    previous='Initial',
    nlgeom=ON,
    maxNumInc=30,
    initialArcInc=0.2
    )
```

Resistance of Polygonal Cross Section of Lattice Wind Tower

```python
# Change to plastic material, optim355
r_model_N.materials['optim355'].Plastic(table=((381.1, 0.0), (
    391.2, 0.0053), (404.8, 0.0197), (418.0, 0.0228), (444.2, 0.0310), (499.8,
    0.0503), (539.1, 0.0764), (562.1, 0.1009), (584.6, 0.1221), (594.4,
    0.1394)))

# Apply concentrated force
N_pl_rd = 510*area

r_model_N.ConcentratedForce(
    cf3=-N_pl_rd,
    createStepName='RIKS',
    distributionType=UNIFORM,
    field='',
    localCsys=None,
    name='compression',
    region=r_model_N.rootAssembly.sets['RP-2-set']
    )

# Field and History output requests

r_model_N.historyOutputRequests.changeKey(
    fromName='H-Output-1',
    toName='load'
    )

r_model_N.historyOutputRequests['load'].setValues(
    rebar=EXCLUDE,
    region=r_model_N.rootAssembly.sets['RP-1-set'],
    sectionPoints=DEFAULT, variables=('RF3', )
    )

r_model_N.HistoryOutputRequest(
    createStepName='RIKS',
    name='disp',
    rebar=EXCLUDE,
    region=r_model_N.rootAssembly.sets['RP-2-set'],
    sectionPoints=DEFAULT,
    variables=('U3', )
    )

r_model_N.HistoryOutputRequest(
    createStepName='RIKS',
    name='moment',
    rebar=EXCLUDE,
    region=r_model_N.rootAssembly.sets['RP-Mid-set'],
    sectionPoints=DEFAULT,
    variables=('UR1', )
    )

r_model_N.fieldOutputRequests.changeKey(
    fromName='F-Output-1',
    toName='fields'
    )
r_model_N.fieldOutputRequests['fields'].setValues(
    variables=('S', 'MISES', 'E', 'PEEQ', 'U')
    )

# Delete keyword nodefile
```

```
r_model_N.keywordBlock.synchVersions(storeNodesAndElements=False)
r_model_N.keywordBlock.replace(GetBlockPosition(r_model_N,'*End Step')-1, '\n')

# Change keywords to include initial imperfections file (filename was given wrong initially and corrected later)
amp_impf = s/2000
#r_model_N.keywordBlock.synchVersions(storeNodesAndElements=False)
r_model_N.keywordBlock.replace(GetBlockPosition(r_model_N, '*step')-1,
'\n** ---------------------------------------------------------------\n** \n**********GEOMETRICAL
IMPERFECTIONS\n*IMPERFECTION,FILE='
+ str(buckle_model) +',STEP=1\n1,'+ str(float(amp_impf)) +'\n2,'+ str(float(amp_impf)) +'\n3,'+
str(float(amp_impf)) +'\n4,'+ str(float(amp_impf)) +'\n**')

# Create Job
mdb.Job(
    atTime=None,
    contactPrint=OFF,
    description='',
    echoPrint=OFF,
    explicitPrecision=SINGLE,
    getMemoryFromAnalysis=True,
    historyPrint=OFF,
    memory=90,
    memoryUnits=PERCENTAGE,
    model='RIKS-N-1-1-1-1',
    modelPrint=OFF,
    multiprocessingMode=DEFAULT,
    name='RIKS-N-1-1-1-1',
    nodalOutputPrecision=SINGLE,
    numCpus=1,
    numGPUs=0,
    queue=None,
    resultsFormat=ODB,
    scratch='',
    type=ANALYSIS,
    userSubroutine='',
    waitHours=0,
    waitMinutes=0
    )

# Write the input file
mdb.jobs[riks_model_N].writeInput()

# RIKS model, Axial snd bending
+++++++++++++++++++++++++++++++++++++++++++++++++++++++++++++++++++++++++++++++++++++++++++++
++++++++++++++++++++++++++

riks_model_NM = 'RIKS-NM-'+str(i+1)+'-'+str(j+1)+'-'+str(k+1)+'-'+str(l+1)

# Copy model from buckling analysis
r_model_NM=mdb.Model(
    name=riks_model_NM,
    objectToCopy=r_model_N
    )

# Apply bending moment at the mid-connection
# Calculate the magnitude of moment as 10% of moment resistance
W = current_Iy/(current_d/2)
M_resist = W*current_fy
M = 0.1*M_resist
```

```python
r_model_NM.Moment(
    cm1=-M,
    createStepName='RIKS',
    distributionType=UNIFORM,
    field='',
    localCsys=None,
    name='moment',
    region=c_assembly.sets['RP-Mid-set']
    )

# Create Job
mdb.Job(
    atTime=None,
    contactPrint=OFF,
    description='',
    echoPrint=OFF,
    explicitPrecision=SINGLE,
    getMemoryFromAnalysis=True,
    historyPrint=OFF,
    memory=90,
    memoryUnits=PERCENTAGE,
    model='RIKS-NM-1-1-1-1',
    modelPrint=OFF,
    multiprocessingMode=DEFAULT,
    name='RIKS-NM-1-1-1-1',
    nodalOutputPrecision=SINGLE,
    numCpus=1,
    numGPUs=0,
    queue=None,
    resultsFormat=ODB,
    scratch='',
    type=ANALYSIS,
    userSubroutine='',
    waitHours=0,
    waitMinutes=0
    )

# Write the input file
mdb.jobs[riks_model_NM].writeInput()



# Save the model -------------------------------------------------------------------------------------------
mdb.saveAs(pathName=os.getcwd()+'\\'+str(i+1)+'-'+str(j+1)+'-'+str(k+1)+'-'+str(l+1)+'.cae')
```

Annex D Python script for history output (N)

```python
import numpy as np
import os
import string
import sys
import odbAccess

from odbAccess import *
from abaqusConstants import *

# Import pickle to load the .pkl database
import pickle

# Open and read the database
profiles_file = open("profiles.pkl",'rb')
profiles = pickle.load(profiles_file)
profiles_file.close()

profiles_file = open("meta8.pkl",'rb')
profiles_meta = pickle.load(profiles_file)
profiles_file.close()


NameOfFile='maxforcedispldata-N.txt'
out = open(NameOfFile,'w')



for b in (3, 4, 5):
    for l in (1, 2, 3):
        for k in (3, 5):
            for j in (2, 3, 4):
                for i in range (1,2,1):

                    # Variables holding information of the current profile
                    name='RIKS-N-1-'+str(j)+'-'+str(k)+'-'+str(l)+'-'+str(b)+'.odb'
                    current_d = float(profiles_meta[i-1][j-1][k-1][l-1][0][0])
                    current_t = float(profiles_meta[i-1][j-1][k-1][l-1][1][0])
                    current_l = float(profiles_meta[i-1][j-1][k-1][l-1][7][0])
                    current_fy = float(profiles_meta[i-1][j-1][k-1][l-1][3][0])
                    current_area = float(profiles_meta[i-1][j-1][k-1][l-1][4][0])
                    current_Iy = float(profiles_meta[i-1][j-1][k-1][l-1][5][0])
                    current_effarea = float(profiles_meta[i-1][j-1][k-1][l-1][8][0])
                    current_class = float(profiles_meta[i-1][j-1][k-1][l-1][9][0])
                    current_It = float(profiles_meta[i-1][j-1][k-1][l-1][10][0])
                    current_Iw = float(profiles_meta[i-1][j-1][k-1][l-1][11][0])
                    E=210000
                    G=81000
                    epsilon=(sqrt(235/current_fy))*(sqrt(235/current_fy))
                    current_lambda = current_l/(pi*sqrt(E*current_Iy/(current_area*current_fy)))

                    nameOfStep='RIKS'
                    myOdb = odbAccess.openOdb(path=name)
                    RIKS= myOdb.steps[nameOfStep]

                    rp1key = RIKS.historyRegions.keys()[1]
                    ho1key = RIKS.historyRegions[rp1key].historyOutputs.keys()[0]
                    rp2key = RIKS.historyRegions.keys()[2]
                    ho2key = RIKS.historyRegions[rp2key].historyOutputs.keys()[0]
```

Resistance of Polygonal Cross Section of Lattice Wind Tower

```python
load_hist = RIKS.historyRegions[rp1key].historyOutputs[ho1key].data
disp_hist = RIKS.historyRegions[rp2key].historyOutputs[ho2key].data
maxpos = load_hist.index(max(load_hist,key=lambda x:x[1]))
load = load_hist[maxpos][1]
disp = -disp_hist[maxpos][1]


# Calculation of resistance according to EC3-1-3 Part 6
# Cross section resistance pure axial compression
gamma_m0 = 1.0
current_Ncrd = current_effarea*current_fy/gamma_m0

#Buckling resistance
#Flexural buckling
alpha=0.21  #buckling coefficient
current_i = sqrt(current_Iy/current_effarea)
current_sigmacrit = ((pi*pi)*E)/((current_l/current_i)*(current_l/current_i))
current_lambdabar = sqrt((current_fy*current_effarea)/(current_sigmacrit*current_effarea))
current_Phi = 0.5*(1+alpha*(current_lambdabar - 0.2)+(current_lambdabar*current_lambdabar))
current_Chi = 1/(current_Phi+sqrt((current_Phi*current_Phi)-
(current_lambdabar*current_lambdabar)))
        if current_Chi>1:
            current_Chi = 1
current_Nbf = current_Chi*current_effarea*current_fy

#Torsional buckling
current_io = sqrt((current_i*current_i)+(current_i*current_i))
current_sigmacritT =
(1/(current_area*(current_io*current_io)))*(G*current_It+((pi*pi*E*current_Iw)/(current_l*current_l)))
current_lambdabarT = sqrt((current_fy*current_effarea)/(current_sigmacritT*current_area))
current_PhiT = 0.5*(1+alpha*(current_lambdabarT -
0.2)+(current_lambdabarT*current_lambdabarT))
current_ChiT = 1/(current_PhiT+sqrt((current_PhiT*current_PhiT)-
(current_lambdabarT*current_lambdabarT)))
        if current_ChiT>1:
            current_ChiT = 1
current_NbT = current_ChiT*current_effarea*current_fy

#Flexural-Torsional buckling
beta = 1.0
current_sigmacritFT = (current_sigmacrit/(2*beta))*(1+(current_sigmacritT/current_sigmacrit)-
(sqrt((1-(current_sigmacritT/current_sigmacrit))*(1-
(current_sigmacritT/current_sigmacrit)))+(4*0*current_sigmacritT/current_sigmacrit)))
current_lambdabarFT = sqrt((current_fy*current_effarea)/(current_sigmacritFT*current_area))
current_PhiFT = 0.5*(1+alpha*(current_lambdabarFT -
0.2)+(current_lambdabarFT*current_lambdabarFT))
current_ChiFT = 1/(current_PhiFT+sqrt((current_PhiFT*current_PhiFT)-
(current_lambdabarFT*current_lambdabarFT)))
        if current_ChiFT>1:
            current_ChiFT = 1
current_NbFT = current_ChiFT*current_effarea*current_fy

# Calculation of resistance according to EC3-1-6 Shell
Cxb = 1  #pinned-pinned BC
Q = 16  #fabrication class C
lambdaxo = 0.2
betax = 0.6
gammam1 = 1.1
current_w = current_l/sqrt((current_d/2)/current_t)
```

Resistance of Polygonal Cross Section of Lattice Wind Tower

```python
                limit = 0.5*(current_d/2)/current_t
                if current_w>limit:
                    current_Cx = 1+((0.2/Cxb)*(1-2*current_w*current_t/(current_d/2)))
                    if current_Cx<0.6:
                        current_Cx=0.6
                    current_sigmaxRcr = 0.605*E*current_Cx*current_t/(current_d/2)  #critical meridional buckling
stress
                    current_alphax = 0.62/(1+(1.91*((1/Q)*sqrt(current_d/2)/current_t)*1.44))
                    current_lambdabarp=sqrt(current_alphax/(1-betax))
                    current_lambdax = sqrt(current_fy/current_sigmaxRcr)
                    current_Chix = 1-betax*((current_lambdax-lambdaxo)/(current_lambdabarp-lambdaxo))
                    current_sigmaRd = current_Chix*current_fy/gammam1       #design resistance
                    current_Ncrdshell = current_sigmaRd*current_area




out.write(str(current_d)+'\t'+str(round(current_d/current_t,2))+'\t'+str(current_lambda)+'\t'+str(b)+'\t'+str(load)+'
\t'+

str(disp)+'\t'+str(current_d/(current_t*epsilon))+'\t'+str(current_area)+'\t'+str(current_effarea)+'\t'+str(current_cl
ass)+'\t'+str(current_Ncrd)+'\t'+str(current_Nbf)+'\t'+str(current_NbT)+'\t'+str(current_NbFT)+'\t'+str(current_N
crdshell)+'\n')
                myOdb.close()
```

Annex E Python script for history output (N+M)

```python
import numpy as np
import os
import string
import sys
import odbAccess

from odbAccess import *
from abaqusConstants import *

# Import pickle to load the .pkl database
import pickle

# Open and read the database
profiles_file = open("profiles.pkl",'rb')
profiles = pickle.load(profiles_file)
profiles_file.close()

profiles_file = open("meta13.pkl",'rb')
profiles_meta = pickle.load(profiles_file)
profiles_file.close()


NameOfFile='maxforcedispldata-NM05.txt'
out = open(NameOfFile,'w')



for b in (3, 4, 5):
   for l in (1, 2, 3):
      for k in (3, 5):
         for j in (2, 3, 4):
            for i in range (1,2,1):

               # Variables holding information of the current profile
               name='1-'+str(j)+'-'+str(k)+'-'+str(l)+'-'+str(b)+'-RIKS-NM-05'+'.odb'
               current_d = float(profiles_meta[i-1][j-1][k-1][l-1][0][0])
               current_t = float(profiles_meta[i-1][j-1][k-1][l-1][1][0])
               current_l = float(profiles_meta[i-1][j-1][k-1][l-1][7][0])
               current_fy = float(profiles_meta[i-1][j-1][k-1][l-1][3][0])
               current_area = float(profiles_meta[i-1][j-1][k-1][l-1][4][0])
               current_Iy = float(profiles_meta[i-1][j-1][k-1][l-1][5][0])
               current_effarealocal = float(profiles_meta[i-1][j-1][k-1][l-1][8][0])
               current_class = float(profiles_meta[i-1][j-1][k-1][l-1][9][0])
               current_It = float(profiles_meta[i-1][j-1][k-1][l-1][10][0])
               current_Iw = float(profiles_meta[i-1][j-1][k-1][l-1][11][0])
               current_cornerround1 = float(profiles_meta[i-1][j-1][k-1][l-1][12][0])
               current_cornerround2 = float(profiles_meta[i-1][j-1][k-1][l-1][13][0])
               current_bp = float(profiles_meta[i-1][j-1][k-1][l-1][14][0])
               current_llip = float(profiles_meta[i-1][j-1][k-1][l-1][15][0])

               E=210000
               G=81000
               epsilon=(sqrt(235/current_fy))*(sqrt(235/current_fy))
               current_lambda = current_l/(pi*sqrt(E*current_Iy/(current_area*current_fy)))

               nameOfStep='RIKS'
               myOdb = odbAccess.openOdb(path=name)
               RIKS= myOdb.steps[nameOfStep]
```

```
rp1key = RIKS.historyRegions.keys()[1]
ho1key = RIKS.historyRegions[rp1key].historyOutputs.keys()[0]
rp2key = RIKS.historyRegions.keys()[2]
ho2key = RIKS.historyRegions[rp2key].historyOutputs.keys()[0]
load_hist = RIKS.historyRegions[rp1key].historyOutputs[ho1key].data
disp_hist = RIKS.historyRegions[rp2key].historyOutputs[ho2key].data
maxpos = load_hist.index(max(load_hist,key=lambda x:x[1]))
load = load_hist[maxpos][1]
disp = -disp_hist[maxpos][1]


## Calculation of elastic buckling based on EC
current_Pb = pi*pi*E*current_Iy/((current_l+1.5*current_d)*(current_l+1.5*current_d))


## Calculation of average yield strength, according to EC-3-1-3
current_fya = current_fy+(520-current_fy)*7*6*current_t*current_t/current_area
limit_fya = (520+current_fy)/2
if current_fya >= limit_fya:
    current_fya = limit_fya

## Calculation of reduction factor due to distortional
# Stiffness of stiffener
current_delta =
((1*current_bp*current_bp*current_bp*current_bp)/(3*(current_bp+current_bp)))*((12*(1-
0.3*0.3))/(E*current_t*current_t*current_t))
u = 1
current_K = u/current_delta
# area of stiffener
current_As = (current_llip*2+current_bp+current_bp)*current_t
# moment of inertia stiffener
current_z
=((current_bp*2*current_t*current_t/2+current_llip*2*current_t*current_llip))/current_As
    current_Is =
(1/12)*current_t*current_t*current_t*2*current_bp+2*current_bp*current_t*(current_z-
current_t/2)*(current_z-
current_t/2)+(1/12)*2*current_llip*2*current_llip*2*current_llip*current_t+2*current_llip*current_t*(current_l
lip-current_z)*(current_llip-current_z)


#critical buckling stress of stiffener
current_sigmacrs = 2*sqrt(current_K*E*current_Is)/current_As
#lambdabar distortional
current_lambdabard = sqrt(current_fy/current_sigmacrs)
#reduction factor distotional
if current_lambdabard <= 0.65:
    current_Chid = 1
else:
    current_Chid = 1.47-0.723*current_lambdabard

# Iteration of reduction factor for less conservative result
#Iteration 1
gamma_m0 = 1.0
current_sigmacomEd_1 = current_Chid*current_fy/gamma_m0
current_lambdap_llip = (current_llip*2/current_t)/(28.4*epsilon*2)
current_lambdap_1 = sqrt(current_Chid)*current_lambdap_llip
current_rop_1 = (current_lambdap_1-0.188)/(current_lambdap_1*current_lambdap_1)
if current_rop_1 > 1:
    current_rop_1 = 1
```

Resistance of Polygonal Cross Section of Lattice Wind Tower

```
            current_llip_1 = current_rop_1*current_llip

            current_lambdap_bp = (current_bp*2/current_t)/(28.4*epsilon*2)
            current_lambdapbp_1 = sqrt(current_Chid)*current_lambdap_bp
            current_ropbp_1 = (current_lambdapbp_1-0.055*4)/(current_lambdapbp_1*current_lambdapbp_1)
            if current_ropbp_1 > 1:
               current_ropbp_1 = 1
            current_bp_1 = current_ropbp_1*current_bp


            current_As_1 = (current_llip_1*2+current_bp_1+current_bp_1)*current_t

            current_z_1
=((current_bp_1*2*current_t*current_t/2+current_llip_1*2*current_t*current_llip_1))/current_As_1
            current_Is_1=
(1/12)*current_t*current_t*current_t*2*current_bp_1+2*current_bp_1*current_t*(current_z-
current_t/2)*(current_z_1-
current_t/2)+(1/12)*2*current_llip_1*2*current_llip_1*2*current_llip_1*current_t+2*current_llip_1*current_t
*(current_llip_1-current_z_1)*(current_llip_1-current_z_1)


            current_sigmacrs_1 = 2*sqrt(current_K*E*current_Is_1)/current_As_1

            current_lambdabard_1 = sqrt(current_fy/current_sigmacrs_1)

            if current_lambdabard_1 <= 0.65:
               current_Chid_1 = 1
            else:
               current_Chid_1 = 1.47-0.723*current_lambdabard_1

            #Iteration 2
            current_sigmacomEd_2 = current_Chid_1*current_fy/gamma_m0
            current_lambdap_2 = sqrt(current_Chid_1)*current_lambdap_llip
            current_rop_2 = (current_lambdap_2-0.188)/(current_lambdap_2*current_lambdap_2)
            if current_rop_2 > 1:
               current_rop_2 = 1
            current_llip_2 = current_rop_2*current_llip

            current_lambdapbp_2 = sqrt(current_Chid_1)*current_lambdap_bp
            current_ropbp_2 = (current_lambdapbp_2-0.055*4)/(current_lambdapbp_2*current_lambdapbp_2)
            if current_ropbp_2 > 1:
               current_ropbp_2 = 1
            current_bp_2 = current_ropbp_2*current_bp


            current_As_2 = (current_llip_2*2+current_bp_2+current_bp_2)*current_t

            current_z_2
=((current_bp_2*2*current_t*current_t/2+current_llip_2*2*current_t*current_llip_2))/current_As_2
            current_Is_2=
(1/12)*current_t*current_t*current_t*2*current_bp_2+2*current_bp_2*current_t*(current_z_2-
current_t/2)*(current_z_2-
current_t/2)+(1/12)*2*current_llip_2*2*current_llip_2*2*current_llip_2*current_t+2*current_llip_2*current_t
*(current_llip_2-current_z_2)*(current_llip_2-current_z_2)


            current_sigmacrs_2 = 2*sqrt(current_K*E*current_Is_2)/current_As_2

            current_lambdabard_2 = sqrt(current_fy/current_sigmacrs_2)
```

```python
        if current_lambdabard_2 <= 0.65:
            current_Chid_2 = 1
        else:
            current_Chid_2 = 1.47-0.723*current_lambdabard_2


        ## Effective area due to distortional
        current_effareadistort = current_effarealocal-((1-
current_Chid_2)*current_t*6*(current_llip+current_bp))


        # Calculation of resistance according to EC3-1-3 Part 6
        # Cross section resistance pure axial compression
        gamma_m0 = 1.0
        current_Ncrd_local = current_area*current_fy/gamma_m0
        current_Ncrd_local_fya = current_area*current_fya/gamma_m0
        current_Ncrd = current_effareadistort*current_fy/gamma_m0
        current_Ncrd_fya = current_effareadistort*current_fya/gamma_m0

        # Cross section resistance pure bending moment
        current_W = current_Iy/(current_d/2)
        current_Mcrd = current_W*current_fy/gamma_m0


        #Buckling resistance
        #Flexural buckling
        alpha=0.34  #buckling coefficient
        current_lcr = current_l
        current_i = sqrt(current_Iy/current_area)   #radius of gyration
        current_sigmacrit = ((pi*pi)*E)/((current_lcr/current_i)*(current_lcr/current_i))
        current_lambdabar = sqrt((current_fy*current_effareadistort)/(current_sigmacrit*current_area))
        current_Phi = 0.5*(1+alpha*(current_lambdabar - 0.2)+(current_lambdabar*current_lambdabar))
        current_Chi = 1/(current_Phi+sqrt((current_Phi*current_Phi)-
(current_lambdabar*current_lambdabar)))
        if current_Chi>1:
            current_Chi = 1
        current_Nbf = current_Chi*current_effareadistort*current_fy

        #Torsional buckling
        current_io = sqrt((current_i*current_i)+(current_i*current_i))
        current_sigmacritT =
(1/(current_area*(current_io*current_io)))*(G*current_It+((pi*pi*E*current_Iw)/(current_lcr*current_lcr)))
        current_lambdabarT = sqrt((current_fy*current_effareadistort)/(current_sigmacritT*current_area))
        current_PhiT = 0.5*(1+alpha*(current_lambdabarT -
0.2)+(current_lambdabarT*current_lambdabarT))
        current_ChiT = 1/(current_PhiT+sqrt((current_PhiT*current_PhiT)-
(current_lambdabarT*current_lambdabarT)))
        if current_ChiT>1:
            current_ChiT = 1
        current_NbT = current_ChiT*current_effareadistort*current_fy

        #Flexural-Torsional buckling
        beta = 1.0
        current_sigmacritFT = (current_sigmacrit/(2*beta))*(1+(current_sigmacritT/current_sigmacrit)-
(sqrt((1-(current_sigmacritT/current_sigmacrit))*(1-
(current_sigmacritT/current_sigmacrit)))+(4*0*current_sigmacritT/current_sigmacrit)))
        current_lambdabarFT =
sqrt((current_fy*current_effareadistort)/(current_sigmacritFT*current_area))
```

```python
            current_PhiFT = 0.5*(1+alpha*(current_lambdabarFT -
0.2)+(current_lambdabarFT*current_lambdabarFT))
            current_ChiFT = 1/(current_PhiFT+sqrt((current_PhiFT*current_PhiFT)-
(current_lambdabarFT*current_lambdabarFT)))
                if current_ChiFT>1:
                    current_ChiFT = 1
                current_NbFT = current_ChiFT*current_effareadistort*current_fy

                #Final buckling
                current_Nbrd = current_effareadistort*current_fy*min(current_Chi, current_ChiT, current_ChiFT)
                current_Nbrd_fya = current_effareadistort*current_fya*min(current_Chi, current_ChiT,
current_ChiFT)

                ## Calculation of resistance according to EC3-1-6 Shell
                Cxb = 1  #pinned-pinned BC
                Q = 16  #fabrication class C
                lambdaxo = 0.2
                betax = 0.6
                gammam1 = 1.1
                current_w = current_l/sqrt((current_d/2)/current_t)
                limit = 0.5*(current_d/2)/current_t
                if current_w>limit:
                    current_Cx = 1+((0.2/Cxb)*(1-2*current_w*current_t/(current_d/2)))
                    if current_Cx<0.6:
                        current_Cx=0.6
                current_sigmaxRcr = 0.605*E*current_Cx*current_t/(current_d/2)  #critical meridional buckling
stress
                current_alphax = 0.62/(1+(1.91*((1/Q)*sqrt(current_d/2)/current_t)*1.44))
                current_lambdabarp=sqrt(current_alphax/(1-betax))
                current_lambdax = sqrt(current_fy/current_sigmaxRcr)
                current_Chix = 1-betax*((current_lambdax-lambdaxo)/(current_lambdabarp-lambdaxo))
                current_sigmaRd = current_Chix*current_fy/gammam1      #design resistance
                current_Ncrdshell = current_sigmaRd*current_area

                ## Calculation of weight of the member
                gamma_steel = 7850
                current_weight = current_area*(current_l*2+current_d*3)*gamma_steel*0.000000001


out.write(str(j)+'\t'+str(k)+'\t'+str(l)+'\t'+str(b)+'\t'+str(current_d)+'\t'+str(current_t)+'\t'+str(current_l*2+current_
d*3)+'\t'+str(round(current_d/current_t,2))+'\t'+str(current_lambda)+'\t'+str(b)+'\t'+str(load)+'\t'+

str(disp)+'\t'+str(current_d/(current_t*epsilon))+'\t'+str(current_area)+'\t'+str(current_effarealocal)+'\t'+str(curre
nt_effareadistort)+'\t'+str(current_class)+'\t'+str(current_Ncrd_local)+'\t'+str(current_Ncrd)+'\t'+str(current_Ncr
d_local_fya)+'\t'+str(current_Ncrd_fya)+'\t'+str(current_Chi)+'\t'+str(round(current_ChiT,0))+'\t'+str(current_Ch
iFT)+'\t'+str(current_Nbrd)+'\t'+str(current_Nbrd_fya)+'\t'+str(current_Ncrdshell)+'\t'+str(current_fya)+'\t'+str(c
urrent_corneround1)+'\t'+str(current_corneround2)+'\t'+str(current_Chid_2)+'\t'+str(current_bp)+'\t'+str(current
_Pb)+'\t'+str(current_weight)+'\t'+str((load/1000)/current_weight)+'\n')
                myOdb.close()
out.close()
```

Annex F Buckling modes
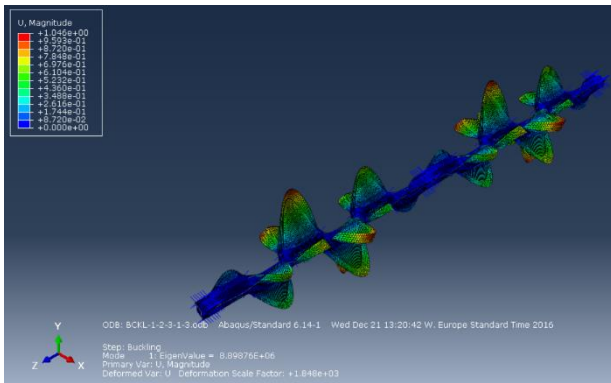
1-2-3-1-3
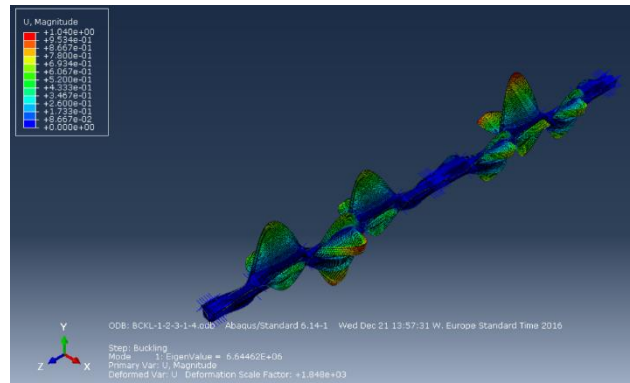
1-2-3-1-4
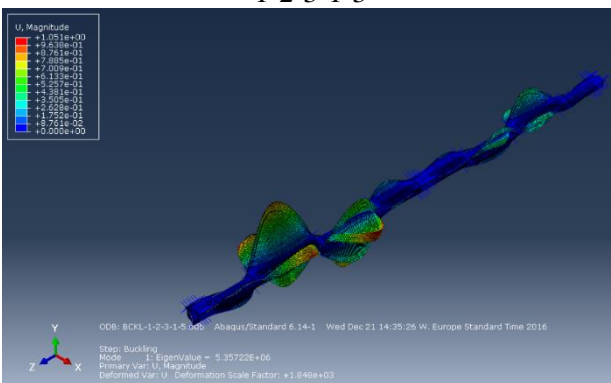
1-2-3-1-5
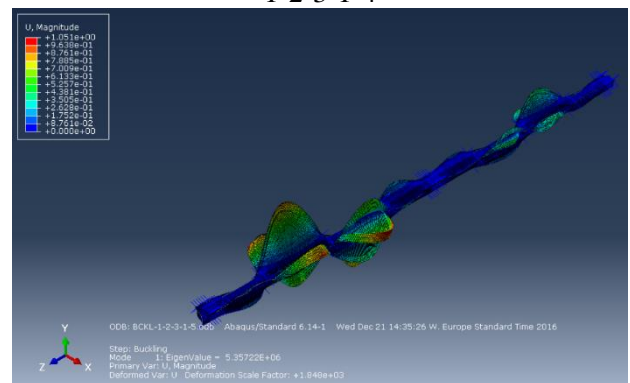
1-2-3-2-3
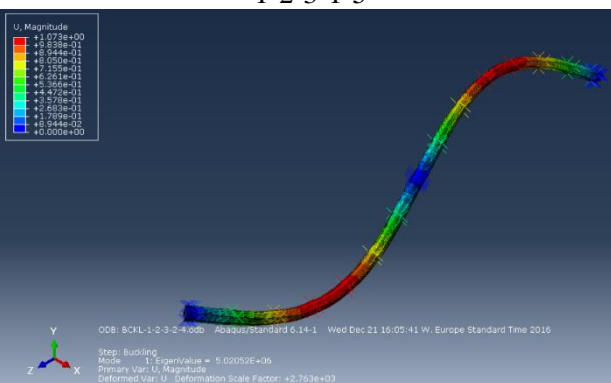
1-2-3-2-4
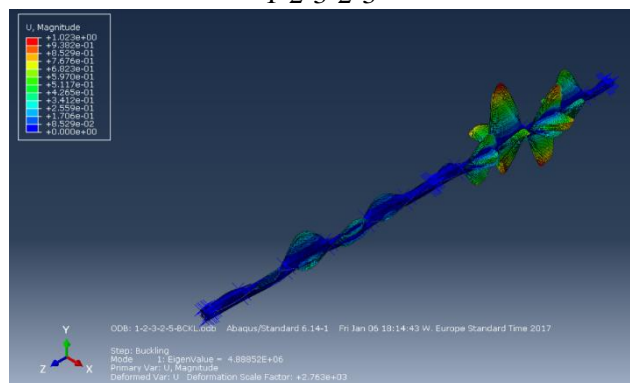
1-2-3-2-5
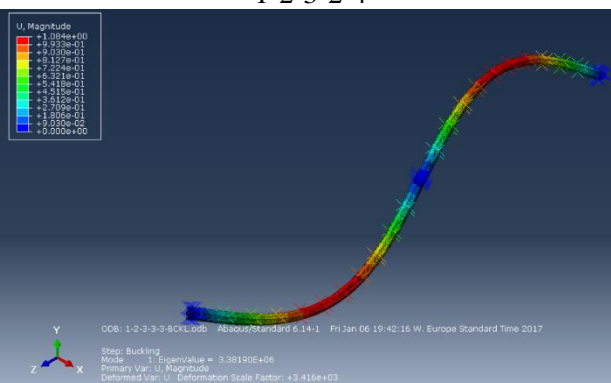
1-2-3-3-3

1-2-3-3-4

124
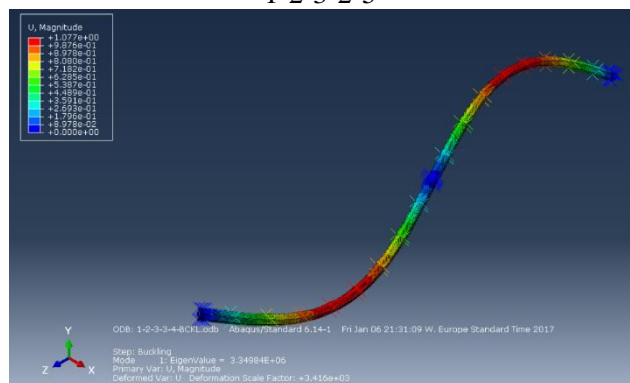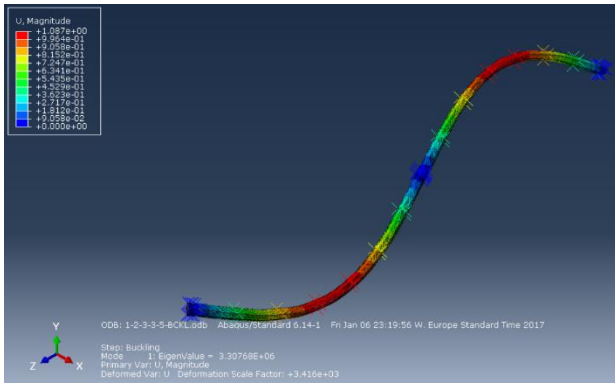
1-2-3-3-5
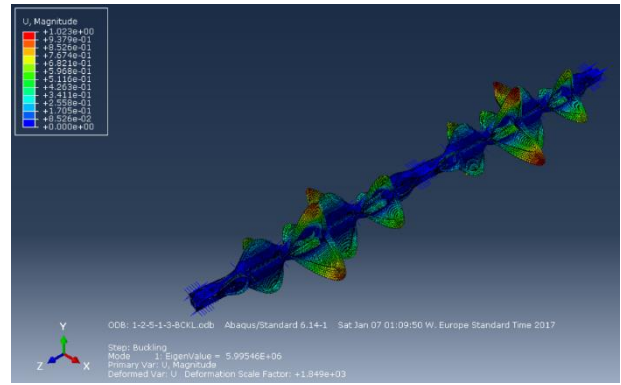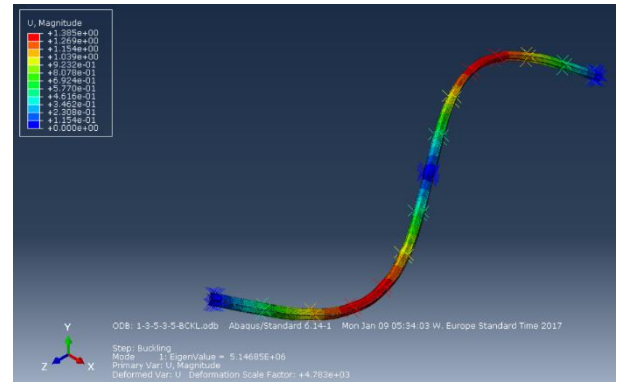

1-2-5-1-3
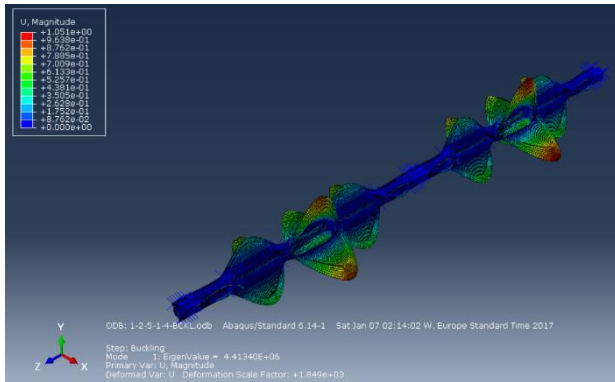
1-2-5-1-4
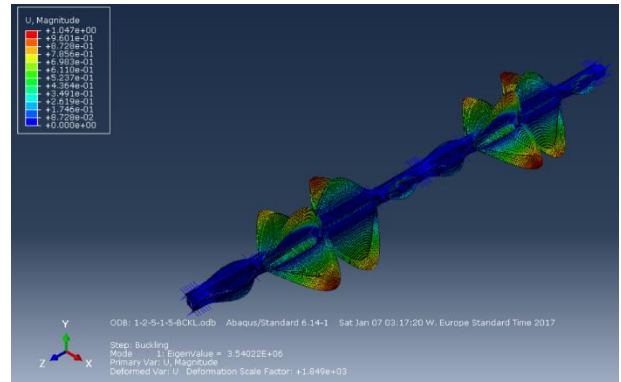
1-2-5-1-5
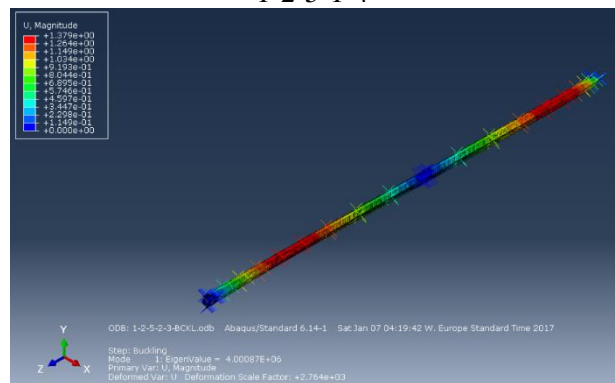
1-2-5-2-3
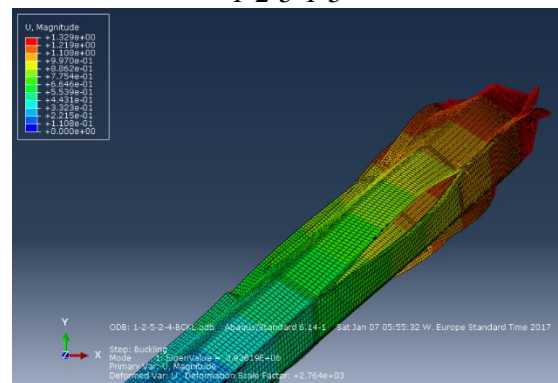
1-2-5-2-4
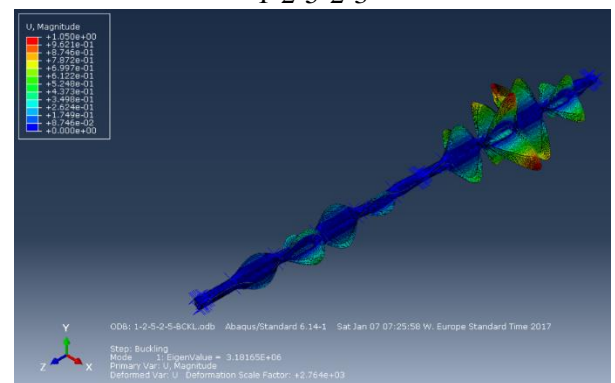
1-2-5-2-5
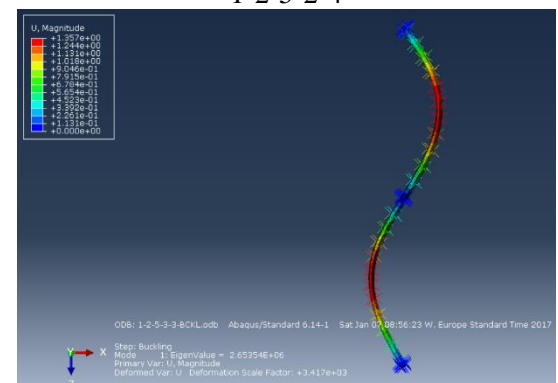
1-2-5-3-3
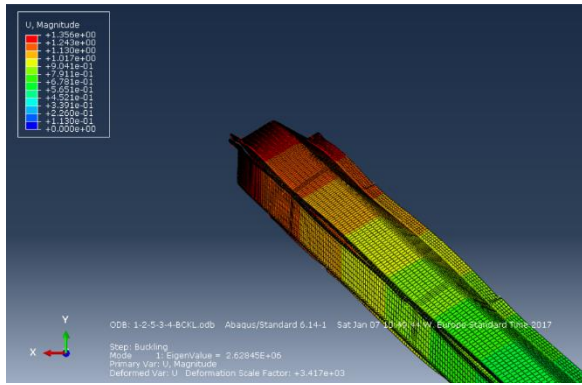
1-2-5-3-4
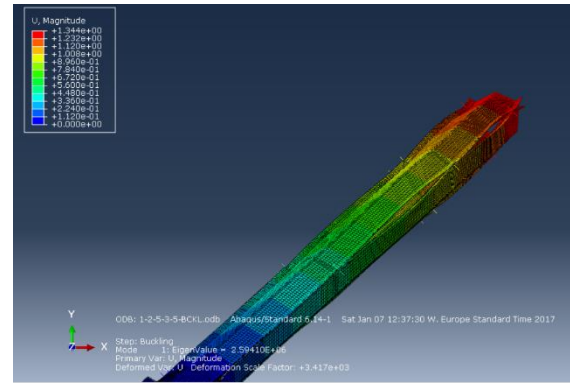
1-2-5-3-5
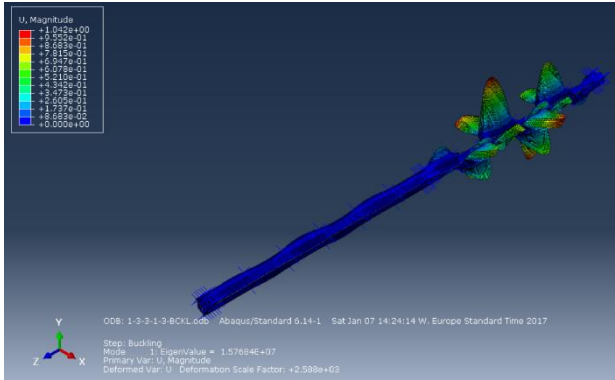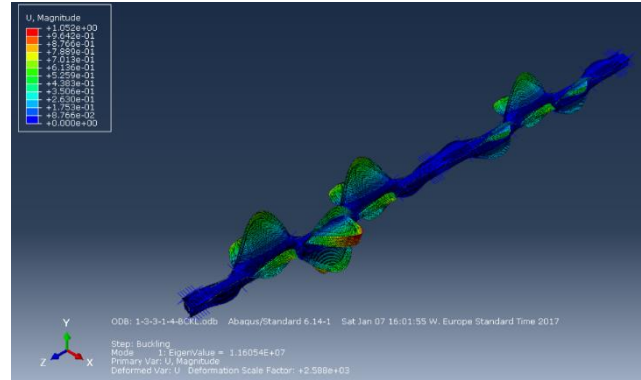
1-3-3-1-3

1-3-3-1-4
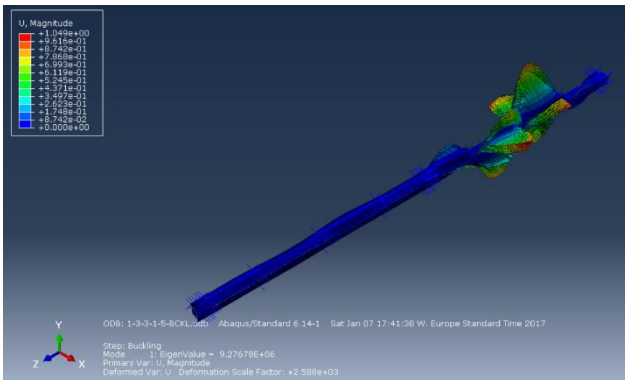
1-3-3-1-5
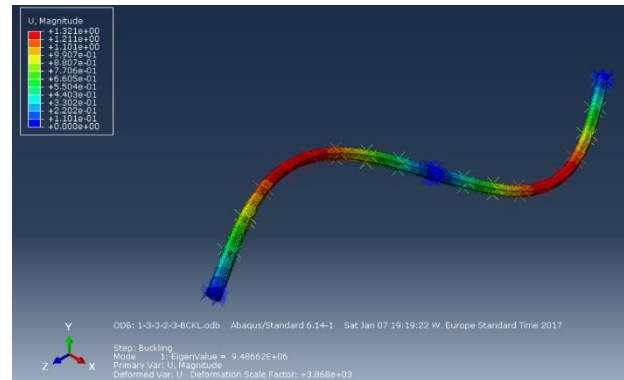
1-3-3-2-3
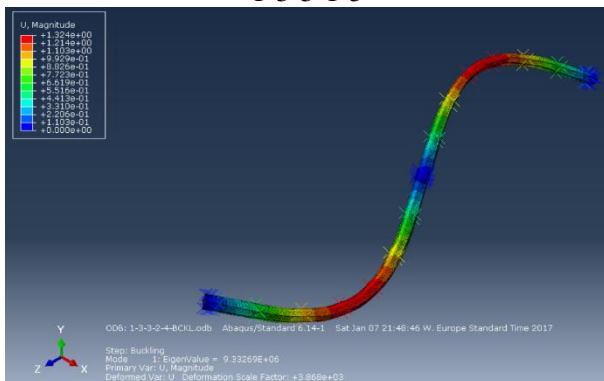
1-3-3-2-4
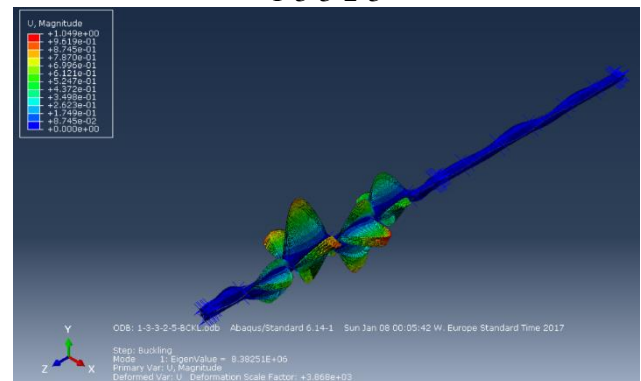
1-3-3-2-5

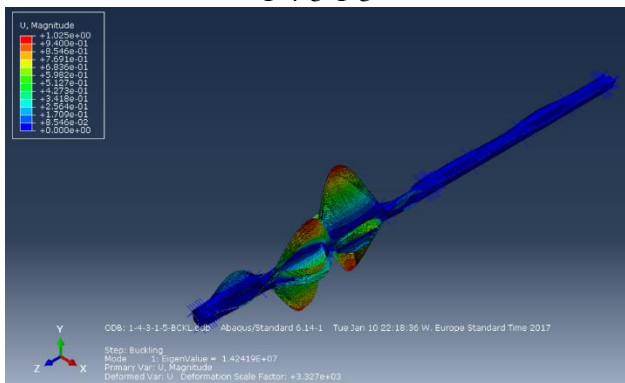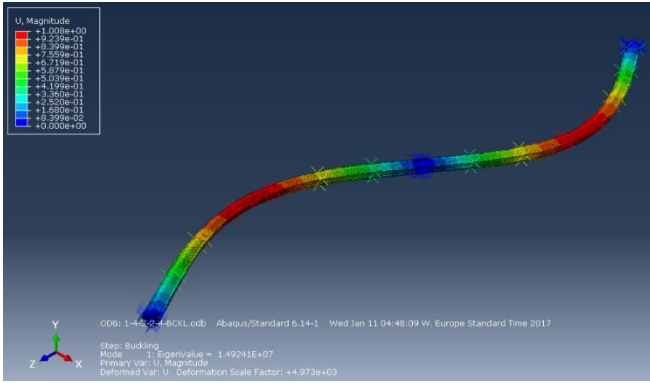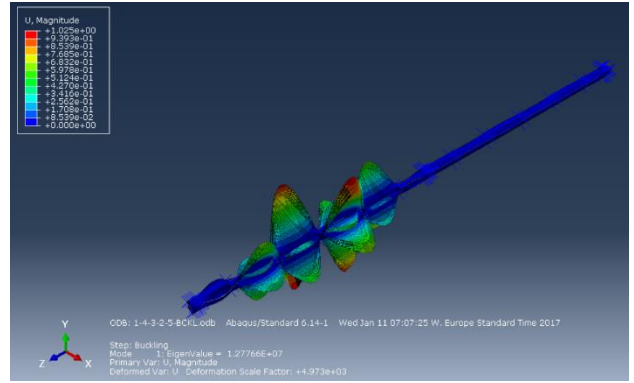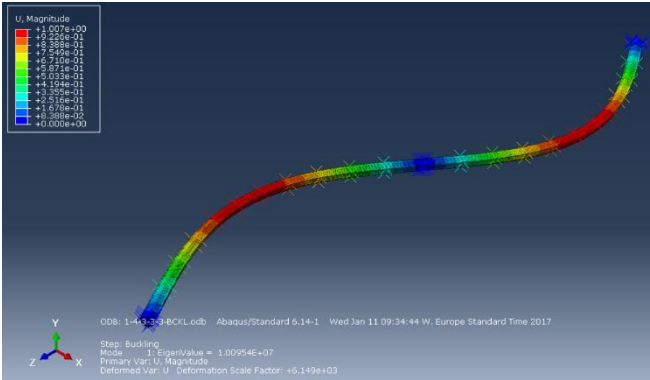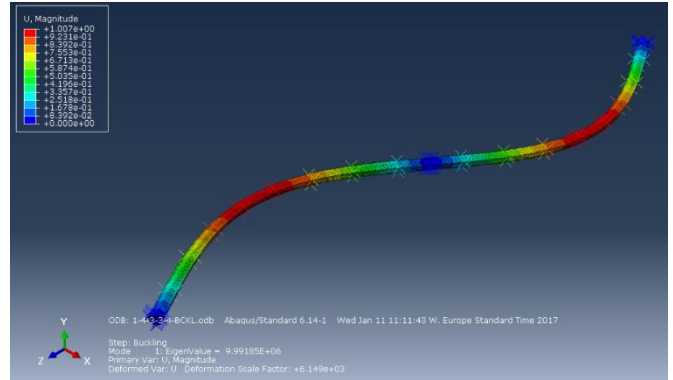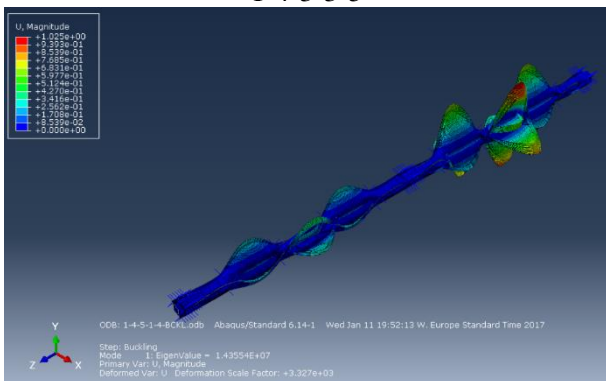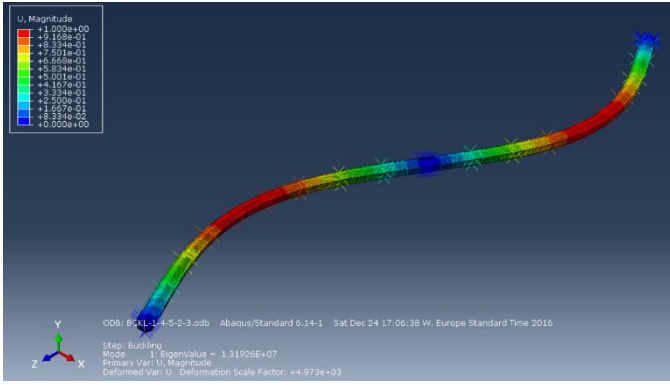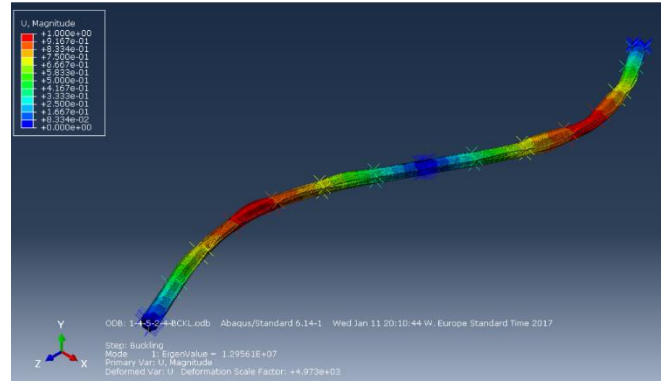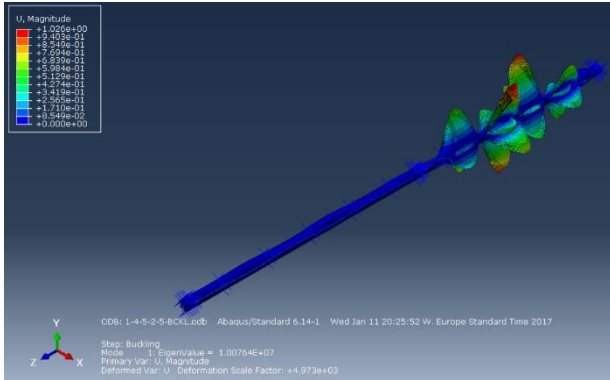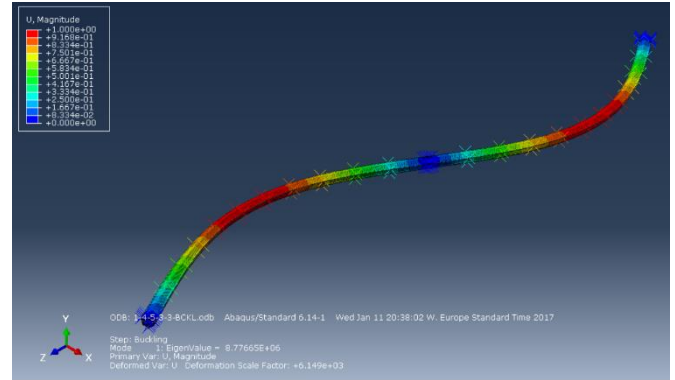Resistance of Polygonal Cross Section of Lattice Wind Tower
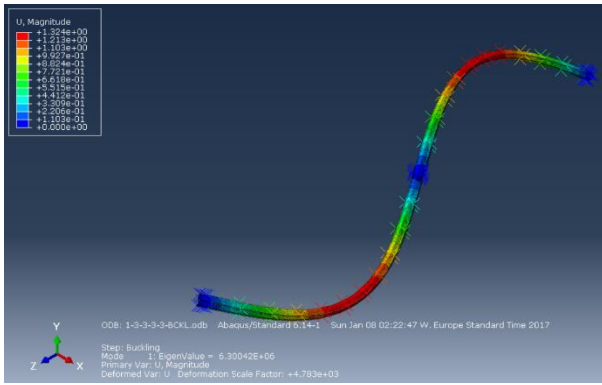
1-3-3-3-3
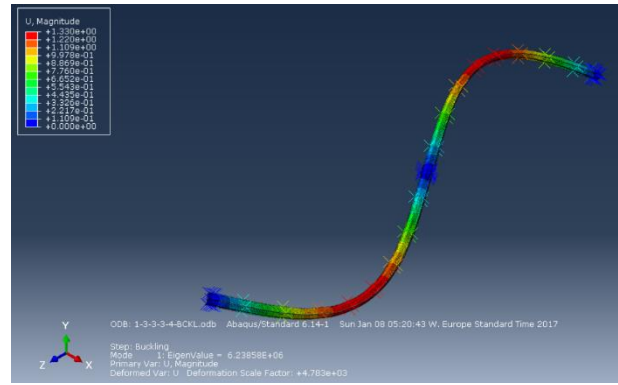
1-3-3-3-4
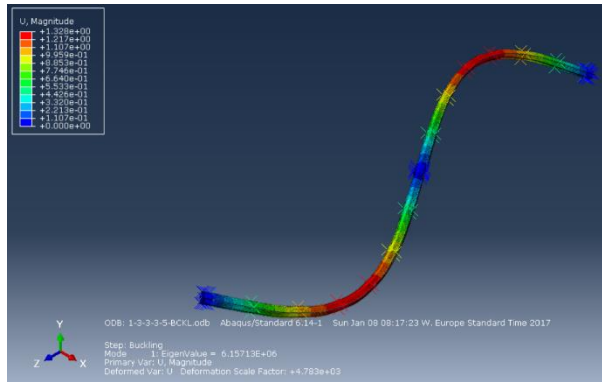
1-3-3-3-5
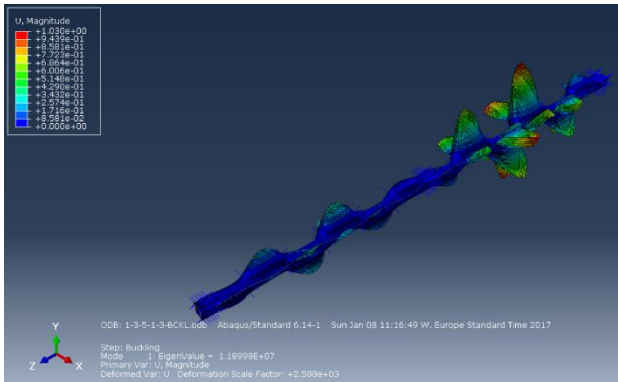
1-3-5-1-3
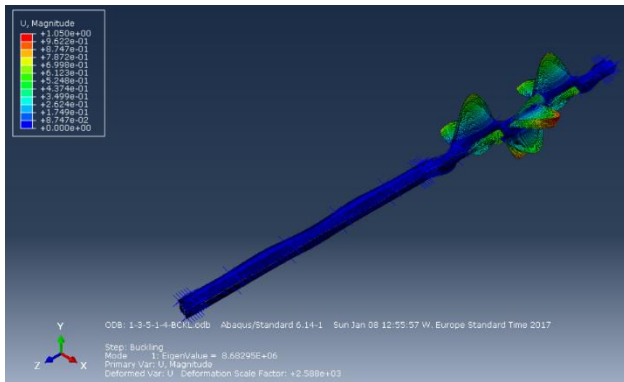
1-3-5-1-4
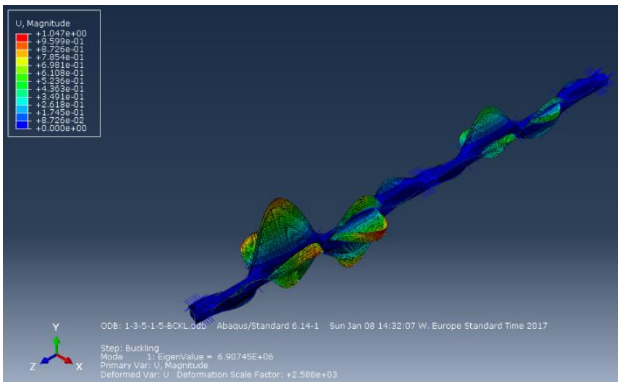
1-3-5-1-5
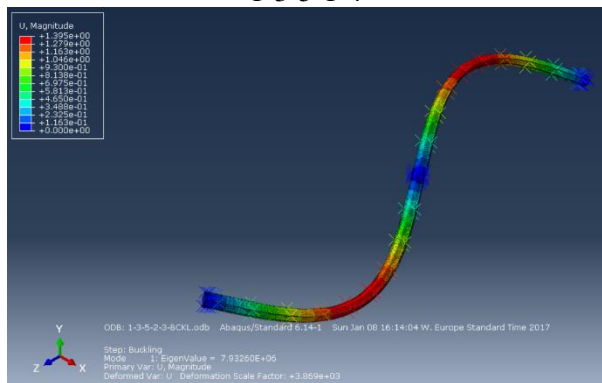
1-3-5-2-3
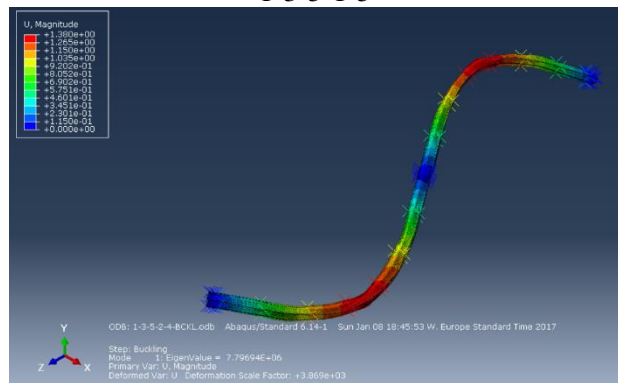
1-3-5-2-4
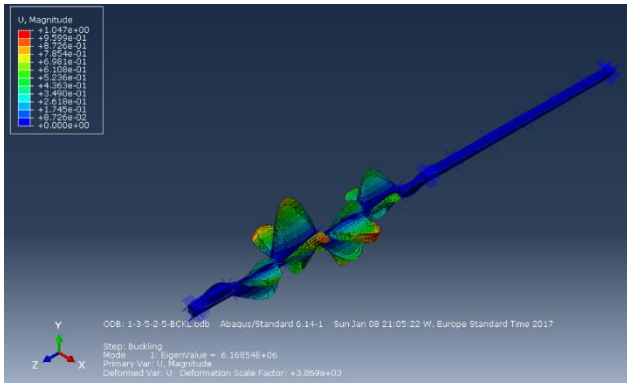
1-3-5-2-5
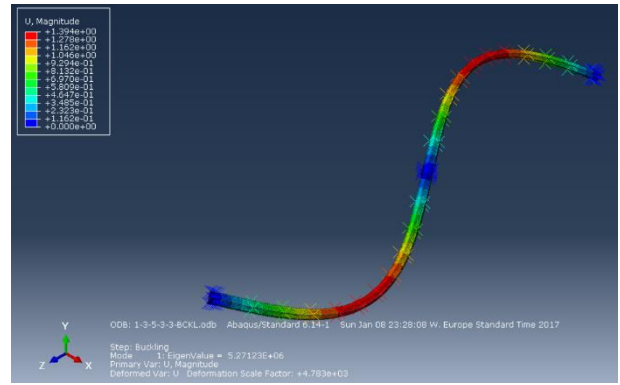
1-3-5-3-3
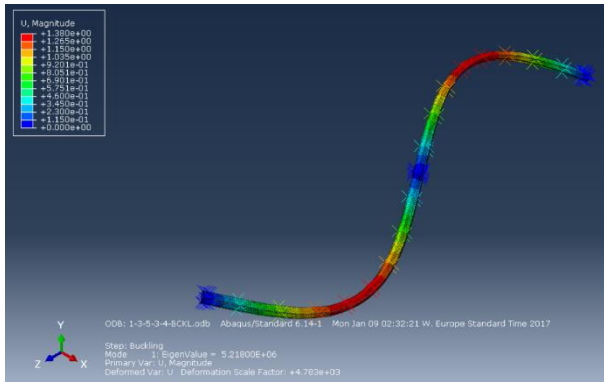
1-3-5-3-4

1-3-5-3-5

1-4-3-1-3
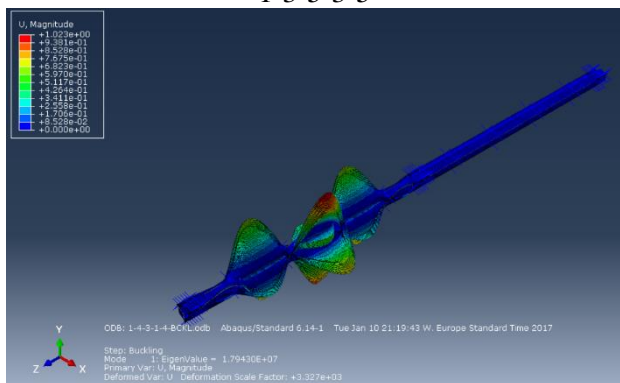
1-4-3-1-4

1-4-3-1-5

1-4-3-2-3

128
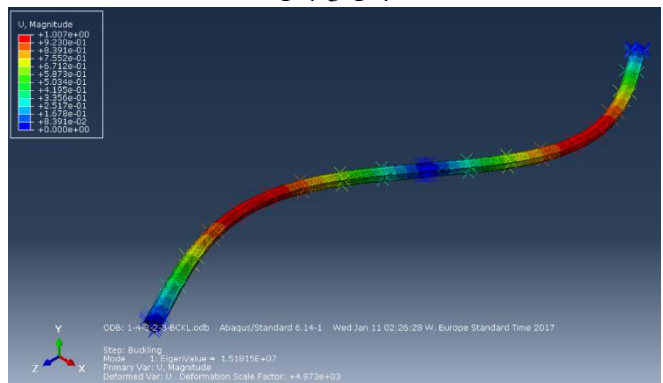
1-4-3-2-4

1-4-3-2-5

1-4-3-3-3

1-4-3-3-4

1-4-3-3-5
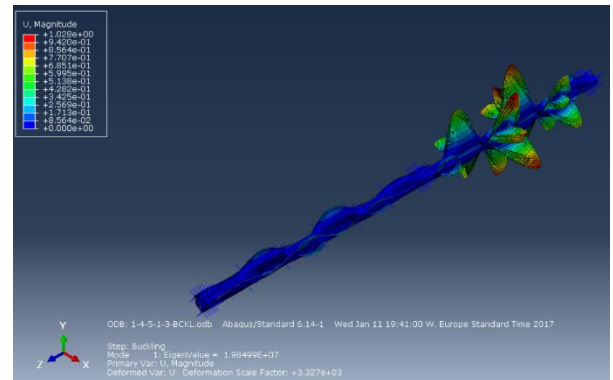
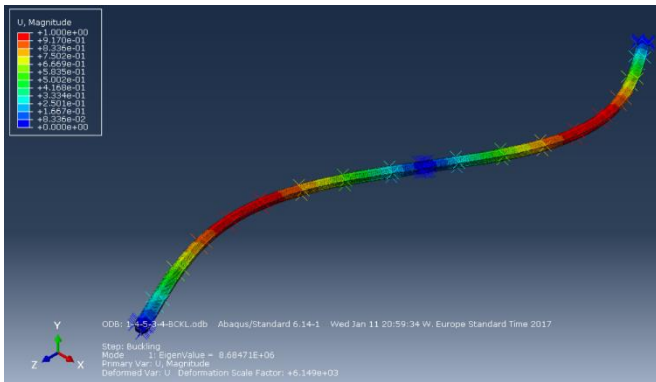
1-4-5-1-3
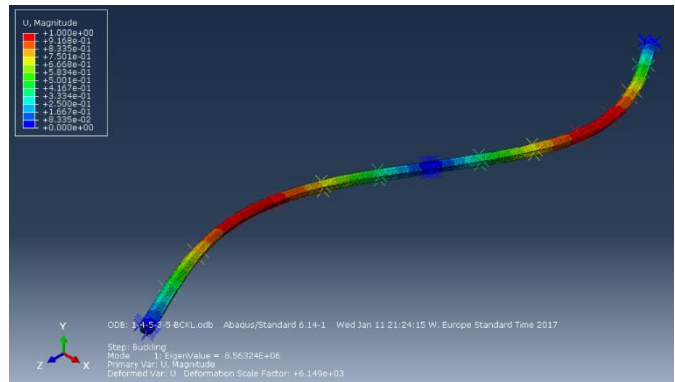

1-4-5-1-4

1-4-5-1-5

129
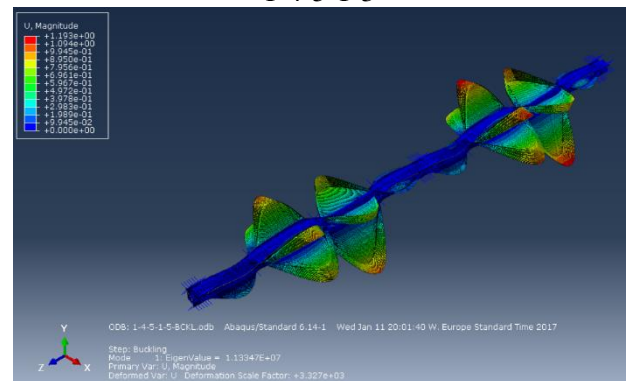
1-4-5-2-3

1-4-5-2-4

1-4-5-2-5

1-4-5-3-3

1-4-5-3-4

1-4-5-3-5